UPPER RIO GRANDE WATER OPERATIONS MODEL PHYSICAL MODEL DOCUMENTATION: THIRD TECHNICAL REVIEW COMMITTEE DRAFT

Contents

Figures

Tables

UPPER RIO GRANDE WATER OPERATIONS MODEL PHYSICAL MODEL DOCUMENTATION: THIRD TECHNICAL REVIEW COMMITTEE DRAFT

INTRODUCTION

This is the third Technical Review Committee draft of the Upper Rio Grande Basin Water Operations Model (URGWOM) physical model documentation. The document describes the data, methods, and assumptions used by RiverWare to simulate streamflow, water accounting, and reservoir operation in the Upper Rio Grande Basin. Because this document represents the model's state of development as of the date of the document's release, it is considered a "working" document—that is, it will be updated further as the model changes. The relations developed in this physical model are also used in other URGWOM models, such as the accounting, planning, and water operations models. Discussion of these other models, however, is beyond the scope of this document.

The documentation describes and analyzes river routing techniques; describes the development of travel time lags used in the variable time lag method, which is the adopted river routing method; and describes the methods and assumptions used to develop river-channel loss coefficients. The routing methods and procedures for estimating river-channel loss mechanisms are described in the document. Because application of these techniques is repetitive, tables summarize the results for each reach. Plots of data used to develop travel times and loss rates are in the **Physical Model Appendix (PHYGRAPH)**.

The geographic extent of the reaches simulated in the URGWOM model include the main stem of the Rio Grande between Lobatos, Colorado, and El Paso, Texas; Willow Creek and the Rio Chama main stem downstream from the mouth of Willow Creek; and the lower 30 miles (mi) of the Jemez River **(fig. 1)**. The model simulates streamflow and operation of the major reservoirs in these reaches. Maps throughout the document provide details of physical features of each reach.

Datasets used to determine travel times and loss rates for the reaches above Cochiti Dam and travel times for the reaches between Cochiti Dam and Elephant Butte Dam are from U.S. Geological Survey (USGS) stream-gage calibration data and Bureau of Reclamation (USBR) and Corps of Engineers (Corps) reservoir records. Data from gages at the upstream and downstream ends of URGWOM reaches that are available in electronic format, which are generally for the most recent 30-year period, were used in these calculations. Datasets used to determine loss rates and travel times for reaches between Elephant Butte Dam and El Paso are based on stream-gage calibration and reservoir data collected by the USGS, USBR, and Elephant Butte Irrigation District during 1984-99.

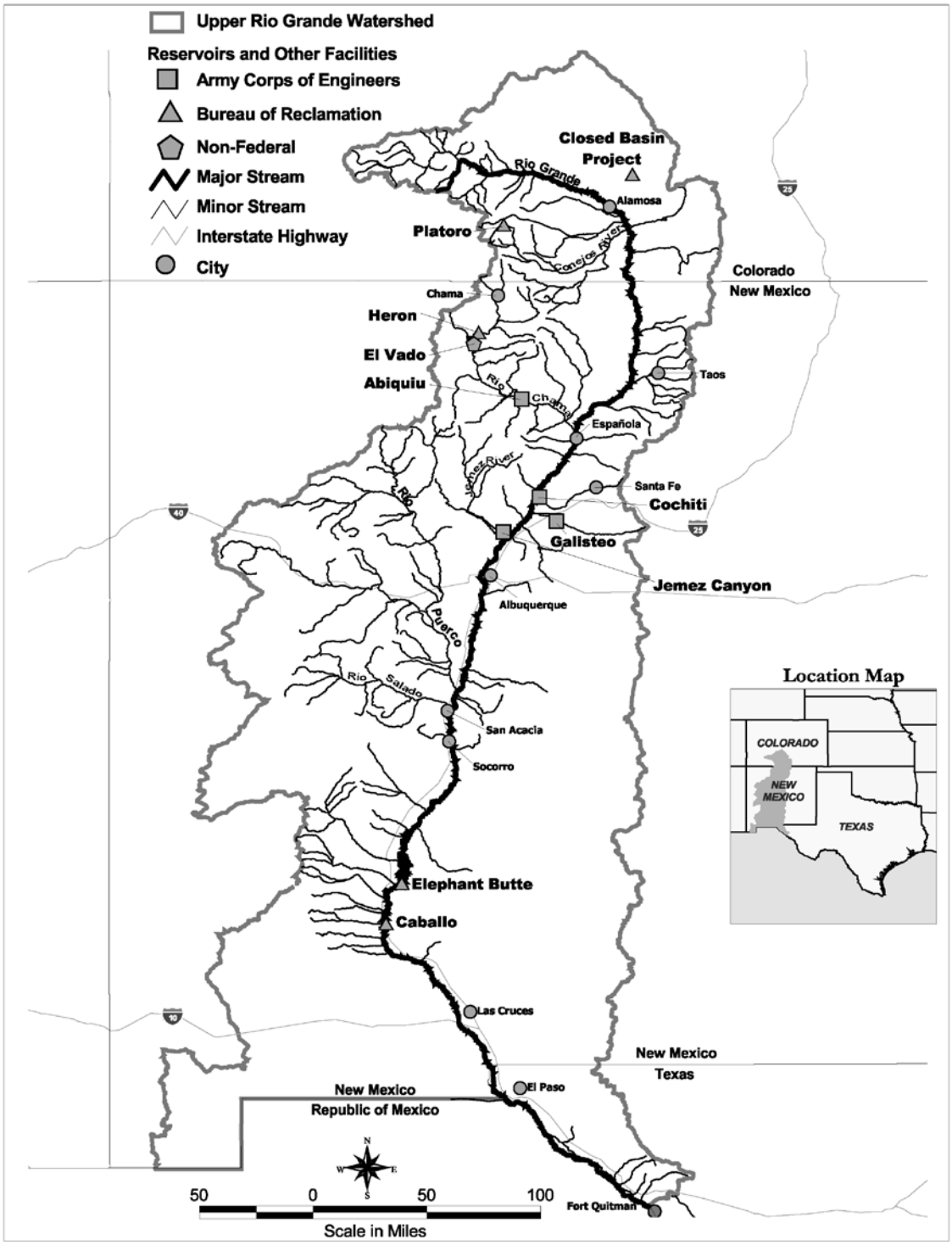

Figure 1. Rio Grande Basin from headwaters to Fort Quitman, Texas.

UPPER RIVER

SUMMARY OF REACH ANALYSIS METHODS – ROUTING AND LOSSES

Comparison of River Routing Methods

River (streamflow) routing is a method used to compute the effect of channel storage on the shape (reduction in peak, or attenuation) and downstream movement (translation, or travel time) of a hydrograph. Standard empirical river routing methods are available in RiverWare, such as the Muskingum-Cunge, kinematic wave, Muskingum, variable time lag, time lag, variable Muskingum, storage (SSARR), variable storage, impulse response, and MacCormack methods. The theory of each of these methods can be found in documents such as hydrology textbooks or engineering manuals developed by the Corps, the USBR, or the USGS. RiverWare was evaluated to assure that it computes the proper results for each routing method. Because URGWOM is a daily time step model, river routing is an important computation needed for the development of loss computations and the proper functioning of all RiverWare models being developed for URGWOM and thus is discussed first.

A river reach (the stretch of river between control points) from Rio Chama below El Vado Dam to above Abiquiu Reservoir was analyzed using several of these routing methods. Not all routing methods available in RiverWare were used in this analysis (SSARR, impulse response, and MacCormack methods). The purpose was to determine an appropriate method to use for this reach and other reaches in the model and to compare the results of the different methods and the sensitivity of the results of one method with another. The period of data analyzed generally was 1962 to 1996 because 1962 is the beginning of the complete record for the gage Rio Chama above Abiquiu Reservoir.

The routing coefficients and parameters for each method were estimated or optimized in the Hydrologic Engineering Center Hydrologic Modeling System (HEC-HMS), the Corps' precipitation-runoff computer software program. The lag and Muskingum K values for the Muskingum, variable time lag, and time lag methods were determined using measured data for the Rio Chama gages below El Vado Dam and above Abiquiu Reservoir, as described in the next section, "Time lags based on wave velocity." The input data required for the Muskingum-Cunge and kinematic wave methods were determined from cross section data from a previous study (U.S. Army Corps of Engineers, 1995). The reach length and energy slope input values were derived from gage information included in USGS Water Resources Data Reports. The Manning's roughness coefficient, n (n-value), was initially estimated using "Handbook of Hydraulics" (Brater and King, 1976) and "Open Channel Hydraulics" (Chow, 1959) as references. HEC-HMS was then used to optimize the n-value for the Muskingum-Cunge method. The initial estimated n-value was 0.04, and HEC-HMS optimized the value to 0.05. An n-value of 0.05 was used in RiverWare for the Muskingum-Cunge and kinematic wave routing methods. The Muskingum X value was optimized to a value of 0.3 in HEC-HMS, when the Muskingum K value was locked at 12 hours. A Muskingum X value of 0.3 was tried in RiverWare, resulting in negative flows. Negative flows were computed because negative coefficients are derived from the Muskingum method when K is much less than the computational time interval. Negative coefficients will result for short travel times, depending on the value of X. Because of the instability of the method for short routing reaches (travel time lags less than 24 hours), the X value was adjusted to 0.1 so that negative values would not be computed. The coefficients and parameters for each routing method are listed in **table 1**.

Table 1. Routing coefficients and parameters for the reach of the Rio Chama from below El Vado Dam to above Abiquiu Reservoir

Routing method	Reach length (miles)	Energy slope	Bottom width (feet)	Side slope (xH:1V)	Man-ning's n-value	Channel shape	Flow rate	Mus-kingum K or lag (hours)	Mus-Kingum X
Mus-kingum-Cunge	28.8	0.0027	70	2	0.05	Trape-zoid	---	---	---
Kine-matic wave	28.8	0.0027	70	2	0.05	Trape-zoid	---	---	---
Mus-kingum	---	---	---	---	---	---	---	12	0.1
Variable time lag	---	---	---	---	---	---	50	29	---
	---	---	---	---	---	---	200	15	---
	---	---	---	---	---	---	500	9	---
	---	---	---	---	---	---	750	8	---
	---	---	---	---	---	---	1000	7	---
	---	---	---	---	---	---	3000	4	---
	---	---	---	---	---	---	6000	3	---
½ -day time lag	---	---	---	---	---	---	---	12	---
1-day time lag	---	---	---	---	---	---	---	24	---

The model was then set up to run the various routing methods, and the results were plotted for comparison using selected hydrographs. Periods of little or no local inflow were selected so that only water being released could be analyzed for routing. These selected hydrographs are shown in **graphs 1-8** (all graphs are in **appendix (PHYGRAPH)** unless otherwise stated).

To define the variable time lag method, the time lag method is first defined. The time lag method applies a single time lag to all flows. On a daily time step, a daily flow volume begins arriving downstream at the specified number of hours of lag and continues through a 24-hour period. If this lag is not an integer number of days, the volume of water is apportioned between 2 days. For example, if a volume of 100 cubic-foot-per-second (cfs)-days (100 cfs for a day) has an 8-hour time lag, it begins arriving at the eighth hour of the current day and ends at the eighth hour of the next day. Apportioned, this provides (16/24) x 100 = 67 cfs-days downstream the current day and (8/24) x 100 = 33 cfs-days the next day.

Although the variable time lag method uses the same procedure, it allows breaking the total flow range into as many as 10 flow ranges, each with associated varying time lags. It also allows as many as 12 seasons to be defined with different flow range/time lag sets.

The Muskingum-Cunge and variable time lag methods appear to provide the most consistent results for timing and matching peak flows in the reach Rio Chama below El Vado Dam to above Abiquiu Reservoir. All the methods, however, provide acceptable results, except for the 1-day time lag, which tended to peak later than the other methods. Although the simple time lag routing method is also sometimes effective, the variable time lag method was chosen because of several considerations. First, the variable time lag method is fairly easy to develop if measurement data are available. Second, it can be developed throughout the model for reaches with differing geomorphic and hydrologic conditions. Third, the variable time lag routing method takes advantage of the known direct relation between velocity and flow.

Time Lags Based on Wave Velocity

Wave velocity is also known as the Klietz-Seddon or Seddon law (Seddon, 1900). In 1900, J.A. Seddon published a paper regarding the computation of wave velocity. His study concentrated on unsteady flow in rivers. He concluded that the wave velocity, V_w, is equal to *dQ/dA*. By using the power relations developed from historical USGS cross section and measurement data, travel time relations (time lags) can be computed for their corresponding reaches:

$$A=\alpha Q^{\beta}$$

where:

A = cross section area, in square feet (ft^2);
Q = discharge, in cfs; and
α *and* β = regression power coefficients and exponents.

The cross section area equation can be rearranged to solve flow as a function of area:

$$Q=\left(\frac{1}{\alpha}\right)^{\frac{1}{\beta}} A^{\frac{1}{\beta}}$$

Solving for *dQ/dA*:

$$\frac{dQ}{dA}=\frac{1}{\beta}\left(\frac{1}{\alpha}\right)^{\frac{1}{\beta}} \frac{A^{\frac{1}{\beta}}}{A}$$

since:

$$Q=\left(\frac{1}{\alpha}\right)^{\frac{1}{\beta}} A^{\frac{1}{\beta}}$$

substituting *Q*:

$$\frac{dQ}{dA}=\frac{1}{\beta}\frac{Q}{A}$$

also:

$$\frac{Q}{A}=V_{avg}$$

where:

V_{avg} is the average velocity, in feet per second (ft/s).

Therefore, substituting for *Q/A*:

$$\frac{dQ}{dA}=\frac{1}{\beta}V_{avg}$$

Because the wave velocity is equal to *dQ/dA*:

where:

$$V_w = \frac{dQ}{dA} = \frac{1}{\beta} V_{avg}$$

V_w is the wave velocity, in ft/s.

The lag time is then estimated by dividing the reach length by the wave velocity (with the appropriate conversions of time and distance units). Because wave velocity varies with discharge, travel time varies with discharge. The relation of time lag as a function of discharge can then be incorporated into a table for use in the model. The following is an example calculation of the time lag for a reach length of 28.8 mi (Rio Chama from below El Vado Dam to above Abiquiu Reservoir).

First, by using data from USGS discharge measurements, measured cross section area (ft^2) is plotted against stream discharge (cfs), and a power relation is derived (**fig. 2**).

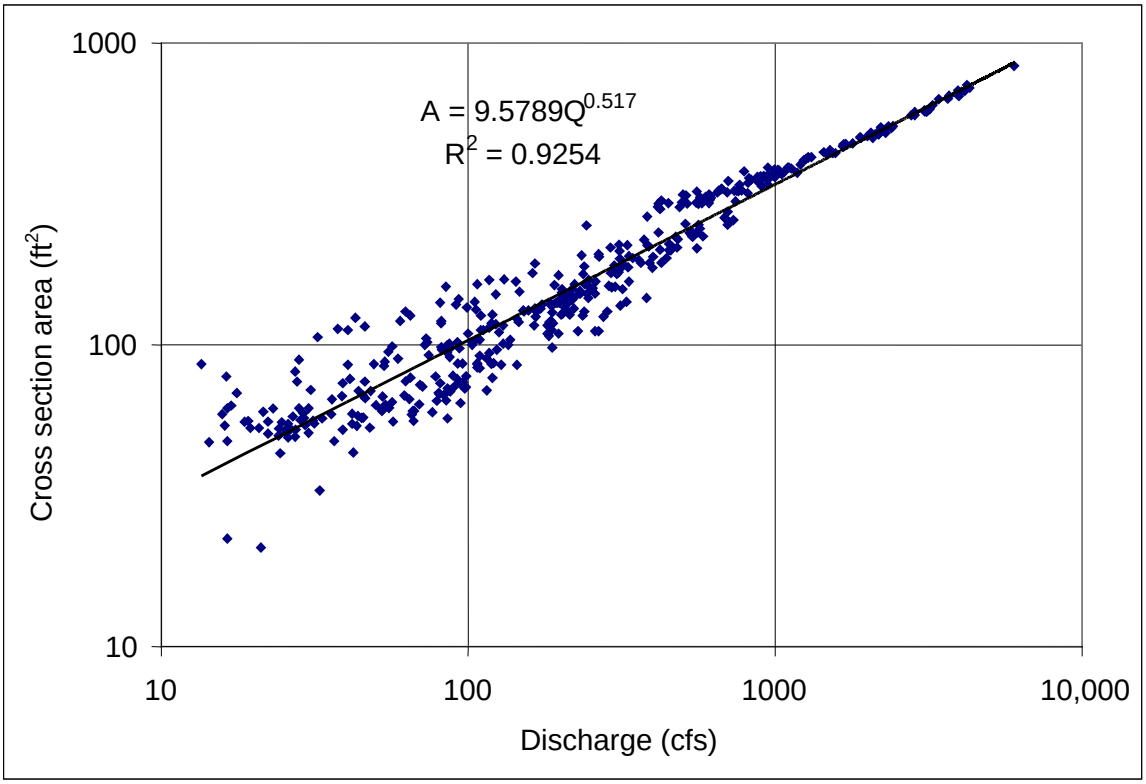

Figure 2. Cross-section area versus discharge, Rio Chama below El Vado Dam, 1969-98.

From this power equation, $\beta = 0.517$. Each measured average velocity (V_{avg}) is then divided by β to derive the wave velocity for a given discharge measurement:

$$V_w = \frac{V_{avg}}{\beta} = \frac{1.68}{0.517} = 3.25 \, ft/s$$

Once the wave velocity is known, the time lag can be computed for a given discharge by dividing reach length by wave velocity and making the appropriate conversions:

$$TL = \frac{L}{V_w} \frac{5280 \frac{ft}{mi}}{3600 \frac{s}{hr}} = \frac{28.8 mi}{3.25 \frac{ft}{s}} \frac{5280 \frac{ft}{mi}}{3600 \frac{s}{hr}} = 13.0 hr$$

where:

TL = time lag, in hours; and
L = routing reach length, in mi.

Travel time versus discharge can then be plotted on a scatter graph and a power equation derived, as shown in **figure 3.**

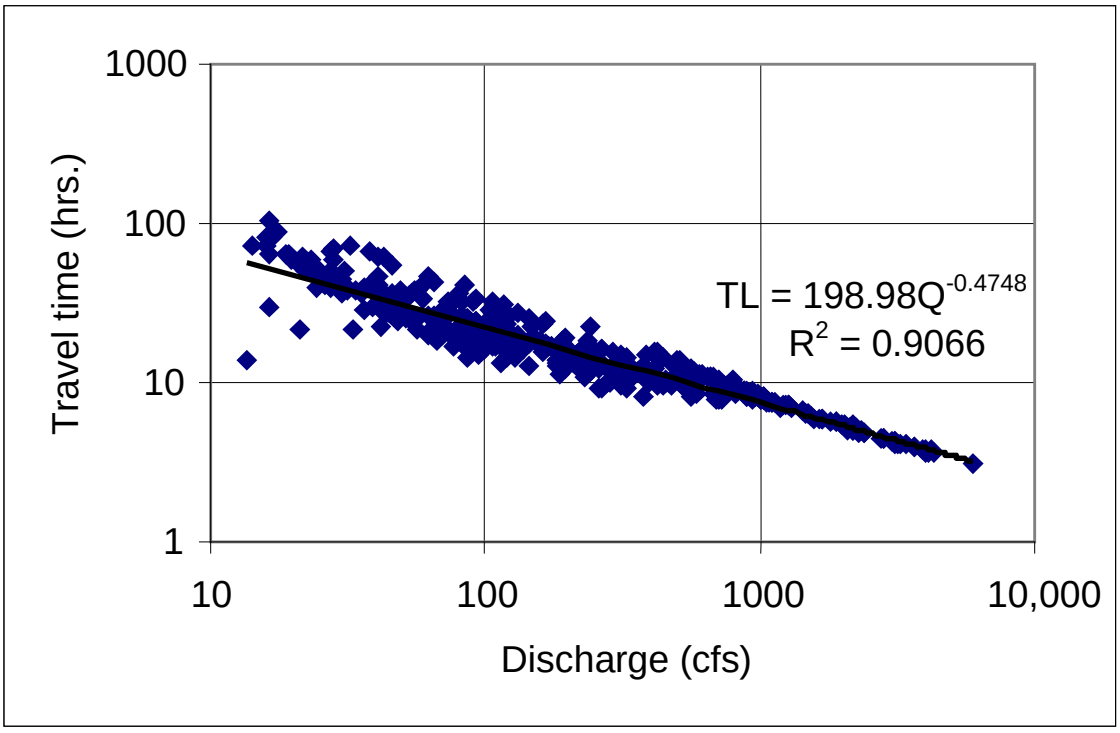

Figure 3. Travel time versus discharge, Rio Chama below El Vado Dam to above Abiquiu. Reservoir (based on gage Rio Chama below El Vado Dam, 1969-98).

Because RiverWare does not accept power equations, a table of travel time versus discharge must be developed for use in the model. Travel time for varying discharge ranges can be calculated using the power equation derived in **figure 3** ($TL = 198.98Q^{-0.4748}$). **Table 2** uses the same example reach.

Table 2. Discharge rates and travel times for the reach of the Rio Chama from below El Vado Dam to above Abiquiu Reservoir (based on gage Rio Chama below El Vado Dam)

Discharge rate used to determine travel time (cfs)	Travel time (hours)
50	31
200	16
500	10
750	9
1000	7
3000	4
6000	3

When this procedure is used to estimate travel time lags, the gage cross section is assumed to be representative of the entire routing reach. If both upstream and downstream gage measurements are available, the results of wave velocity analysis are averaged to represent the entire reach. Analyzing the upstream and downstream hydrographs at various discharge rates verifies the results.

If no measurement or hydrograph data are available for a given reach, a ratio method can be used to derive a wave velocity. The average velocities are calculated from Manning's equation with a representative cross section and varying discharges for the routing reach. For various channel shapes, wave velocity has been found to be a direct ratio of average velocity (**table 3**). For natural channels, a ratio of 1.5 is suggested.

Table 3. Wave velocity ratios for various channel shapes

Channel width	Ratio V_w/V_{avg}
Wide rectangular	1.67
Wide parabolic	1.44
Triangular	1.33

This procedure can also be used to estimate the K value required for the Muskingum routing method or a single or average time lag for use in the time lag routing method.

Reach Loss Analysis and Gains Determination

The following steps are necessary for implementing the variable time lag routing method to develop monthly loss rates and local inflow (gains) in a reach:

1. Select an overall dataset. Datasets used to determine travel times for the reaches above Cochiti Dam are based on USGS discharge data for gages at the upstream and downstream ends of each URGWOM reach that are available in electronic format, generally the most recent 30-year period. Loss rates computed for the URGWOM reaches use data based on the available period of record or the most recent 30 years, whichever is greater. Using variable time periods in model development is considered reliable because most of the

channel sections above Cochiti Dam are relatively stable, and travel times and loss rates are not substantially affected by the use of any specific time period. For those reaches below Cochiti Dam, the channel is unstable: the channel has changed since the construction of Cochiti Dam and continues to change. The period of record used in the analysis of each URGWOM reach is included in the description of each reach.

2. Model all significant human effects in the reach, including diversions.

3. Calibrate the variable time lag routing method for each reach using the methods described in the previous section.

4. Create a routed hydrograph by routing the upstream-observed hydrograph using the overall dataset.

5. Create a filtered dataset to determine only loss relations; keep data for the days when routed flow is greater than downstream-observed flow in groups of 3 or more consecutive days.

6. Plot the (filtered) downstream-observed hydrograph versus the (filtered) routed hydrograph and perform a regression analysis on the data.

7. Create a monthly regression coefficient for each calendar month by using daily data in the regression analyses of the filtered dataset. The slope of the linear regression line of best fit represents the loss coefficient. Regression lines of best fit are computed with y-intercepts and with the line forced through the zero y-intercept. After an analysis of loss rates computed using both regression lines and an analysis of the results, which were not significantly different, it was decided that the use of the y = 0 intercept regression line could be used.

8. Create a “routed with losses” hydrograph using the monthly regression coefficient minus one on the daily numbers (of the corresponding months), for the overall routed hydrograph.

9. Create a local inflow hydrograph that represents gains within the reach by subtracting the routed with losses hydrograph from the downstream-observed flow hydrograph, both for the overall dataset.

10. (Optional) Smooth the local inflow hydrograph with a moving average technique to minimize large negative daily local inflows.

RIO CHAMA REACHES

A 73.4-mi section of the Rio Chama is divided into two reaches. The first reach begins at the gage Rio Chama below El Vado Dam and extends to the next downstream gage Rio Chama above Abiquiu Reservoir. The second reach is from below Abiquiu Dam downstream to the Chamita gage, which is considered the confluence of the Rio Chama and the Rio Grande. San Juan-Chama Project water diversion and delivery into Heron Reservoir are included in the physical model. The transport of San Juan-Chama Project water from the Azotea Tunnel portal to Heron Reservoir is not based on physical gains/losses and lags, but on an approved loss rate of 0.002 with no travel time lag. The locations of reaches used in the Rio Chama Basin are shown in **figure 4**.

Willow Creek above Heron Reservoir

Although the reach of Willow Creek between the Azotea Tunnel portal and Heron Reservoir is simulated in the physical model, neither natural flows nor San Juan-Chama Project water was routed through this reach. A fixed loss rate is applied to San Juan-Chama Project water between the Azotea Tunnel portal and Heron Reservoir.

This reach flows down a short reach of Azotea Creek and a portion of Willow Creek for about 12 mi at a slope of about 25 feet per mile (ft/mi). The channel varies from 30 to 65 feet (ft) wide and is characterized as a mountainous stream.

Rio Chama from Heron Reservoir to above El Vado Reservoir

This reach of the Rio Chama is not included in the model because of a lack of data necessary to develop travel time lags and river-channel losses. In addition, no need has been identified that requires inclusion of this reach. The Natural Resources Conservation Service/National Weather Service runoff forecast point is at the inflow to El Vado Reservoir, which precludes the need for river routing above this point.

Rio Chama from below El Vado Dam to above Abiquiu Reservoir

Inflow to this reach is water released from El Vado Reservoir, which is measured at a gaging station 1.5 mi downstream from the dam (Rio Chama below El Vado Dam). The downstream end of the reach is the gage above Abiquiu Reservoir (Rio Chama above Abiquiu Reservoir). The reach is 28.8 mi long. The upper part of this reach is a canyon section with a rocky, narrow river channel and flood plain. The lower 6 mi flows through a broad alluvial plain that supports a small amount of irrigable land and a riparian bosque.

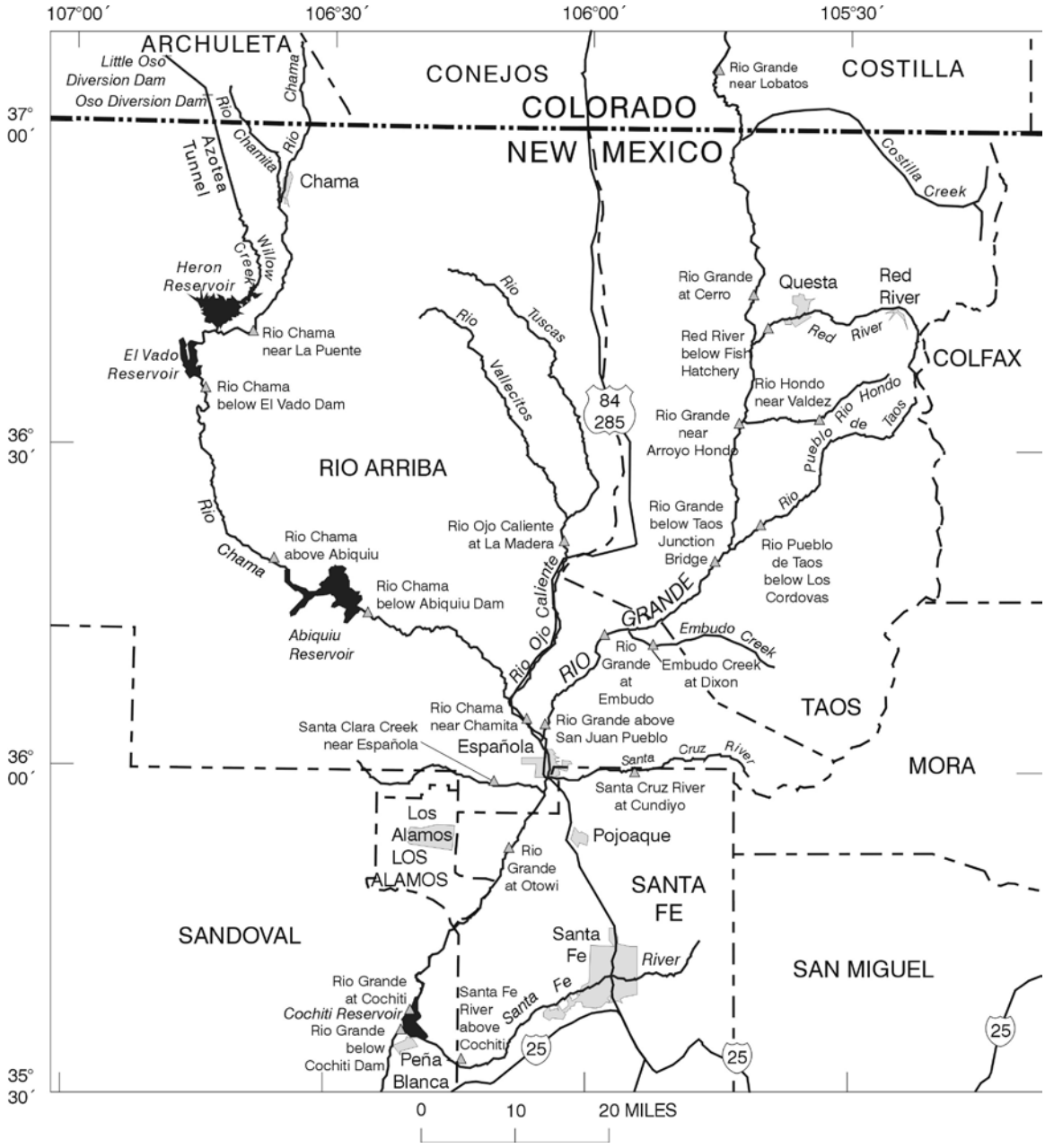

Figure 4. Rio Grande from near Lobatos, Colorado, to Cochiti, New Mexico.

The reach between the gage above Abiquiu Reservoir and Abiquiu Dam is about 15.3 mi long. However, the distance to the headwaters of the reservoir at the top of the existing storage easement (elevation 6220 ft) is only about 4 mi and at the top of the flood control (elevation 6283.5 ft) is less than 2 mi. Because of the short length to the head of the reservoir during normal operations, the reach from the gage above Abiquiu Reservoir to Abiquiu Reservoir will not include any routing or losses.

Table 4 summarizes stream-gage and calibration data used in determining the power coefficient (wave velocity exponent) that is applied to average velocity measurements to determine river travel time lags in the reach from below El Vado Dam to above Abiquiu Reservoir (**fig. 2 and graph 9**).

Table 4. Summary of stream-gage and calibration data for the reach of the Rio Chama from below El Vado Dam to above Abiquiu Reservoir

	Rio Chama below El Vado Dam	Rio Chama above Abiquiu Reservoir	Total Δ
Period of analysis	10/14/69 – 8/9/98	8/28/69 – 8/5/98	
River mile (above mouth)	76.2	47.4	28.8
Elevation (feet above sea level)	6696	6280	416
Drainage area (square miles)	877	1600	723
Number of measurements	446	373	
Wave velocity exponent (β)	0.517	0.486	
Coefficient of determination (R^2)	0.93	0.93	

Table 5 summarizes factors used to determine travel time lags in this reach (**fig. 3 and graph 10).**

Table 5. Adopted travel time lags (TL) for the reach of the Rio Chama from below El Vado Dam to above Abiquiu Reservoir

			Time lag (hours) for indicated flow rate (cfs)						
Gage	TL vs. Q equation	R^2	50	200	500	750	1000	3000	6000
El Vado	$TL = 198.98Q^{-0.4748}$	0.91	31	16	10	9	7	4	3
Abiquiu	$TL = 206.53Q^{-0.5137}$	0.94	28	14	8	7	6	3	2
Adopted travel times for reach→			29	15	9	8	7	4	3

Once the routing parameters were determined and verified for the reaches of the Rio Grande above Cochiti, the loss expected in each reach was analyzed using the filtering procedure described previously. These losses represent losses of flow from surface-water evaporation, seepage to ground water, and bank storage. The river losses are combined in these reaches because of a lack of readily available data for each of these effects. If data to isolate these losses become available in the future, these loss coefficients can be revised. In RiverWare, the loss coefficient is multiplied by the routed flow and the resulting value is subtracted from the upstream-routed flow, resulting in a loss at the downstream point.

Sixteen data points were removed from the analysis of wave velocity and travel time using the gage Rio Chama below El Vado Dam because of errors in or reporting of the measurement data. Some data points were removed from the loss analysis because of timing errors in the routed hydrograph or possible measurement error at one or both of the upstream and downstream gages. Four points were removed from the analysis that uses the gage above Abiquiu Reservoir.

Table 6 summarizes the adopted loss coefficients for this reach (**graphs 11-22**).

Table 6. Correlations between routed flow and observed flow and adopted monthly loss coefficients for the reach of the Rio Chama from below El Vado Dam to above Abiquiu Reservoir, 1962-96

Month	n (days)	Slope (y=0)	R^2	Adopted monthly loss coefficient
Jan	156	0.966	0.99	-0.03
Feb	53	0.966	0.99	-0.03
Mar	93	0.960	0.99	-0.04
Apr	84	0.964	1.00	-0.04
May	162	0.965	1.00	-0.04
June	347	0.946	0.99	-0.05
July	363	0.942	0.99	-0.06
Aug	210	0.946	0.99	-0.05
Sept	284	0.962	0.99	-0.04
Oct	227	0.958	0.99	-0.04
Nov	254	0.973	1.00	-0.03
Dec	217	0.980	1.00	-0.02

Rio Chama from below Abiquiu Dam to near Chamita

This reach of the river is 28.5 mi long and includes numerous agricultural diversions. Inflow to the reach is water released from Abiquiu Dam, as recorded by the gage Rio Chama below Abiquiu Dam. Outflow is measured at the gage Rio Chama near Chamita. The only diversion data (monthly) available are for the Rio Chama main-stream acequias from 1971 to 1985**.** These data were uniformly converted to daily values for each measured diversion. Because no data are available for return flows, 50 percent of the diversion was assumed to return to the Rio Chama.

The Rio Ojo Caliente, a major tributary to this reach, discharges into the Rio Chama about 6 mi above its mouth. This tributary is not included in river routing for this reach because of a lack of data needed to reliably estimate time lags and losses between the gage Rio Ojo Caliente at La Madera (20 mi above mouth) and the Rio Chama confluence. About 500 acres of land can be irrigated from the Rio Ojo Caliente below the gage at La Madera. Discharges to the Rio Chama during spring runoff can be substantial, and the lack of reliable estimates of this discharge to the Rio Chama complicates the reliability of loss estimates for the Abiquiu to Chamita reach. El Rito Creek, which discharges into the Rio Chama about 16 mi above the mouth of the Rio Chama, is not specifically represented in the model because of similar circumstances. These two tributaries, along with other flows, are included in the local inflow between Abiquiu Dam and Chamita.

Table 7 summarizes stream-gage and calibration data used in determining the power coefficient (wave velocity exponent) that is applied to average velocity measurements to determine river travel time lags in this reach (**graphs 23 and 24**)**.**

Table 7. Summary of stream-gage and calibration data for the reach of the Rio Chama from below Abiquiu Dam to near Chamita

	Rio Chama below Abiquiu Dam	Rio Chama near Chamita	Total Δ
Period of analysis	4/15/70 – 8/5/98	7/2/69 – 8/5/98	
River mile (above mouth)	31.3	2.8	28.5
Elevation (feet above sea level)	6040	5654	386
Drainage area (square miles)	2147	3144	997
Number of measurements	332	410	
Wave velocity exponent (β)	0.587	0.620	
Coefficient of determination (R^2)	0.94	0.91	

Table 8 summarizes factors used to determine travel time lags in this reach (**graphs 25 and 26**).

Table 8. Adopted travel time lags (TL) for the reach of the Rio Chama from below Abiquiu Dam to near Chamita

			Time lag (hours) for indicated flow rate (cfs)						
Gage	TL vs. Q equation	R^2	50	200	500	750	1000	3000	6000
Abiquiu	$TL = 132.75Q^{-0.414}$	0.877	26	15	10	9	8	5	4
Chamita	$TL = 94.68Q^{-0.380}$	0.783	21	13	9	8	7	5	3
Adopted travel times for reach→			24	14	10	8	7	5	4

The same procedure used to determine losses for the reach from below El Vado Dam to above Abiquiu Reservoir was applied to this reach. Isolating the losses for this reach is less reliable because of the uniform distribution of monthly diversions and substantial unmeasured tributary inflow. The assumed 50-percent return flow is for each Rio Chama main-stream section ditch. Therefore, the results of the regression analyses for the irrigation months (April through October) do not result in the expected pattern of seasonal losses, such as the results for the reach from below El Vado Dam to above Abiquiu Reservoir (see computed monthly loss coefficients for the reach from below Abiquiu Dam to near Chamita in **table 9**). The pattern of the results for winter (December through February) is the same as that for the reach from below El Vado Dam to above Abiquiu Reservoir, each month being -0.01 lower for the reach from below Abiquiu Dam to near Chamita, and the other non-irrigation months (November and March) being -0.02 lower (**graphs 27-38**). Because of assumptions made for the distribution of monthly diversion data and return flow and the substantial unmeasured tributary inflow, the adopted monthly loss coefficients for the reach from below Abiquiu Dam to near Chamita are based on adding -0.01 to the values for the reach from below El Vado Dam to above Abiquiu Reservoir. **Table 9** summarizes the computed and adopted loss coefficients for this reach.

Table 9. Correlations between routed flow and observed flow and adopted monthly loss coefficients for the reach of the Rio Chama from below Abiquiu Dam to near Chamita, 1973-96

Month	N (days)	Slope (y=0)	R^2	Computed loss coefficient	Adopted loss coefficient, below El Vado to above Abiquiu	Adopted loss coefficient
Jan	25	0.962	0.99	-0.04	-0.03	-0.04
Feb	34	0.956	0.99	-0.04	-0.03	-0.04
Mar	67	0.941	1.00	-0.06	-0.04	-0.05
Apr	9	0.917	0.99	-0.08	-0.04	-0.05
May	52	0.938	0.99	-0.06	-0.04	-0.05
June	200	0.958	0.99	-0.04	-0.05	-0.06
July	228	0.943	0.99	-0.06	-0.06	-0.07
Aug	138	0.939	0.99	-0.06	-0.05	-0.06
Sept	144	0.926	0.97	-0.07	-0.04	-0.05
Oct	61	0.952	0.99	-0.05	-0.04	-0.05
Nov	73	0.946	1.00	-0.05	-0.03	-0.04
Dec	72	0.969	0.99	-0.03	-0.02	-0.03

Rio Chama from near Chamita to Rio Grande Confluence

This reach of the Rio Chama is not modeled in RiverWare because it is very short (2.8 mi) and no gage is located at the confluence.

UPPER RIO GRANDE REACHES

The 132-mile reach of the Rio Grande between the Colorado-New Mexico State line and Cochiti Dam is divided into six reaches. The first reach begins at the gage Rio Grande near Lobatos, CO; the second at the gage near Cerro, NM; the third at the gage below Taos Junction Bridge; the fourth at the gage at Embudo; the fifth at the Rio Chama confluence; and the sixth at the gage at Otowi Bridge. The discontinued gages, Rio Grande above San Juan Pueblo and Rio Grande near Arroyo Hondo, were used to help estimate travel times and loss rates in the reaches in which the gages formerly operated.

Rio Grande Basin in Colorado

Streamflow and reservoir operation in the Rio Grande Basin above the gage Rio Grande near Lobatos, Colorado, are not modeled at this time. Discharge from the Rio Grande in Colorado will be represented by the discharge measured at the gaging station near Lobatos. In the future, the results from models developed by the State of Colorado's Rio Grande Decision Support System may be linked to URGWOM.

Rio Grande from near Lobatos to near Cerro

The stream gage near Lobatos, Colorado, located 6 mi above the Colorado/New Mexico State line, marks the location where the Rio Grande enters a canyon carved through basalt lava flows and gradually increases in depth to about 1200 ft at Embudo, about 70 mi south of the State line (**fig. 4**). The river channel in this reach is rocky and has little riparian vegetation. Costilla Creek is a major east-side tributary to the Rio Grande in this reach. Costilla Creek contributes very little

water to the Rio Grande because its waters are largely regulated and diverted for irrigation before they reach the Rio Grande. Costilla Creek discharges into the Rio Grande during years of very high runoff, but no stream gage is located near its mouth. It is incorporated with local inflows in the river routing of this reach.

Table 10 summarizes stream-gage and calibration data used in determining the power coefficient (wave velocity exponent) that is applied to average velocity measurements to determine river travel time lags in this reach (**graphs 39 and 40**).

Table 10. Summary of stream-gage and calibration data for the reach of the Rio Grande from near Lobatos, Colorado, to near Cerro, New Mexico

	Rio Grande near Lobatos	Rio Grande near Cerro	Total Δ
Period of analysis	5/8/85 – 8/4/87 10/2/90 – 6/1/99	8/26/69 – 6/25/98	
River mile (above mouth)	1719	1693	26
Elevation (feet above sea level)	7428	7110	318
Drainage area (square miles)	7700	8440	740
Number of measurements	323	290	
Wave velocity exponent (β)	0.7273	0.6976	
Coefficient of determination (R^2)	0.90	0.86	

Table 11 summarizes factors used to determine travel time lags in this reach (**graphs 41 and 42**).

Table 11. Adopted travel time lags (TL) for the reach of the Rio Grande from near Lobatos, Colorado, to near Cerro, New Mexico

			Time lag (hours) for indicated flow rate (cfs)						
Gage	TL vs. Q equation	R^2	50	200	500	750	1000	3000	6000
Lobatos	$TL = 74.73Q^{-0.2744}$	0.57	25	17	14	12	11	8	7
Cerro	$TL = 112.43Q^{-0.3}$	0.524	28	19	15	13	12	9	7
	Adopted travel times for reach→		27	18	14	13	12	9	7

Table 12 summarizes the adopted loss coefficients for this reach.

Table 12. Adopted monthly loss coefficients for the reach of the Rio Grande from near Lobatos, Colorado, to near Cerro, New Mexico, 1965-94[1]

Month	Adopted loss coefficient
Jan	-0.02
Feb	-0.03
Mar	-0.03
Apr	-0.05
May	-0.05
June	-0.04
July	-0.04
Aug	-0.04
Sept	-0.03
Oct	-0.03
Nov	-0.02
Dec	-0.03

[1]Based on data developed for the reach from near Arroyo Hondo to below Taos Junction Bridge, near Taos.

The records of discharge measurements at the gage near Lobatos were obtained from the Colorado State Engineer Office in Alamosa. Those for the gage near Cerro were obtained from the USGS New Mexico District Office in Albuquerque.

Rio Grande flow from near Lobatos, Colorado, to near Cerro, New Mexico, shows a substantial accretion. This gain in flow is discharge from the ground-water reservoir beneath the lava-capped plateau to the west, Colorado to the north, the Sunshine Valley to the east, and occasional surface water from Costilla Creek. The unmeasured gain in flow in this reach was great enough in most months to mask losses determined by routing the upstream flow down to the gage near Cerro and comparing this routed flow to the observed or recorded flow near Cerro. Except for the months of May, June, and July, applying the filtering criteria to calibrate losses resulted in an average 28 data points per month for an average of about 4 of the 30 years of flow that were routed. In addition, analysis of streamflow data shows a substantial change in the rate of gain between these two stations in 1987. Therefore loss rates developed for the reach of the Rio Grande between the gage Rio Grande near Arroyo Hondo and the gage Rio Grande below Taos Junction Bridge, near Taos were applied to this reach by adjusting the losses proportionally by the length of the two reaches. Flow of the Rio Grande in the reach from near Arroyo Hondo to below Taos Junction Bridge, near Taos is not significantly augmented by unmeasured flow accretions; thus, reasonable monthly loss rates were developed and applied to the reach from near Lobatos to near Cerro. Four outlying data points were removed from the dataset used to develop the wave velocity exponent for this reach.

Rio Grande from near Cerro to below Taos Junction Bridge, near Taos

In this reach the Rio Grande continues its descent into the basalt canyon, with very steep gradients of as much as 75 ft/mi between the Cerro gage and the mouth of Red River. The river channel is rocky, with no alluvial material in the bed or banks and a lack of riparian vegetation. Three major tributaries draining the Sangre de Cristo Mountains to the east enter the Rio Grande in this reach: Red River, Rio Hondo, and Rio Pueblo de Taos. Only the gages Red River below Fish Hatchery near Questa and Rio Pueblo de Taos below Los Cordovas are used in the river routing in this reach. The only gage on the Rio Hondo is 9 mi above its mouth and above all irrigation diversions; therefore, this tributary is modeled as a local inflow component.

Table 13 summarizes stream-gage and calibration data used in determining the power coefficient (wave velocity exponent) that is applied to average velocity measurements to determine river travel time lags in this reach (**graphs 40 and 43)**.

Table 13. Summary of stream-gage and calibration data for the reach of the Rio Grande from near Cerro to below Taos Junction Bridge, near Taos

	Rio Grande near Cerro	Rio Grande below Taos Junction Bridge, near Taos	Total Δ
Period of analysis	8/26/69 – 6/25/98	6/24/69 – 5/18/99	
River mile (above mouth)	1693	1658	35
Elevation (feet above sea level)	7110	6050	1060
Drainage area (square miles)	8440	9730	1290
Number of measurements	290	331	
Wave velocity exponent (β)	0.6976	0.5412	
Coefficient of determination (R^2)	0.86	0.80	

Table 14 summarizes factors used to determine travel time lags in this reach. The stream gage Rio Grande near Arroyo Hondo, which was discontinued in 1996, is included to help define travel time lags for this reach (**graphs 44-46).**

Table 14. Adopted travel time lags (TL) for the reach of the Rio Grande from near Cerro to below Taos Junction Bridge, near Taos

			Time lag (hours) for indicated flow rate (cfs)						
Gage	TL vs. Q equation	R^2	50	200	500	750	1000	3000	6000
Cerro	$TL = 151.35Q^{-0.3}$	0.524	38	26	20	18	17	12	10
Arroyo Hondo	$TL = 266.77Q^{-0.5108}$	0.969	36	18	11	9	8	4	3
Taos	$TL = 186.81Q^{-0.4607}$	0.738	31	16	11	9	8	5	3
	Adopted travel times for reach→		35	21	15	13	12	8	7

The adopted travel times for this reach are weighted more heavily toward the travel times developed using data for the Arroyo Hondo and Taos gages. Velocity data for the Cerro gage are not representative of the entire Cerro to Taos reach because the channel gradient (and hence, velocity) of the Rio Grande increases just downstream from the Cerro gage. Data indicate that a minimum lag time of 4 hours should be used for this reach.

Table 15 summarizes the adopted loss coefficients for this reach.

Table 15. Adopted monthly loss coefficients for the reach of the Rio Grande from near Cerro to below Taos Junction Bridge, near Taos, 1965-94[1]

Month	Adopted loss coefficient
Jan	-0.02
Feb	-0.04
Mar	-0.04
Apr	-0.07
May	-0.07
June	-0.05
July	-0.05
Aug	-0.05
Sept	-0.04
Oct	-0.04
Nov	-0.03
Dec	-0.04

[1]Based on data developed for the reach from near Arroyo Hondo to below Taos Junction Bridge, near Taos.

Substantial accretions of flow to the Rio Grande continue in this reach, as visibly evidenced by Big Arsenic and Little Arsenic Springs discharging directly into the Rio Grande and springs discharging into the lower Red River. The unmeasured gain in flow was great enough to mask any losses in the reach determined by routing the lagged upstream flow down to the Taos gage and comparing this flow with observed flow at the Taos gage. As a result, the filtered data generated for this reach were insufficient for developing reliable monthly loss relations. Therefore, as in the upstream reach, loss rates developed for the reach of the Rio Grande between the gages Rio Grande near Arroyo Hondo and Rio Grande below Taos Junction Bridge, near Taos were applied to this reach. The Arroyo Hondo to Taos reach, which is a subreach of the Cerro to Taos reach, does not have significant unmeasured flow accretion; reasonable monthly loss rates were developed and prorated by the difference in length between the two reaches.

Rio Grande from near Arroyo Hondo to below Taos Junction Bridge, near Taos

This reach, located within the Cerro to Taos reach, is not in the model (streamflow measurements at the gage Rio Grande near Arroyo Hondo were discontinued in 1996) and is presented here only because it was used to develop river-channel loss rates for the reaches near Lobatos to near Cerro and near Cerro to below Taos Junction Bridge, near Taos. The gage Rio Pueblo de Taos below Los Cordovas is used in the river routing in this reach.

Table 16 summarizes stream-gage and calibration data used in determining the power coefficient (wave velocity exponent) that is applied to average velocity measurements to determine river travel time lags in this reach (**graphs 43 and 47**).

Table 16. Summary of stream-gage and calibration data for the reach of the Rio Grande from near Arroyo Hondo to below Taos Junction Bridge, near Taos

	Rio Grande near Arroyo Hondo	Rio Grande below Taos Junction Bridge	Total Δ
Period of analysis	11/12/69 – 10/9/96	6/24/69 – 5/18/99	
River mile (above mouth)	1677	1658	19
Elevation (feet above sea level)	6470	6050	420
Drainage area (square miles)	8760	9730	970
Number of measurements	315	331	
Wave velocity exponent (β)	0.4889	0.5412	
Coefficient of determination (R^2)	0.97	0.80	

Table 17 summarizes factors used to determine travel time lags in this reach (**graphs 48 and 49**).

Table 17. Adopted travel time lags (TL) for the reach of the Rio Grande from near Arroyo Hondo to below Taos Junction Bridge, near Taos

			Time lag (hours) for indicated flow rate (cfs)						
Gage	TL vs. Q equation	R^2	50	200	500	750	1000	3000	6000
Arroyo Hondo	$TL = 150.16Q^{-0.5108}$	0.969	20	10	6	5	4	3	2
Taos	$TL = 101.41Q^{-0.4607}$	0.738	17	9	6	5	4	3	2
	Adopted travel times for reach→		19	9	6	5	4	4	4

Table 18 summarizes the adopted loss coefficients for this reach. See **graphs 50-61** for plots of observed flow versus routed flow, filtered for losses, and regression analysis for this reach.

Table 18. Correlations between routed flow and observed flow and adopted monthly loss coefficients for the reach of the Rio Grande from near Arroyo Hondo to below Taos Junction Bridge, near Taos, 1965-94

Month	n (days)	Slope (y=0)	R^2	Adopted loss coefficient
Jan	60	0.9871	0.99	-0.01
Feb	63	0.9779	1.00	-0.02
Mar	216	0.9779	1.00	-0.02
Apr	187	0.9629	0.99	-0.04
May	167	0.9621	1.00	-0.04
June	166	0.9709	1.00	-0.03
July	116	0.9726	1.00	-0.03
Aug	95	0.9710	1.00	-0.03
Sept	101	0.9805	1.00	-0.02
Oct	54	0.9807	1.00	-0.02
Nov	100	0.9827	1.00	-0.02
Dec	102	0.9784	0.99	-0.02

Data indicate that at high flows (greater than 5000 cfs), the plot of travel time versus discharge approaches 4 hours asymptotically. Therefore, a minimum travel time of 4 hours will be used.

Plots of data for the gage Rio Grande below Taos Junction Bridge, near Taos reveal a cluster of data points segregated from the other data and located above the line of best fit (**graph 43**). These data points are based on data collected during a short period of time prior to and immediately following 1982. This segregation of data points likely results in part from the use of multiple locations of cross sections, depending on the level of discharge, measured by the USGS. One measurement section used during low flows is controlled by a riffle section, which can change depending on the movement of sediment from the Rio Pueblo de Taos through the control section. Another section with different control is waded to measure flows less than 1000 cfs, and the cableway at a third location is used to measure flows in excess of 1000 cfs.

Rio Grande from below Taos Junction Bridge, near Taos to Embudo

In this reach, the Rio Grande enters the deepest portion of the gorge, and the river channel begins to widen. Alluvial deposits compose the bed and banks of the river here with the first appearance of any significant riparian vegetation. About 200 acres of irrigable land are served by direct diversion from the Rio Grande in the vicinity of Pilar and Rinconada. Embudo Creek is the major tributary in this reach, entering the Rio Grande about 3 mi above the Rio Grande at Embudo gage. The Embudo Creek at Dixon gage measures the discharge of Embudo Creek into the Rio Grande and is included in the river routing for this reach.

Table 19 summarizes stream-gage and calibration data used in determining the power coefficient (wave velocity exponent) that is applied to average velocity measurements to determine river travel time lags in this reach (**graphs 43 and 62**).

Table 19. Stream-gage and calibration data for the reach of the Rio Grande from below Taos Junction Bridge, near Taos to Embudo

	Rio Grande below Taos Junction Bridge, near Taos	Rio Grande at Embudo	Total Δ
Period of analysis	6/24/69 – 5/18/99	7/25/69 – 6/2/98	
River mile (above mouth)	1658	1643.1	14.9
Elevation (feet above sea level)	6050	5789	261
Drainage area (square miles)	9730	10,400	670
Number of measurements	331	342	
Wave velocity exponent (β)	0.5412	0.593	
Coefficient of determination (R^2)	0.80	0.87	

Table 20 summarizes factors used to determine travel time lags in this reach (**graphs 63 and 64**).

Table 20. Adopted travel time lags (TL) for the reach of the Rio Grande from below Taos Junction Bridge, near Taos to Embudo

			Time lag (hours) for indicated flow rate (cfs)						
Gage	TL vs. Q equation	R^2	50	200	500	750	1000	3000	6000
Taos	$TL = 80.1Q^{-0.4607}$	0.738	13	7	5	4	3	2	1
Embudo	$TL = 66.1Q^{-0.4078}$	0.750	13	8	5	4	4	3	2
Adopted travel times for reach→			13	7	5	4	4	2	2

Table 21 summarizes the adopted loss coefficients for this reach (**graphs 65-76**).

Table 21. Correlations between routed flow and observed flow and adopted monthly loss coefficients for the reach of the Rio Grande from below Taos Junction Bridge, near Taos to Embudo, 1962-96

Month	n (days)	Slope (y=0)	R^2	Adopted loss coefficient
Jan	470	0.9771	0.99	-0.02
Feb	401	0.9764	1.00	-0.02
Mar	437	0.9777	1.00	-0.02
Apr	458	0.9706	1.00	-0.03
May	606	0.9625	1.00	-0.04
June	596	0.9646	1.00	-0.04
July	592	0.9617	1.00	-0.04
Aug	508	0.9637	1.00	-0.04
Sept	471	0.9672	1.00	-0.03
Oct	497	0.972	1.00	-0.03
Nov	496	0.9735	1.00	-0.03
Dec	443	0.9701	0.99	-0.03

Rio Grande from Embudo to Rio Chama Confluence

The 13-mi reach of the Rio Grande between the stream gage at Embudo and the site of the discontinued stream gage above San Juan Pueblo was used to determine time lags and loss relations for the 15-mi reach from Embudo to the Rio Chama confluence. Because the gage above San Juan Pueblo was discontinued in 1987, it is not used in the model to route flow or to

compute local inflow. Approximately 5000 acres of irrigable land in this reach are served by direct diversion from the Rio Grande.

Table 22 summarizes stream-gage and calibration data used in determining the power coefficient (wave velocity exponent) that is applied to average velocity measurements to determine river travel time lags in this reach (**graphs 62 and 77**).

Table 22. Stream-gage and calibration data for the reach of the Rio Grande from Embudo to above San Juan Pueblo

	Embudo	Above San Juan Pueblo	Total Δ
Period of analysis	7/25/69 – 6/2/98	6/4/69 – 10/20/87	
River mile (above mouth)	1643.1	1630.1	13
Elevation (feet above sea level)	5789	5630	159
Drainage area (square miles)	10,400	10,550	150
Number of measurements	344	239	
Wave velocity exponent (β)	0.593	0.5796	
Coefficient of determination (R^2)	0.87	0.95	

Table 23 summarizes factors used to determine travel time lags in this reach (**graphs 78 and 79**).

Table 23. Adopted travel time lags (TL) for the reach of the Rio Grande from Embudo to above San Juan Pueblo

			Time lag (hours) for indicated flow rate (cfs)						
Gage	TL vs. Q equation	R^2	50	200	500	750	1000	3000	6000
Embudo	$TL = 65.97Q^{-0.405}$	0.724	14	8	5	5	4	3	2
San Juan	$TL = 69.75Q^{-0.425}$	0.919	13	7	5	4	4	2	2
Adopted travel times for reach→			13	8	5	4	4	2	2

Table 24 summarizes the adopted loss coefficients for this reach (**graphs 80-91**).

Table 24. Correlations between routed flow and observed flow and adopted monthly loss coefficients for the reach of the Rio Grande from Embudo to above San Juan Pueblo, 1976-86

Month	n (days)	Slope (y=0)	R^2	Adopted loss coefficient[1]
Jan	176	0.967	0.98	-0.03
Feb	174	0.967	0.99	-0.03
Mar	180	0.951	0.99	-0.05
Apr	260	0.942	1.00	-0.06
May	294	0.928	0.99	-0.07
June	279	0.920	0.99	-0.08
July	289	0.891	0.99	-0.11
Aug	328	0.921	0.98	-0.08
Sept	312	0.917	0.97	-0.08
Oct	225	0.945	0.99	-0.06
Nov	185	0.942	1.00	-0.06
Dec	201	0.965	0.99	-0.04

[1]Includes losses from irrigation diversions.

Rio Chama / Rio Grande Confluence to Rio Grande at Otowi Bridge

The Rio Chama enters the Rio Grande 14 mi above Otowi Bridge. In this reach, the Rio Grande continues to flow through the alluvium of the Española Valley. Water is diverted to serve a small area of irrigable land on the west side of the river. Santa Clara Creek, Santa Cruz River, and Pojoaque Creek discharge to the Rio Grande in this reach, but are not represented in the model, except as a component of local inflow.

Table 25 summarizes stream-gage and calibration data used in determining the power coefficient (wave velocity exponent) that is applied to average velocity measurements to determine river travel time lags in this reach (**graphs 77 and 92**). Data for the reach from above San Juan Pueblo to Otowi Bridge can be representative of the Rio Chama confluence to Otowi Bridge reach without any significant loss in reliability.

Table 25. Summary of stream-gage and calibration data for the reach of the Rio Grande from above San Juan Pueblo to Otowi Bridge

	Above San Juan Pueblo	Otowi Bridge	Total Δ
Period of analysis	6/4/69 – 10/20/87	7/2/69 – 7/9/98	
River mile (above mouth)	1630.1	1614.2	15.9
Elevation (feet above sea level)	5630	5488.9	141.1
Drainage area (square miles)	5630	14,300	8670
Number of measurements	239	596	
Wave velocity exponent (β)	0.5796	0.663	
Coefficient of determination R^2)	0.95	0.91	

Table 26 summarizes factors used to determine travel time lags in this reach (**graphs 93 and 94**).

Table 26. Adopted travel time lags (TL) for the reach of the Rio Grande from Rio Chama confluence to Otowi Bridge

			Time lag (hours) for indicated flow rate (cfs)						
Gage	TL vs. Q equation	R^2	50	200	500	750	1000	3000	6000
Above San Juan Pueblo	$TL = 47.24Q^{-0.420}$	0.917	9	5	3	3	3	2	1
Otowi Bridge	$TL = 35.03Q^{-0.338}$	0.716	9	6	4	4	3	2	2
	Adopted travel times for reach→		9	5	4	3	3	2	2

Table 27 summarizes the adopted loss coefficients for this reach.

Table 27. Correlations between routed flow and observed flow and adopted monthly loss coefficients for the reach of the Rio Grande from Rio Chama confluence to Otowi Bridge

Month	n (days)	Slope (y=0)	R^2	Adopted loss coefficient
Jan	12	0.727	0.98	-0.03
Feb	27	0.981	0.99	-0.03
Mar	8	0.984	1.00	-0.05
Apr	28	0.967	1.00	-0.06
May	48	0.973	0.96	-0.07
June	79	0.978	1.00	-0.08
July	42	0.974	1.00	-0.11
Aug	15	0.967	0.99	-0.08
Sept	13	0.978	1.00	-0.08
Oct	16	0.968	1.00	-0.06
Nov	4	0.997	1.00	-0.06
Dec	5	0.970	0.98	-0.04

Flow-loss analysis of this reach was inconclusive because of a large variation in percentage of flow loss and a lack of sufficient data for some months. Because the data cannot be used to produce monthly loss rates that demonstrate a reasonable loss pattern, the losses developed for the reach from Embudo to above San Juan Pueblo were applied to this reach. Application of these loss rates is appropriate because of the similarities of the two reaches. The two reaches combined constitute the Española Valley, a broad alluvial valley where land use comprises mainly riparian vegetation and irrigated agriculture.

Within this reach two tributaries, in addition to the Rio Chama and the Pojoaque/Nambe, join the Rio Grande and allow inflow to the Rio Grande. At present no effective way is available to estimate inflow from Santa Clara Creek, so the confluence becomes a placeholder. The Santa Cruz River is also represented in the model but has no current source for real-time data. Because the upstream gage at Cundiyo is above the Santa Cruz Dam and the gage at Riverside was discontinued in 1951, there is no meaningful relation between the Cundiyo gage and inflow to the Rio Grande. Flows from Nambe Dam will be modeled in the future. Wastewater-treatment plant inflow from Española to the reach is represented.

Rio Grande from Otowi Bridge to Cochiti

Although this reach is 27 mi long, it is considered to be 22 mi for computing time lag and loss because the reservoir above the dam is about 5 mi long at the permanent pool elevation of 5335.92 ft (U.S. Army Corps of Engineers, 1990, 1996a). The model for this reach includes the gages Rio Grande at Otowi Bridge and Rio Grande at Cochiti, which are used to determine gain-loss relations. Although Santa Fe River data are not available for this reach for calibration within the selected time period (1926-70), this tributary will be represented in the model.

The gage Rio Grande at Cochiti was discontinued in 1970 at the closing of Cochiti Dam. The period of record from 1926 to 1970, for which data are available for the Otowi Bridge gage, was used for routing calibration of this reach. No measurement data since 1970 are available for the downstream end of this reach at Cochiti Reservoir. Time lags between the Otowi Bridge and the old Cochiti gages were established using USGS discharge-measurement data for only the Otowi Bridge gage.

Table 28 summarizes stream-gage and calibration data used in determining the power coefficient (wave velocity exponent) that is applied to average velocity measurements to determine river travel time lags in this reach (**graph 92**)**.** Because data for the gage Rio Grande at Cochiti are not available, travel time lags for this reach will be based solely on the gage at Otowi Bridge.

Table 28. Summary of stream-gage and calibration data for the reach of the Rio Grande from Otowi Bridge to Cochiti

	Otowi Bridge	Cochiti	Total Δ
Period of analysis	7/2/69 – 7/9/98	n/a	
River mile (above mouth)	1614.2	1587	27.2
Elevation (feet above sea level)	5489	5225	264
Drainage area (square miles)	14,300	14,600	300
Number of measurements	596	290	
Wave velocity exponent (β)	0.663	n/a	
Coefficient of determination (R^2)	0.91	n/a	

Table 29 summarizes factors used to determine travel time lags in this reach (**graph 95**).

Table 29. Adopted travel time lags (TL) for the reach of the Rio Grande from Otowi Bridge to Cochiti

			Time lag (hours) for indicated flow rate (cfs)						
Gage	TL vs. Q equation	R^2	50	200	500	750	1000	3000	6000
Otowi Bridge	$TL = 99.99Q^{-0.4006}$	0.894	21	12	8	7	6	4	3
	Adopted travel times for reach→		21	12	8	7	6	4	3

Table 30 summarizes the monthly loss coefficients for this reach.

Table 30. Correlations between routed flow and observed flow and adopted monthly loss coefficients for the reach of the Rio Grande from Otowi Bridge to Cochiti

Month	n (days)	Slope (y=0)	R^2	Adopted loss coefficient
Jan	374	0.934	0.94	-0.03
Feb	428	0.945	0.98	-0.03
Mar	931	0.913	0.98	-0.04
Apr	1016	0.926	0.99	-0.04
May	999	0.943	0.99	-0.04
June	1013	0.947	0.99	-0.05
July	1096	0.916	0.98	-0.06
Aug	1082	0.874	0.97	-0.05
Sept	1157	0.864	0.98	-0.04
Oct	1203	0.857	0.96	-0.04
Nov	574	0.928	0.98	-0.03
Dec	400	0.955	0.99	-0.02

Analyzing flow loss for this reach was complicated because flows to the Sili and East Side Main Canals were diverted above the old Cochiti gage. Losses computed using the routed flow from Otowi Bridge and the gaged flow at Cochiti includes canal diversions. Diversion data for 1926 to 1970 are not available, but data after 1970 are available. Diversions before and after 1970 should be about the same because 6,000 acres were irrigated before and after 1970 (U.S. Geological Survey, 1964; Ortiz and others, 1998). Average daily diversions were determined by month, using data from 1970 to 1997, and were added to each daily flow at the old Cochiti gage from 1926 to 1970. The gaged flow at the old Cochiti gage and the routed flow from Otowi Bridge were filtered, so the dataset contained only days of losses in the reach. January, February, November, and

December were the only months having numerous days with losses. Average daily diversions for these months are near zero, so the gaged flow at Cochiti was not adjusted significantly. May, June, and July each had fewer than 7 days of flow losses in the reach for the complete 1926-70 dataset. Data analysis for these months showed losses near 0. The small losses do not seem appropriate and probably are a result of adding the average daily canal diversions to actual daily flows at the old Cochiti gage. In the absence of daily diversion data prior to 1970 and no loss estimates for the reach during the irrigation season, loss rates developed for the Rio Chama reach from below El Vado Dam to above Abiquiu Reservoir were applied. Applying these loss rates is reasonable because both reaches are in canyon sections that have little or no riparian vegetation. Loss rates for the below El Vado Dam to above Abiquiu Reservoir reach demonstrate a reasonable seasonal loss pattern, which is expected in the Otowi Bridge to Cochiti reach where losses are predominantly from evaporation.

PHYSICAL MODEL VALIDATION

The purpose of the validation process is to describe and evaluate the difference between modeled flows and historical flows. The process used to validate reaches of the Rio Grande above Otowi is described here. Unmeasured tributary inflow to these reaches is significant particularly because of local snowmelt runoff, and validation of these reaches involves estimating unmeasured inflow or local inflow.

Determining the amount of streamflow reaching the downstream point of each reach involves the application of the variable time lag method of routing streamflow through the reach, previously described in this document (**see page 5**). Monthly loss coefficients are developed also using procedures previously described (**see page 8**). A routed-with-losses hydrograph is then created using monthly regression coefficients for the overall routed hydrograph.

Local inflow, which represents the gains or losses within the reach, is determined by subtracting the routed-with-losses flow from the downstream-observed or recorded flow (exact local inflow). With the assumption of proper modeling techniques and accurate stream gaging, the routed-with-losses hydrograph should be contained within the observed hydrograph, and the difference between the two is an estimate of local inflow between the upstream and downstream stream gages. The resulting accepted local inflow dataset is intended for use as input in the planning and water operations models. The following items are represented in local inflow that could not otherwise be accounted for:

- Ungaged diversions and return flows;
- Precipitation;
- Ungaged tributary inflow;
- Streamflow measurement errors;
- Modeling errors; and
- Ground-water interaction.

For many of the reaches above Otowi, the tributary-inflow component of local inflow is significant, most of it a result of snowmelt runoff from the mountains in northern New Mexico. To validate reaches in the Upper Rio Grande above Otowi, a method to estimate values of local inflow is required that minimizes the difference between routed flow and recorded flow. The following alternatives were considered for estimating the local inflow component of routed flow:

- No local inflow component;
- Smoothed local inflow (use 7-day moving average of exact local inflow);
- Development of regression relating local inflow values to nearby measured tributary inflow; and
- Closest 5-year average volume to forecast volume (average of nearest 5 years of local inflow generated in forecast model).

Here, the sum of the local inflow estimates at all seven reaches above Otowi are accumulated and presented as a total at Otowi.

Validation

Reaches above Cochiti were validated using each of the above four methods to estimate values of local inflow to be added to the routed hydrograph for January 1, 1998, through September 30, 1999. **Figure 5** summarizes the differences between modeled and historical flows for the four alternatives for 1998 and 1999. Plots of the routed hydrographs using local inflow estimated by the four alternatives and historical hydrographs are plotted in **figures 6-9** below.

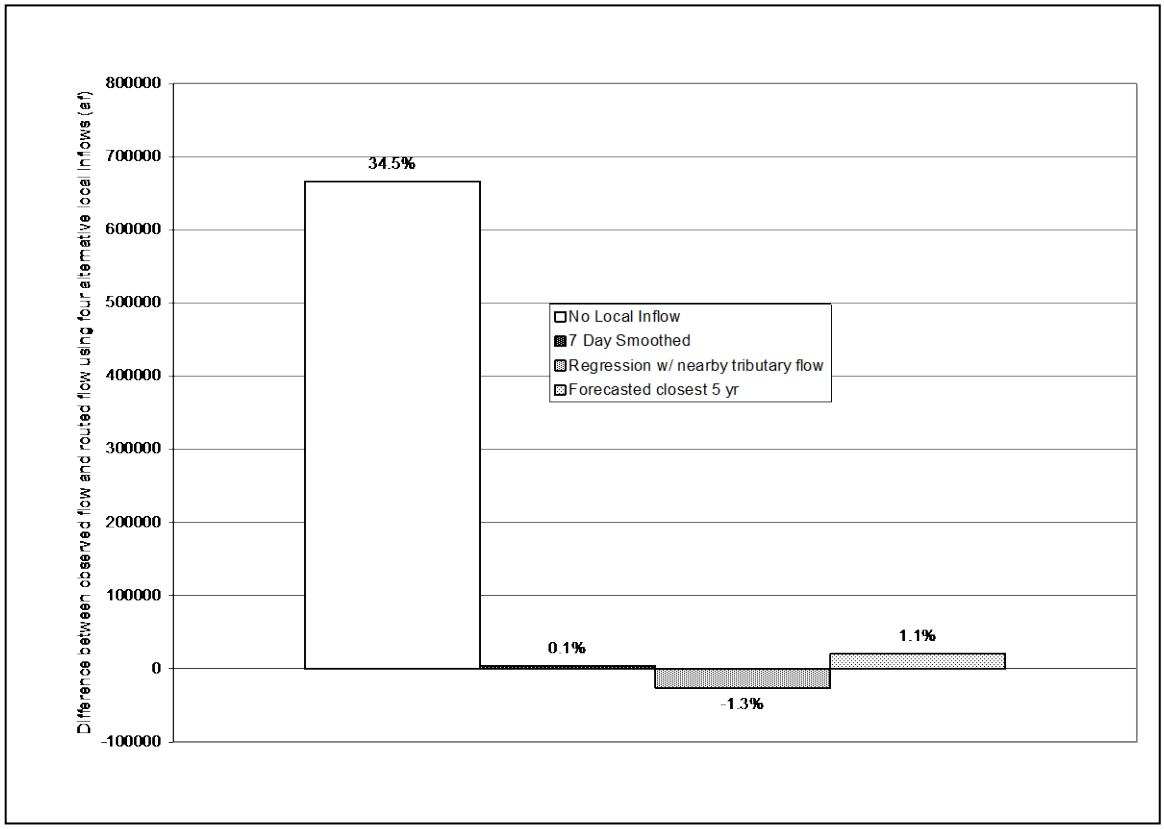

Figure 5. Summary and comparison of alternatives for estimating local inflow, 1998-99.

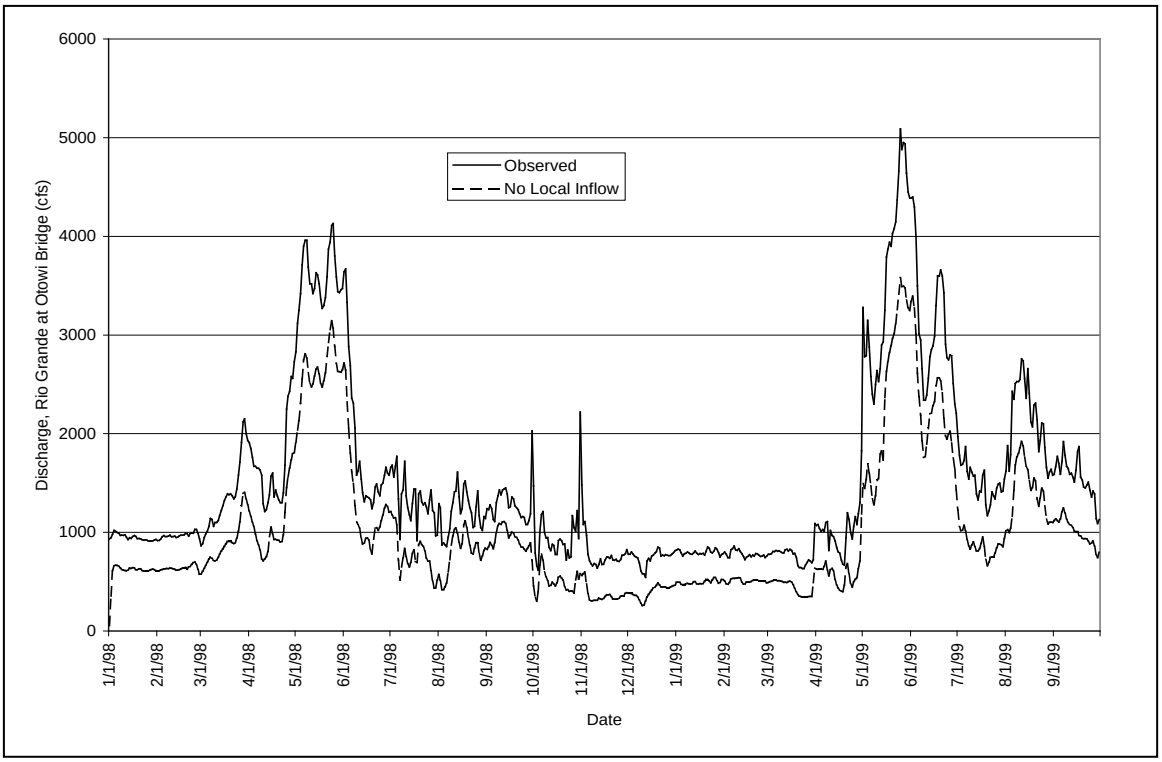

Figure 6. Hydrographs of observed flow and routed flow without local inflow.

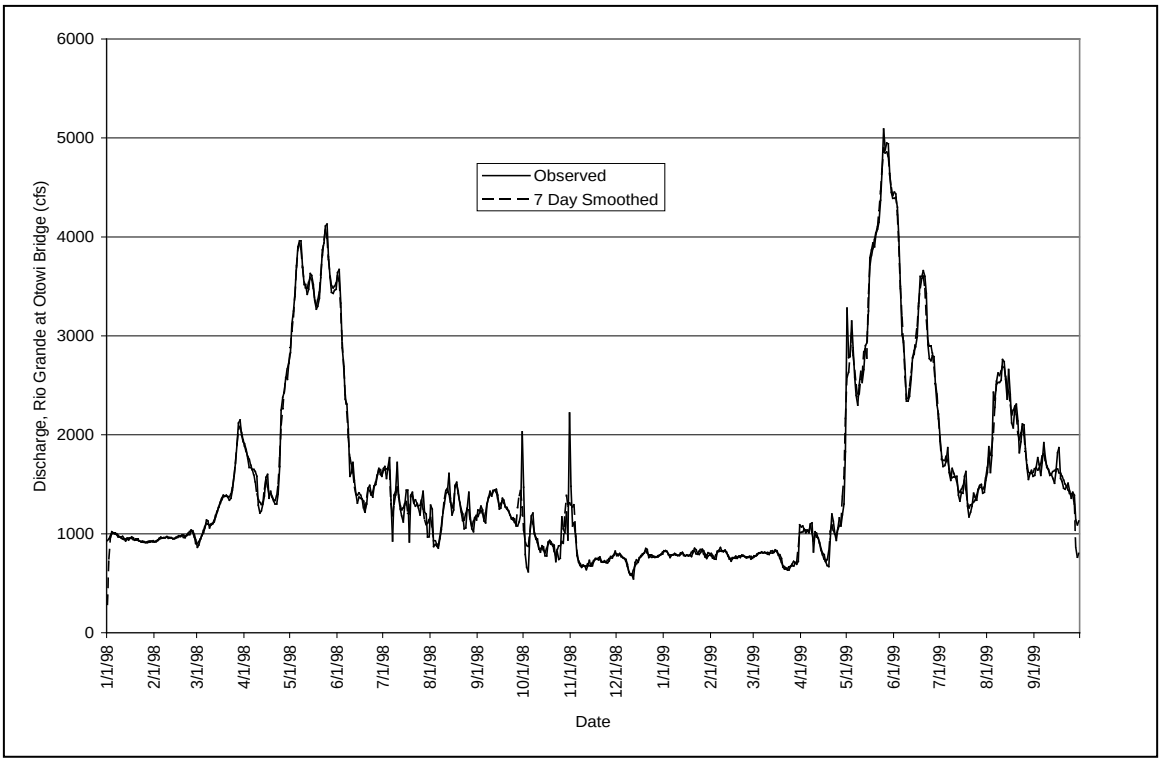

Figure 7. Hydrographs of observed flow and routed flow using local inflow determined by seven-day moving average.

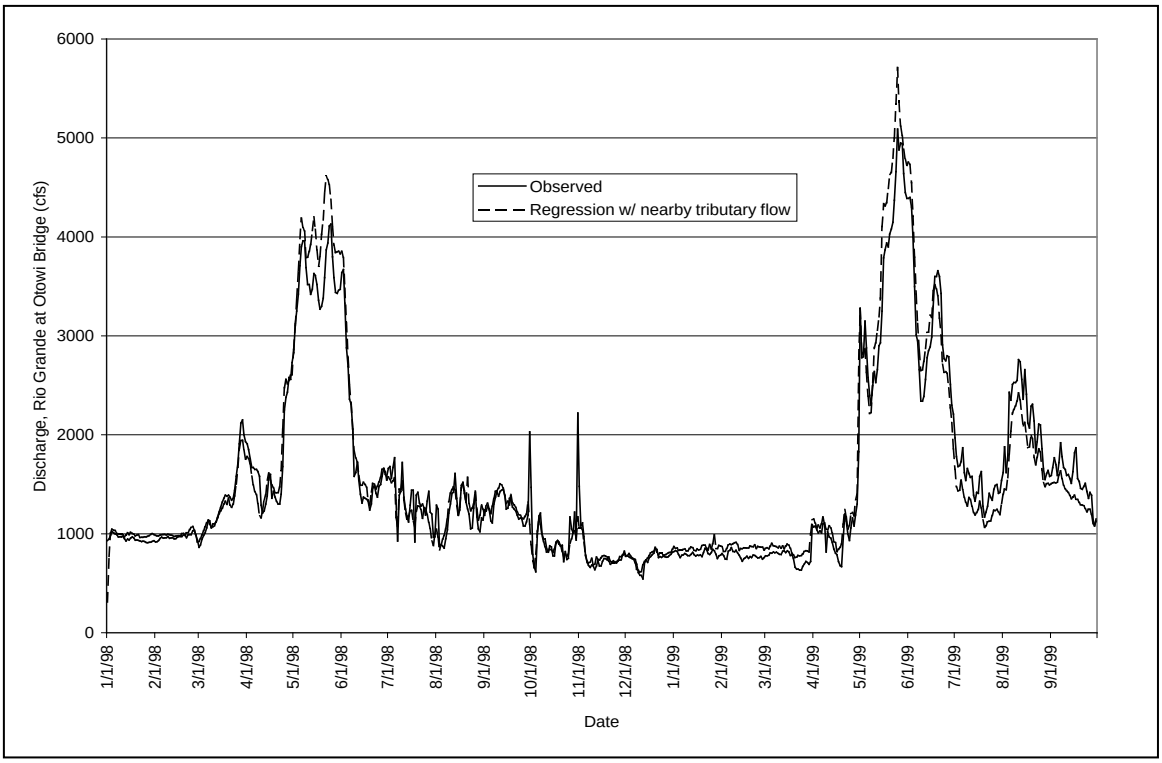

Figure 8. Hydrographs of observed flow and routed flow using local inflow determined by correlation with local tributary.

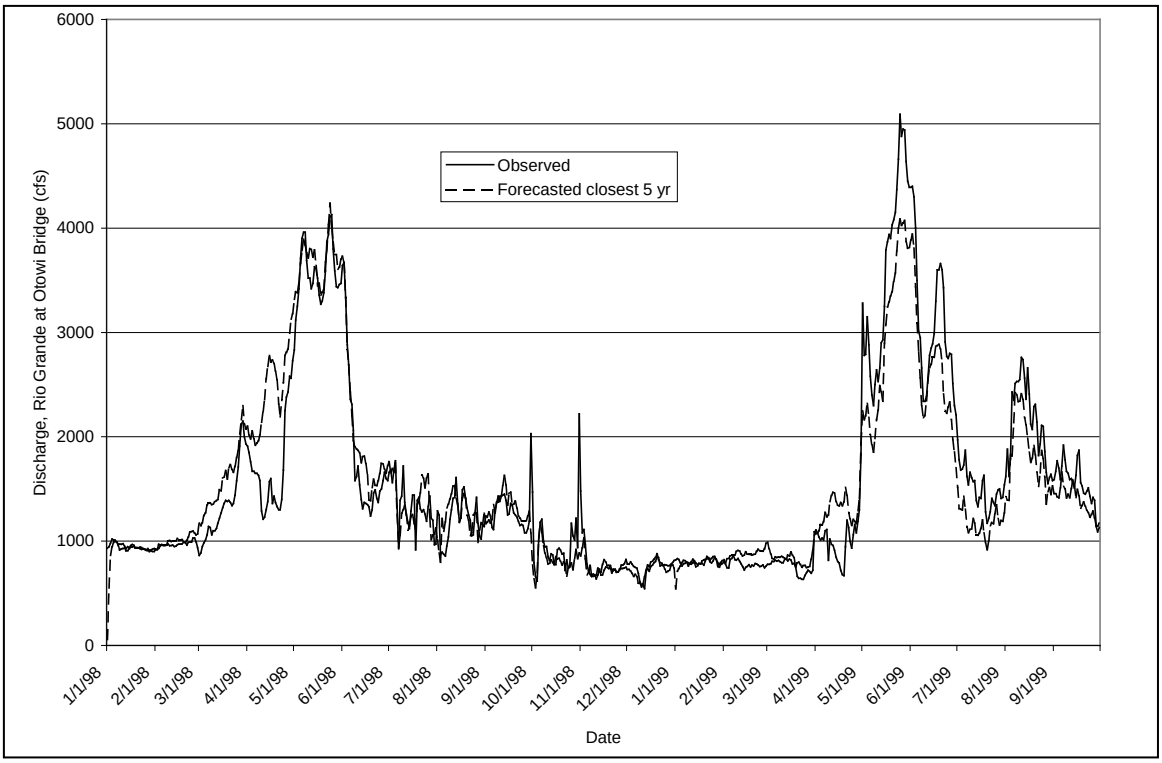

Figure 9. Hydrographs of observed flow and routed flow using local inflow determined by average of nearest five years.

Conclusion

Local inflow is an important calibration component for reaches above Cochiti Dam where snowmelt is a significant component of local inflow. Results of the validation runs appear to be good when estimates of local inflow are included. The smoothed local inflow method, which uses a 7-day moving average, appears to be most suitable for use in the planning and water operations models. Use of this method may result in negative local inflows and reductions in peak flows; however, this method preserves the volume of exact local inflow.

Local inflow developed using a regression describing the relation between computed local inflow to a reach and measured tributary inflow nearby the reach would be beneficial for application in the operations model or planning model. No reliable regressions have been identified as yet for reaches above Otowi.

RESERVOIRS ON THE RIO CHAMA

DESCRIPTION OF PHYSICAL PROPERTIES

Three reservoirs–Heron, El Vado, and Abiquiu–were constructed on the Rio Chama and its tributaries to store water for flood control and water supply. Hydroelectric power plants are located at El Vado Dam and Abiquiu Dam, which are operated as “run-of-the-river” plants–that is, the demand for release for hydroelectric power at these dams is subservient to other demands. **Table 31** summarizes general information about these dams.

Table 31. General information about dams in the Rio Chama Basin

	Heron	El Vado	Abiquiu
Type:	Earth fill	Earth fill	Earth fill
Year completed:	1971	1935	1963
Structural height (feet):	269	230	341
Top width (feet):	40	20	30
Width at base (feet):	1500	642	2000
Dam crest length (feet):	1220	1326	1800
Dam crest elevation (feet above sea level):	7199	6914.5	6381
Outlet works discharge capacity (cfs):	510	6890	8200

Heron Reservoir

Heron Reservoir stores and releases water imported from the San Juan River Basin and is the primary storage feature of the San Juan-Chama Project. Owned and operated by the USBR, Heron Reservoir’s entire capacity of about 401,300 acre-feet (acre-ft) is dedicated to storing San Juan-Chama Project water. All native Rio Grande inflow to Heron Reservoir is bypassed. The water imported to the Rio Grande Basin from the San Juan River Basin provides supplemental water supplies for various communities and irrigation districts. The project also provides fish, wildlife, and recreational benefits from the storage and movement of this water. An average of 91,210 acre-ft per year of the firm yield is allocated annually by contract or project authorization; the remaining 4990 acre-ft is as yet uncontracted. **Table 32** lists elevation information about Heron Reservoir.

Table 32. Elevation-related information about Heron Reservoir

	Elevation (feet)	Area (acres)	Capacity (acre-feet)
Top of dam:	7199.00	--	--
Maximum pool:	7190.80	6148	429,657
Total storage at spillway crest:	7186.10	5905	401,334
Top of dead pool:	7003.00	106	1218

El Vado Reservoir

El Vado Dam was constructed to provide conservation storage for irrigation purposes on Middle Rio Grande Conservancy District (MRGCD) lands along the Rio Grande between Cochiti and Bosque del Apache National Wildlife Refuge. Operated by the USBR, the reservoir is used to store San Juan-Chama and native water for use by the MRGCD and associated subcontractors. **Table 33** lists elevation information about El Vado Reservoir.

Table 33. Elevation-related information about El Vado Reservoir

	Elevation (feet)	Area (acres)	Capacity (acre-feet)
Top of dam:	6914.50	--	--
Maximum pool:	6908.00	--	--
Total active conservation storage:	6902.00	3232	186,252
Total storage at spillway crest:	6879.00	2454	120,544
Top of dead pool:	6775.00	84	480

Abiquiu Reservoir

Abiquiu Dam and Reservoir is operated by the Corps for flood and sediment control in accordance with conditions and limitations stipulated in the Flood Control Act of 1960 (Public Law 86-645). Reservoir regulation for flood control is also coordinated with the operation of Jemez Canyon Reservoir, Cochiti Lake, and Galisteo Reservoir **(figs. 4 and 10**). Abiquiu Reservoir is operated to limit flow in the Rio Chama, to the extent possible, to downstream channel capacities of 1800 cfs for the reach below Abiquiu Dam, 3000 cfs for the reach below the confluence with the Rio Ojo Caliente, and 10,000 cfs through the Española Valley on the Rio Grande main stem. Irrigation releases from El Vado Reservoir pass through Abiquiu Reservoir. Typically, Rio Grande water is stored in Abiquiu Reservoir in April and May, during the peak of snowmelt runoff, and released in June and early July. Any storage remaining in the reservoir after natural flow at the Otowi Bridge gage drops below 1500 cfs is carried over or stored until after November 1, when it may then be released. In 1981, Congress authorized the use of Abiquiu Reservoir to store as much as 200,000 acre-ft of San Juan-Chama Project water. The San Juan-Chama Project water allocated to the City of Albuquerque and other entities is stored in the unused sediment space and a small portion of the flood-control space. **Table 34** lists elevation information about Abiquiu Reservoir.

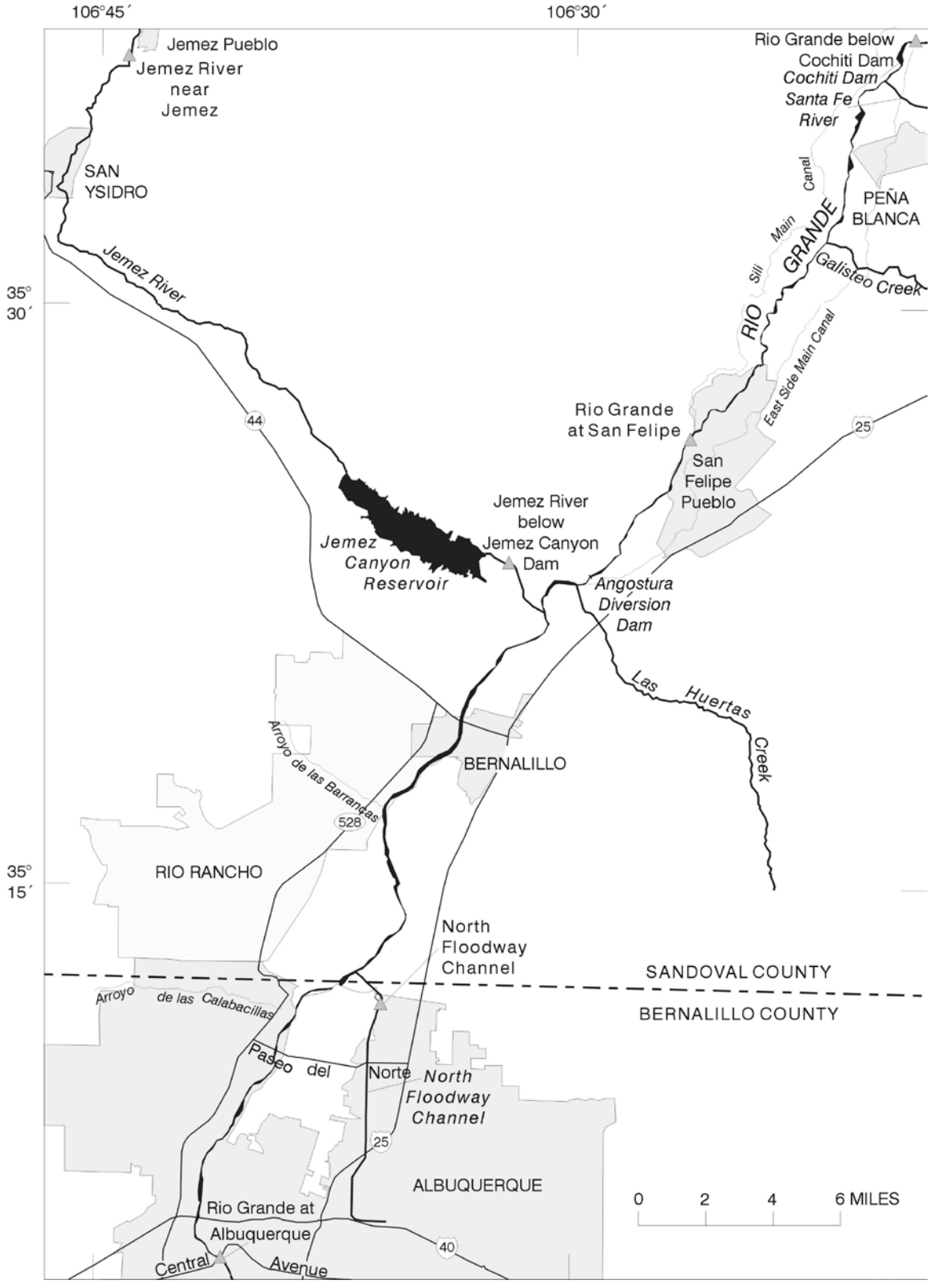

Figure 10. Rio Grande from Cochiti to Albuquerque.

Table 34. Elevation-related information about Abiquiu Reservoir

	Elevation (feet)	Area (acres)	Capacity (acre-feet)
Top of dam:	6381.00	--	--
Maximum pool:	6374.70	--	--
Total storage at spillway crest:	6350.00	--	--
Top of flood-control pool:	6283.50	7439	545,783
Top of San Juan-Chama storage:	6220.00	4029	183,882
Top of dead pool:	6077.00	--	--

MATHEMATICAL DESCRIPTION OF RIO CHAMA RESERVOIR CALCULATIONS

All three Rio Chama Basin reservoirs follow the general mass-balance equation for reservoirs:

$$S_t - S_{t-1} - I - \mathrm{Pt} + E_t + O = 0$$

where:
S_t = total storage today, in acre-ft;
S_{t-1} = total storage yesterday, in acre-ft;
I = inflow into the reservoir, in acre-ft/day;
P_t = physical model precipitation, in acre-ft/day;
E_t = physical model evaporation, in acre-ft/day; and
O = outflow from the reservoir, in acre-ft/day.

Physical model precipitation is determined by using the equation:

$$P_t = R_t(A_{res})/12$$

where:
R_t = rainfall, in inches/day; and
A_{res} = average reservoir area, in acres.

Physical model evaporation is determined by using one of two equations, depending on the time of year. The summer equation is:

$$E_t = E_p(coeff)(A_{res})/12$$

where:
E_p = pan evaporation, in inches per day; and
coeff = pan evaporation coefficient (0.7 for reservoirs in the Rio Grande Basin).

The winter equation is:

$$E_t = [(T_{max} + T_{min}) /2] * (k/days) * (1\text{-}cov) * A_{res}$$

where:
T_{max} = maximum daily temperature, in degrees Fahrenheit (°F);
T_{min} = minimum daily temperature, in °F;
k = factor for month, in inches per °F;
days = days in the month; and
cov = reservoir ice cover, in percent.

MODEL SIMULATION OF RIO CHAMA RESERVOIR SYSTEM

In the model each reservoir is simulated with reservoir objects. Heron and El Vado Reservoirs are simulated with storage reservoir objects, and Abiquiu Reservoir is simulated with a level power reservoir object, which adds the capability of simulating a power-generating plant at the reservoir. Each reservoir object solves a mass-balance equation for the reservoir as well as many user-defined solutions.

Each of the reservoirs in the model can estimate spillway flow using the unregulated spill method. The “pan and ice evaporation” method was used to calculate the amount of evaporation from the surface of each reservoir.

Methods to account for real-time sediment deposition in Abiquiu Reservoir have been developed using empirical data and assumptions unique to that reservoir. These methods provide an estimate of sediment accumulation in storage, resulting in a more accurate accounting of water stored in the reservoir.

MIDDLE VALLEY

HYDROGEOLOGY OF THE MIDDLE VALLEY – ALBUQUERQUE BASIN

The Middle Rio Grande Valley is located in one of several structural basins that are part of the Rio Grande Rift, a region formed by Cenozoic extension that extends from Colorado through the length of central New Mexico into northern Mexico. The Rio Grande flows through constrictions in the northeastern and southern boundaries to form the Albuquerque Basin, where the eastern and western structural features converge. Basin fill is continuous across these boundaries (Hawley and Haase, 1992, p. II-4).

The predominant basin deposit is the Santa Fe Group. The thickness of the Santa Fe Group ranges from about 3000 to 4000 ft along basin margins to greater than 14,000 ft in the center of the basin.

Deposition of post-Santa Fe Group sediments has occurred from 1 million years ago (Ma) to the present. In the early part of this period, the Rio Puerco and Rio Grande deposited channel and flood-plain material during river incision and backfilling episodes. In the last 10,000 to 15,000 years, these rivers have been aggrading. Recent post-Santa Fe Group alluvial deposits average about 80 ft thick. Volcanic rock was emplaced in the central part of the Albuquerque Basin west of the Rio Grande from about 0.2 to 0.1 Ma. Basalt flowed to land surface along presumed fault zones. The exposed part of this rock occupies a small percentage of the basin surface area.

The surface-water hydrology in the inner valley of the Albuquerque Basin includes Rio Grande flow, storage in Jemez Reservoir and Cochiti Lake, and an extensive, interconnected network of canals and drains. In some areas of the inner valley, the Rio Grande, canals, and drains recharge the ground-water system, whereas in other areas ground water discharges to surface water. Seepage from Cochiti Lake also recharges the ground-water system.

Historically, large sediment discharges from tributaries of the Rio Grande resulted in a meandering channel that heightened the threat of flood because of decreased channel capacity, rising ground water, and the establishment of dense stands of phreatophytes. These problems led to the authorization of the Middle Rio Grande Project, which included construction of flood- and sediment-control reservoirs and control of the Rio Grande channel and reclamation of seeped lands through rehabilitation of riverside and interior drains.

The capture of sediment in Jemez Reservoir and Cochiti Lake and the construction of channel control works have changed the channel of the Rio Grande above Bernalillo from a braided

channel with sand bars to a straight, incised channel with an armored bed. The effects of these sediment-control pools are moving downstream. However, the reduced peak flows of the Rio Grande below Cochiti are insufficient to move the sediment contributed by small tributaries, resulting in continued instability in some reaches.

The recent chronic high reservoir stage of Elephant Butte Reservoir has resulted in sediment deposition and aggradation of the Rio Grande Floodway below San Acacia. This aggradation has largely reduced the capacity of the Rio Grande channel above Elephant Butte Reservoir and has required concentrated maintenance on the levee to maintain this unstable channel.

Impoundment of water in Cochiti Reservoir began in 1973, and mean annual water levels in the reservoir from 1974 through 1995 ranged from 5260 to 5390 ft above sea level. Seepage from the reservoir to the ground-water flow system was estimated to be 84,000 acre-ft/year in 1978 and 1979 and 21,000 acre-ft/yr in 1980 and 1981 (Blanchard, 1993). Seepage from Cochiti Lake increases with increased reservoir storage, which occurs during flood-control operations.

PHYSICAL DESCRIPTION OF MODEL REACHES

The Middle Rio Grande Valley is defined in this model as Cochiti Lake to Elephant Butte Reservoir. The Middle Valley was analyzed in reaches that were delineated at points along the river where discharge readings were available for the historical calibration period across the entire river valley. These locations are referred to as “full cross sections” and provide calibration points for each canal and drain as well as the river. The first reach starts at Cochiti Dam and ends at the San Felipe gage. The second reach starts at the San Felipe gage and ends at the Central Avenue Bridge where the gage Rio Grande at Albuquerque is located (**fig. 10**). The third reach starts at the Albuquerque gage and continues to the Rio Grande Floodway near Bernardo gage (**fig. 11**). The fourth reach starts at the gage Rio Grande Floodway near Bernardo and ends at the gage Rio Grande Floodway at San Acacia, just downstream from the San Acacia diversion structure (**fig. 12**). The fifth reach starts at the gage Rio Grande Floodway at San Acacia and ends at the San Marcial Floodway gage. The sixth reach starts at the San Marcial Floodway gage and ends at the inflow to Elephant Butte Reservoir. As seen on the model topology, each reach includes data objects that estimate losses and gains based on available information and data.

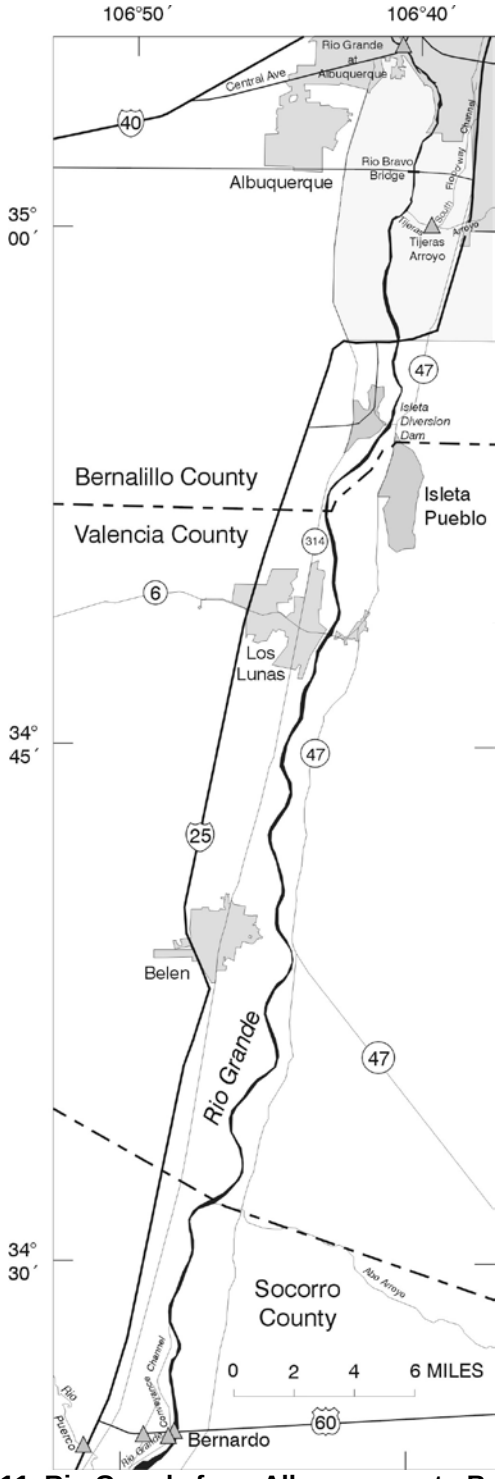

Figure 11. Rio Grande from Albuquerque to Bernardo.

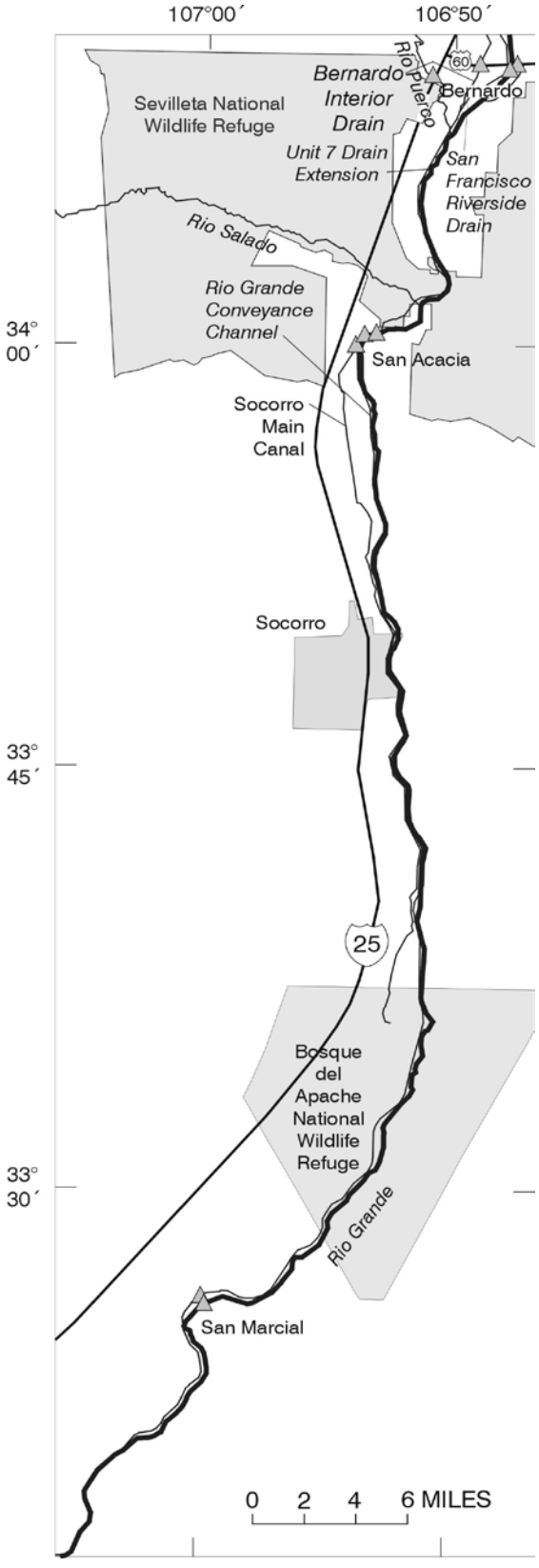

Figure 12. Rio Grande from Bernardo to San Marcial.

DESCRIPTION OF MODEL METHODS

Developing river routing, river-channel leakage, calibrating unmeasured return flows, and solving for local inflow are outlined below:

1. Select an overall dataset that is post-Cochiti Dam construction and has data about major anthropogenic effects (1985-97).

2. Using available gage data, statistically develop time lags for varying flow ranges for each reach in the Middle Valley. The methodology used was similar to all other reaches in the model above Cochiti and is discussed in detail in the Rio Chama section of this document.

3. To calibrate the travel time lags, multiply the travel time lags determined in step 2 by appropriate multipliers—for example, 0.5, 0.8, 1.0, 1.2, and 1.5—to provide a series of routed flows.

4. Compare the series of routed flows to the observed flow at the downstream gage. Use regression analysis and the standard error of the predicted routed flow at the downstream gage, for each observed flow at the downstream gage. On the basis of the series of routed flows that minimize the standard error, choose the appropriate multiplier for the travel time.

5. Compare the multiplier that minimizes the standard error to the observed travel time for identifiable peaks that can be tracked from an upstream to a downstream gage. In the shorter reaches of the Middle Valley the standard error was insensitive and adjusting the multiplier chosen was necessary so that the standard error was small and at the same time the observed travel time for peaks was not violated.

6. Input river-channel leakage and river-channel water surface evaporation.

7. Model all significant and known human effects in the reach such as:
   Agricultural diversions
   Agricultural depletions
   Gaged tributary inflows
   Reservoir effects
   Wastewater returns.

8. Calibrate return flows back into the river within the reach by calibrating against a full downstream cross section—that is, a cross section that has discharge data for across the entire river valley, indicating how much water resides in the irrigation distribution and drainage system, including agricultural diversion flows and ground-water interception.

9. Create an overall routed hydrograph from the upstream-observed hydrograph, accounting for anthropogenic effects, channel losses, routing, and return flows.

10. Compute local inflow by subtracting the downstream-observed river hydrograph from the overall routed hydrograph. This local inflow encompasses effects on the river that could not be accounted for such as:
    Precipitation
    Urban runoff
    Springs or "gains" in the channel
    Ungaged inflow
    Errors resulting from invalid engineering assumptions
    Measurement errors.

Selection of Overall Dataset

The dataset selected for calibrating the model through the Middle Valley extends from Cochiti Lake and Dam to the inflow to Elephant Butte Reservoir. The data include streamflow- or reservoir-gaging stations located on the main stem and on the mouths of tributaries, measurements of diversions and return flows, and climatological data for stations located in the valley or nearby. The dataset period of record used for calibration and validation of the model is 1985-99. The period 1985-97 will be used for calibration of the data, and 1998-99 will be used for validation of the model. The dataset chosen most accurately represents the current geomorphic character of the Middle Valley from Cochiti to Elephant Butte. The construction of levees, drains, and other channel improvement works, as well as the operation of sediment-control pools at Cochiti and Jemez Canyon Reservoirs, has changed the character of the upper river to the extent that records prior to 1985 do not represent current conditions.

Method for Estimating River-Channel Evaporation Loss

The following equations were used to estimate evaporation losses from the water surface and wetted sands within the river channel in the Middle Rio Grande Valley between Cochiti Dam and Elephant Butte Reservoir.

Cochiti to San Felipe (bankfull discharge = 5650 cfs and corresponding surface area = 625 acres):

For $Q < 5650$ cfs; $L = Pan_e (111\ Q^{.20}) + 0.25\ Pan_e (625\text{-}111\ Q^{.20})$

For $Q \geq 5650$ cfs; $L = Pan_e (111\ Q^{.20})$

San Felipe to Albuquerque (bankfull discharge = 4820 cfs and corresponding surface area = 2718 acres):

For $Q < 4820$ cfs; $L = Pan_e (84\ Q^{.41}) + 0.25\ Pan_e (2718\text{-}84\ Q^{.41})$

For $Q \geq 4820$ cfs; $L = Pan_e (84\ Q^{.41})$

Albuquerque to Bernardo (bankfull discharge = 4820 cfs and corresponding surface area = 5175 acres):

For $Q < 4820$ cfs; $L = Pan_e (124\ Q^{.44}) + 0.25\ Pan_e (5175\ \text{-}124\ Q^{.44})$

For $Q \geq 4820$ cfs; $L = Pan_e (124\ Q^{.44})$

Bernardo to San Acacia (bankfull discharge = 4000 cfs and corresponding surface area = 1054 acres):

For $Q < 4000$ cfs; $L = Pan_e (13\ Q^{.53}) + 0.25\ Pan_e (1054 - 13\ Q^{.53})$

For $Q \geq 4000$ cfs; $L = Pan_e (13\ Q^{.53})$

San Acacia to San Marcial (bankfull discharge = 9100 cfs and corresponding surface area = 2913 acres):

For $Q < 9100$ cfs; $L = Pan_e (158\ Q^{.32}) + 0.25\ Pan_e (2913 - 158\ Q^{.32})$

For $Q \geq 9100$ cfs; $L = Pan_e (158\ Q^{.32})$

San Marcial to Elephant Butte Reservoir (bankfull discharge = 2400 cfs and corresponding surface area = 166 acres):

For $Q < 2400$ cfs; $L = Pan_e (60\ Q^{.13}) + 0.25\ Pan_e (166 - 60\ Q^{.13})$

For $Q \geq 2400$ cfs; $L = Pan_e (60\ Q^{.13})$

where:

Q = Mean daily discharge at the upstream end of the reach, in cfs;
L = Loss from water surface evaporation and wetted sands in the reach, in acre-ft/day; and
Pan_e = Pan evaporation data for the site nearest to the reach under consideration, in ft/day.

Data used to develop the stream discharge/loss equations were obtained from three sources: Fenton (1996); USBR and U.S. Army Corps of Engineers (1998); and USBR (1985). The USBR mapped river-channel areas in 1992 during high-flow and low-flow conditions (Fenton, 1996). The water surface areas of the main channel were tabulated for each reach during high flow and low flow. River-channel bankfull widths at the computed channel maintenance discharge for each reach (USBR and U.S. Army Corps of Engineers, 1998) also were included in the development of the water surface area/stream-discharge relation. Finally, data developed in the San Juan-Chama incremental loss study (USBR, 1985) were incorporated into the analysis for reaches between Cochiti Dam and San Acacia. These data include river-channel cross section data obtained from an ongoing program to measure river-channel response to the construction and operation of flood-control works in the Middle Rio Grande Valley and data collected by the USGS during the course of stream-gage calibration.

Leopold and Maddock (1953) described the relation between channel width and stream discharge in the form $w = aQ^b$, where w is channel width, Q is discharge, and a and b are constants. This equation was used to develop the loss equations described above. River-channel areas were developed by multiplying the channel width times the length of the reach. Losses are estimated by multiplying the areas by an evaporation rate, such as that measured at a nearby evaporation pan.

For this analysis, at the bankfull discharge, all sand bars in the river channel are assumed to be covered with water and the wetted sands not subject to evaporation loss. This bankfull discharge generally has a 1- to 2-year return interval (Leopold and others, 1964). A peak annual discharge with a 2-year return interval for each reach was used to estimate the bankfull discharge (USBR and U.S. Army Corps of Engineers, 1998). As stream discharge drops below the bankfull discharge, sand bars become exposed and subject to evaporative losses. A factor of 0.25 is used to correlate the evaporation of water by capillary action through sand bars in the river channel to an adjacent evaporation pan measurement (Sorey and Matlock, 1969).

Some data used in this analysis were collected before the influence of the construction and operation of Cochiti and Jemez Canyon Dams were obvious on the river channel. The construction and operation of these flood- and sediment-control facilities have resulted in deeper and narrower river-channel cross sections in the upper reaches. Data are inadequate to evaluate the changes in river-channel cross sections or to predict future changes in river-channel cross sections.

The constant used to correlate evaporation from wetted sand surfaces with pan evaporation data for a nearby station varies between 0.25 for wetted sands within 1 ft above the water surface to 0.05 for wetted sands between 1 and 4 ft above the water surface (Sorey and Matlock, 1969). A constant of 0.25 is used here for all water levels.

Graph 96 shows plots of the relation between water surface area and streamflow discharge for each reach of the Middle Valley.

Method for Modeling Ground Water (Channel Leakage)

The Albuquerque Basin is an important part of the RiverWare model. The complexity of the surface-water system, the effects of storage and delivery requirements of water users in the basin on the upstream river system, the large population that depends on surface and ground water, the importance of ground water as a public water supply, and the interaction of the surface- and ground-water systems require defining the complete hydrologic system. Surface-water/ground-water exchange can be estimated in the Albuquerque Basin because data are available that are needed to calibrate the analytical solution of ground-water flow equations. In addition, leakage has been measured in specific reaches of the Rio Grande that can be compared to other methods.

A preliminary estimate of leakage to or from the river and shallow ground-water system was made to compare to actual seepage measurements in the reach from just below the Highway 44 Bridge (**fig. 10**) to the Rio Bravo Bridge (**fig. 11**). This estimate was made using a FORTRAN program developed for the Rio Grande reach from Cochiti Dam to San Acacia. The leakage estimate is based on hydraulic gradients between the river and riverside drains. USBR-reported hydraulic-conductivity values of the shallow aquifer sediments were used as initial values in the calculations (Bureau of Reclamation, 1997, p.17). Daily ground-water head data were not available for the shallow aquifer adjacent to this reach. Drain water surface elevations of 5 ft below land surface at each Albuquerque Basin model drain cell (Kernodle and others, 1995) were used to establish a constant ground-water elevation in the shallow aquifer. Daily river surface elevations at each model river cell were estimated using daily river surface gradients from the Cochiti to San Felipe gages, the San Felipe to Albuquerque gages, and the Albuquerque to San Acacia gages and the length of each model cell. River cell surface areas were taken from the model. The estimated channel bank area, through which water flows, was estimated by assuming a 3-ft-deep flow in the river times the length of the cell, which also was taken from the model. The channel bank area was multiplied by two to account for both sides of the river. Vertical or horizontal hydraulic conductivity times an estimated vertical gradient (Jim Bartolino, U.S. Geological Survey, oral commun.) and the calculated horizontal gradient, were used to calculate flow to or from the river, respectively. Seepage was estimated for October 1, 1994, to September 30, 1998. Estimates of leakage to or from the river for December, January, and February were compared to actual seepage measurements made by Jack Veenhuis, oral commun.). Close agreement was obtained between the measured seepage rate of 85 to 95 cfs and the estimated (discussed above) leakage rates derived using horizontal and vertical hydraulic-conductivity values of 160 and 1.6 ft/day, respectively.

In February 1999, computer programs became available for analytical solutions of the ground-water flow equation using a surface-water stage hydrograph as input and the convolution method of solution (Barlow and Moench, 1998). The solutions are based on the partial differential equation of transient ground-water flow in a saturated, homogeneous, slightly compressible, and anisotropic aquifer in which the principal directions of hydraulic conductivity are oriented parallel to the coordinate axes. The most general case of the equation written in two dimensions is:

$$K_x \frac{\partial^2 h}{\partial x^2} + K_z \frac{\partial^2 h}{\partial z^2} = S_s \frac{\partial h}{\partial t} + q'$$

where:

K_x, K_z = horizontal and vertical hydraulic conductivity of the aquifer, respectively (units of length per time);
h = ground-water head (units of length);
x,z = horizontal and vertical coordinate directions, respectively (units of length);
S_s = specific storage of the aquifer (units of inverse length);
t = time (units of time); and
q' = a volumetric flow rate to or from the aquifer per unit volume of aquifer, representing sources or sinks of water to the aquifer (units of inverse time).

The solutions are for confined aquifers (program STLK1) and for unconfined aquifers (program STWT1). One of the hydrologic requirements for using the programs properly is that ground-water flows are primarily perpendicular to the river channel and, for unconfined aquifers, vertical below the channel.

Next attempted was calibrating the analytical solution, using measured leakage from the river in the reach from just below the Highway 44 Bridge to the Rio Bravo Bridge, to actual seepage

measurements made by Jack Veenhuis, (oral communication). The actual seepage measurements determined that 85 to 95 cfs leaks from the river in this reach during December, January, and February. The depth of the aquifer was set at 250 ft, a depth at which changes in river stage are not noticed in nearby piezometers. The width of the aquifer, from the midpoint of the river to one side of the aquifer, was set at 5600 ft, again a distance at which stage changes are not noticed in the aquifer. With the aquifer at these dimensions, boundary conditions, including the drains and canals within the specified area, were thought to be insignificant. Analytical solution results could not match this leakage rate. Horizontal hydraulic conductivity of 500 ft/day, a vertical to horizontal hydraulic-conductivity ratio of 0.5, storage coefficient of 1×10^{-3}, and a specific yield of 0.25 were tried in the solutions to obtain the measured leakage rate. Although these input values were greater than any reported values in the area, the maximum leakage rate was only about 30 cfs. The method and calibrations were reviewed with staff of the USGS. Even with the aquifer dimensions set beyond apparent influences of the drain, the methods and calibrations created a significant boundary condition. The constant head of the drain and the drainage of water out of the system created a condition that could not be duplicated by the STWT program.

Computation of daily leakage to or from the river and the shallow ground-water system was made account for river channel losses. These calculations are based on gradients using water-surface elevations of the Rio Grande and riverside drain(s). Flow of water from the river was calculated using the equation Q=KIA where Q= flow in cubic feet per day, K is the hydraulic conductivity in feet per day , I is the average gradient from the river to the drain(s), and A is the area through which water will flow to or from the river, in square feet. The methods and data used in this computation are summarized below.

River elevations were derived using the U.S. Bureau of Reclamation (USBR) aggredation-degradation data and maps (USBR, 1992). A range line was selected by the USBR for about each 500 feet of river length from Cochiti Dam to range line 1794, at the headwaters of Elephant Butte reservoir. For each of these range lines, land and water surface elevations were estimated using orthophotgraphic maps through work done by a USBR contractor. In estimating river elevations in the river leakage study a range line was selected at about each river mile starting at Cochiti Dam and ending at Bernardo. The selected range lines formed the upper and lower ends of a cell that contained the river and adjacent riverside drains, if there was a riverside drain. River bottom elevations were estimated by subtracting the estimated depth of flow at each of the selected range lines from the water surface elevation. The depths of flow were estimated using U.S. Geological Survey (USGS) flow measurement data that corresponded to a flow that was in the river on February 21, 1992 from Cochiti Dam to near the Alameda Boulevard bridge in Albuquerque and on February 24, 1992 from near the Alameda bridge to Bernardo. Average measured depth of flow was taken from flow measurement data at gages Rio Grande below Cochiti Dam (08317400), Rio Grande near Alameda (08329928), Rio Grande at Albuquerque (08330000), and Rio Grande at Rio Bravo Bridge (08330150), and Rio Grand Floodway near Bernardo (08332010). Depth of flow for each cell between the gages was estimated by dividing the difference in depth of flow of 2 adjacent gages by the number of cells. This value was then added to the depth of the upstream gage.

Riverside drain bottom elevations were taken from digital data obtained from original drain engineering plans. Digital data were created by the USGS through a cooperative project with the City of Albuquerque, Office of the New Mexico State Engineer, and the Middle Rio Grande Conservancy District. Riverside drain traces were digitized and divided into many arcs with top and bottom nodes at each arc. Drain bottom elevation and drain slope that corresponded to the upstream most node of each arc were part of the digital data set. A digital trace of the river, riverside drains, and cells corresponding to selected range lines were overlain using ARC/INFO. Drain bottom elevation data at the same location of the river bottom data were not available. Riverside drain bottom elevation data were estimated at each range line using the slope of the drain and the distance from a node on a riverside drain arc to the next range line.

River water-surface elevations for each cell were estimated using the gradient from the upstream to a downstream gage used to define a river reach. This gradient was multiplied by the distance from the upstream gage to the top of the second cell then the distance from the second cell to next cell etc. The product of the above operation was subtracted from the water surface elevation at the upstream gage or cell to estimate the water surface elevation for the next downstream cell. A river water surface elevation for each cell was estimated using this procedure for each day. A riverside drain water surface elevation was estimated for each cell by averaging the drain bottom elevation at the top and bottom of each cell and adding the average monthly drain depth of flow shown in **table 35**.

The gradient from the river to the drain(s) was estimated using the estimated river water-surface elevation in each cell, the distance from the river to the drain(s), and the estimated water-surface elevation in the drain(s). This gradient is assumed to be the driving force for leakage to or from the river. Positive gradients generate flow from the river. The cells were used to define discrete parts of the floodplain. Within each cell the parameters of the flow equation were defined and the flow to or from the river computed.

Table 35. Average monthly depth of water in riverside drains

Month	Corrales average depth	Atrisco average depth	Albuquerque average depth	Bernardo average depth	Average depth
January	1.18			0.99	1.09
February	1.66	1.18	1.13	1.00	1.24
March	1.42	1.29	2.21	1.31	1.56
April	1.97	1.24	2.19	1.50	1.73
May	1.91	2.43	2.18	1.69	2.05
June	1.97	1.57	2.57	1.62	1.93
July	1.79	1.36	2.55	1.69	1.85
August	1.95	1.13	2.43	1.77	1.82
September	1.82	1.18	2.60	2.19	1.95
October	2.09	1.34	2.43	2.20	2.02
November	1.29	1.23	1.54	1.04	1.28
December	1.25	1.20	1.28	1.05	1.20

A FORTRAN program was developed to compute river leakage. The program calculates a water surface elevation for the river and for each riverside drain in each cell for each day. The average gradient from the river to the east and to the west drains are computed separately. Input to the program are gage heights for Rio Grande below Cochiti Dam (08317400), Rio Grande at Albuquerque (08330000), and Rio Grande Floodway near Bernardo (08332010) and horizontal and vertical hydraulic conductivity for each reach. The average distance from the east side of the river to the riverside drain east of the river, using distances at each of the range lines that form the upper and lower boundaries of the cell are used. Distances from the river to the east side riverside drains were measured from orthophotoquad maps at a scale of 1 inch equal to 400 feet on the ground (USBR, 1992). The average distance from the west side of the river to the riverside drain west of the river, using distances at each of the range lines that form the upper and lower boundaries of the cell are also used. The surface area of the river was obtained using ARC/INFO by intersecting the bounding traces of the river edges with the cells. The surface area of the river was assumed to be equal to the bottom area and this value was used to compute vertical leakage from the river. The distance from the river to the riverside drains and the river surface area were adjusted using relationships between river stage and the change in river area derived from USGS flow measurement data. If the river surface area decreased then the distance from the river to the drains increased. The area through which horizontal flowing river leakage had to pass was the length of each side of the river in each cell times the estimated depth of flow of the river in that cell times 2. The depth of flow was multiplied by 2 assuming that flow lines from river to the

shallow ground-water system would not be straight lines from the river bank to the ground water system but that there would be some curvature at the river bank and bottom that would create an effective area of flow from the river greater than the depth of river flow. River depth is varied according to the relationships established between gage height and flow depth for each gage in the middle valley. Depth of flow was changed daily based on the gage height-flow depth relationships shown in **graphs 97-104**. In order to assure consistency in the daily depth of flow between gages and reaches the difference in depth of flow at an upstream and a downstream gage in a reach was divided by the number of cells in that reach and the depth for each cell incremented by that value. Vertical flow from the river used average gradients and vertical hydraulic conductivities from Bartalino and Niswonger (1999).

The FORTRAN program was calibrated using river to drain gradient and leakage data from Hansen (no date). This investigation established temporary surface-water elevation gages at the river, the east riverside drain at some sites, and selected canals. Shallow piezometers at five sites in the Middle Valley were also installed. Site 1 was near the confluence of the North Diversion channel and the Rio Grande, the Sandia Site; site 2 at the Paseo del Norte bridge crossing, the Paseo del Norte site; site 3 near the Interstate 40 bridge, the I-40 site; site 4 near the Albuquerque zoo, the Tingley site; and site 5 at the Rio Bravo Boulevard bride, the Rio Bravo site. Cells used in this investigation that corresponded to the five sites in the Hansen (no date) investigation were used to compare river to drain gradients and to match river leakage values by varying horizontal hydraulic conductivity in the FORTRAN program until river leakage values were similar to those reported by Hansen (no date).

River to drain gradients were not computed by Hansen (no date) but data were available to compute these gradients at the Sandia and Rio Bravo sites. At the Sandia site there were 4 days when river to drain gradients could be computed using the USBR elevation data. Using FORTRAN estimated river to drain gradients for those same 4 days the average FORTRAN gradients are .00728 greater than the average gradients computed using USBR data. For the Rio Bravo site there were 11 days when USBR data were available to compute river to drain gradients. The average FORTRAN computed river to drain gradients for the same 11 days that have USBR data available to compute gradients are .00516 greater than the average USBR river to drain gradients.

Hansen (no date) reported gradient values from a piezometer near the river to a piezometer on the river side of the east riverside drain at all sites (USBR gw grad). The gradients computed by the FORTRAN program are from the river to the east riverside drain (mod sw grad) so these two gradient data sets are not exactly comparable. River to drain gradients computed by the FORTRAN program were compared to gradients between a piezometer near the river and a piezometer near the east side drain (Hansen, no date). Plots comparing USBR well-to-well gradients and FORTRAN computed river to drain gradients are shown in **figures 13-17**.

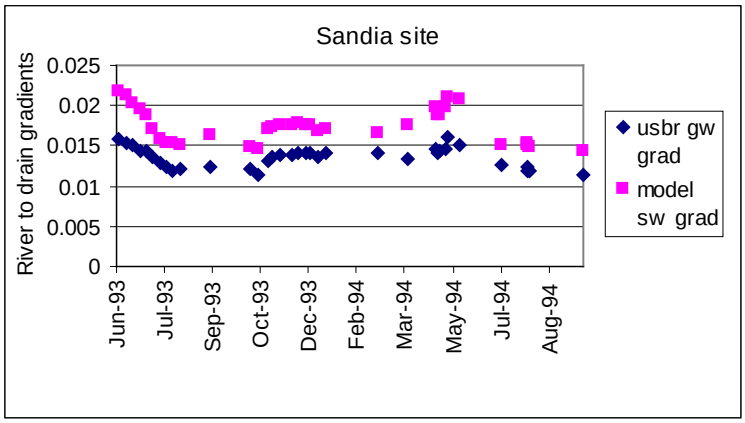

Figure 13. Comparison of USBR well-to-well gradients with FORTRAN computed river to drain gradients at Sandia site

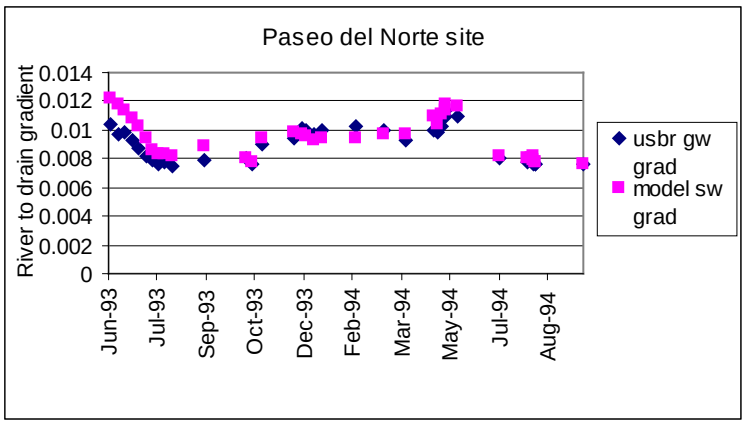

Figure 14. Comparison of USBR well-to-well gradients with FORTRAN computed river to drain gradients at Paseo del Norte site

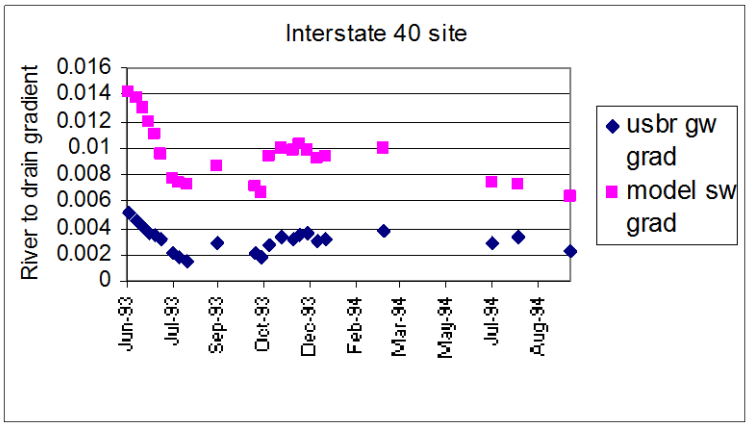

Figure 15. Comparison of USBR well-to-well gradients with FORTRAN computed river to drain gradients at Interstate 40 site

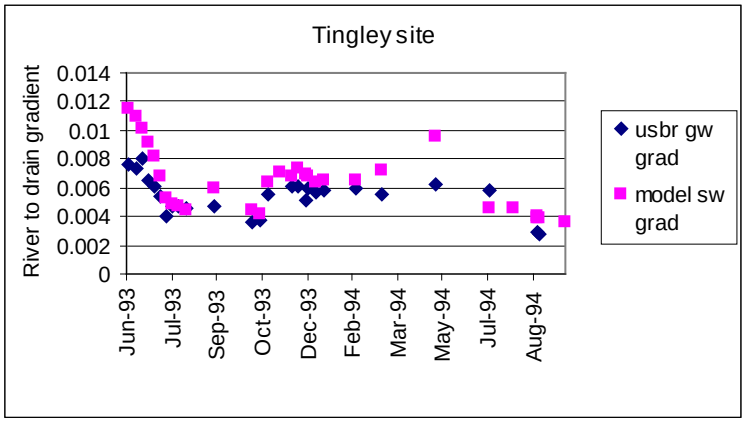

Figure 16. Comparison of USBR well-to-well gradients with FORTRAN computed river to drain gradients at Tingley site

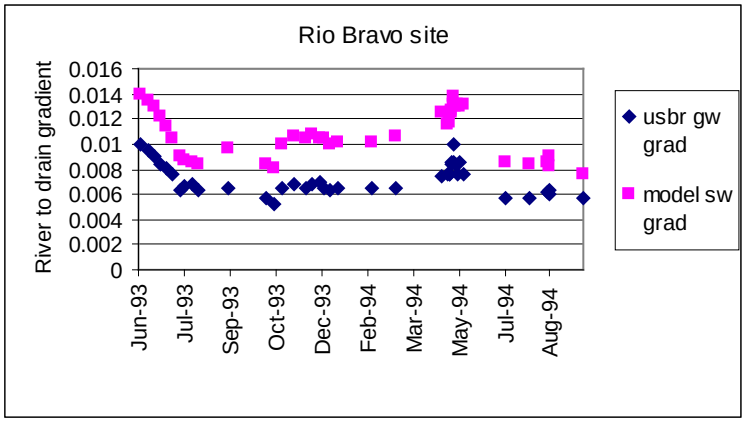

Figure 17. Comparison of USBR well-to-well gradients with FORTRAN computed river to drain gradients at Rio Bravo site

Table 36 presents the average USBR hydraulic gradients from a piezometer near the river to a piezometer near the east riverside drain and the average FORTRAN hydraulic gradient from the river to the east riverside drain. In all cases the FORTRAN computed gradient is greater than the USBR gradient. The gradient differences are caused by one or more of the following: the gradients are not based on the same water elevations, the FORTRAN computed gradients use different river to drain distances than the USBR gradients and the FORTRAN river to drain distances are varied each day depending on the gage height of the river, and the FORTRAN gradients are based on average estimated river water surface elevations for a cell that is about 1 mile in length. Considering these differences the FORTRAN river to drain gradients probably represents an appropriate gradient that can be used in estimating river leakage

Table 36. Comparison of USBR measured gradients with FORTRAN computed gradients

Site	Number of days	USBR average gradient	FORTRAN average gradient	Average gradient difference
Sandia	36	0.01352	0.01739	-0.00509
Paseo del Norte	36	0.00899	0.00948	-0.00049
Interstate 40	23	0.00308	0.00943	-0.00635
Tingley	30	0.00541	0.00642	-0.00101
Rio Bravo	41	0.00721	0.01077	-0.00356

River leakage reported by Hansen (no date) are cubic feet per second (cfs) per mile of river. Depths used by Hansen (no date) to compute leakage from the river ranged from 65 to 80 feet depending on the site. Using the reported depths assumes the river is this deep and is not valid. The reported river leakage values (Hansen (no date) were divided by the depth used in the leakage calculations and river leakage computed in the FORTRAN program were divided by the river depth used in these calculations. These unit leakage values were compared in the calibration procedure. **Figures 18-22** show the USBR leakage (USBRleak) and the FORTRAN computed leakage (modleak).

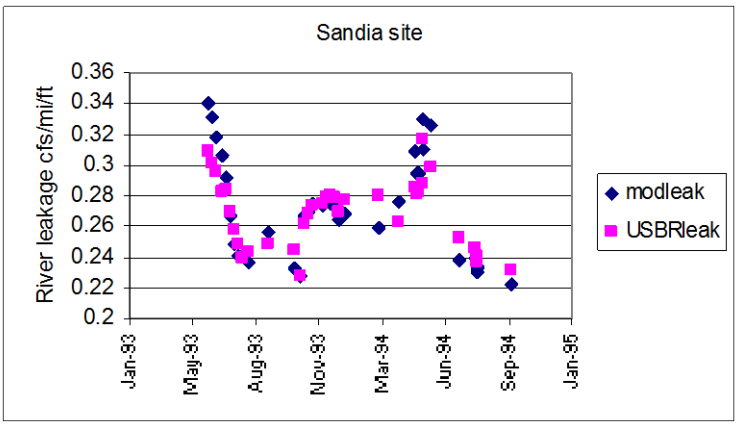

Figure 18. Comparison of USBR leakage rates with FORTRAN computed leakage rates at Sandia site.

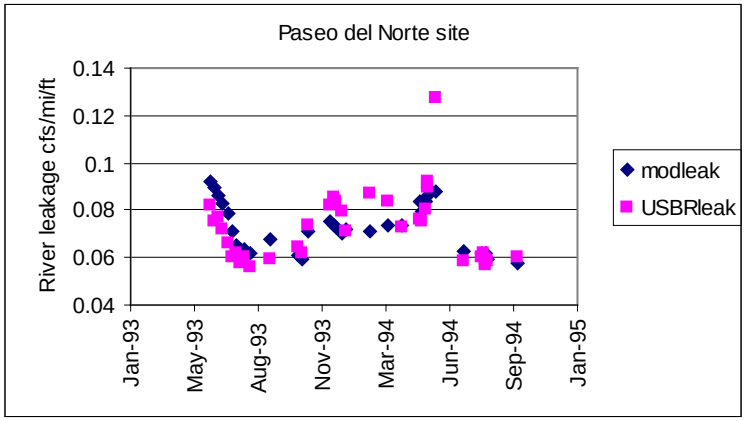

Figure 19. Comparison of USBR leakage rates with FORTRAN computed leakage rates at Paseo del Norte site.

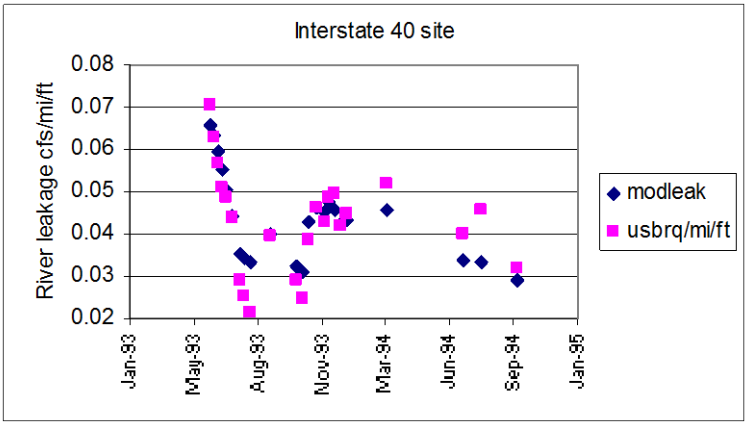

Figure 20. Comparison of USBR leakage rates with FORTRAN computed leakage rates at Interstate 40 site.

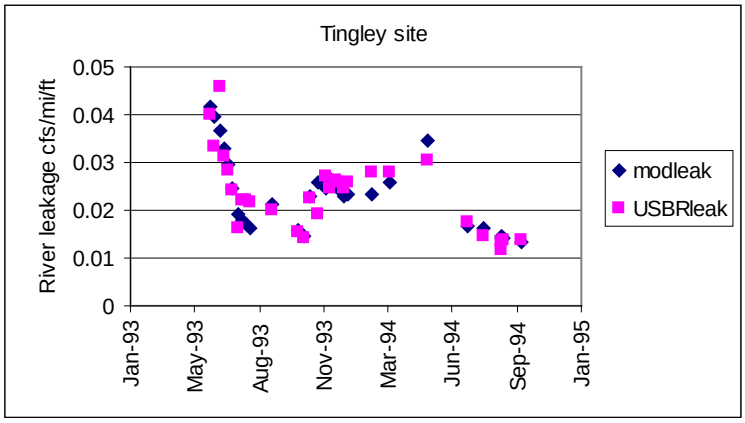

Figure 21. Comparison of USBR leakage rates with FORTRAN computed leakage rates at Tingley site.

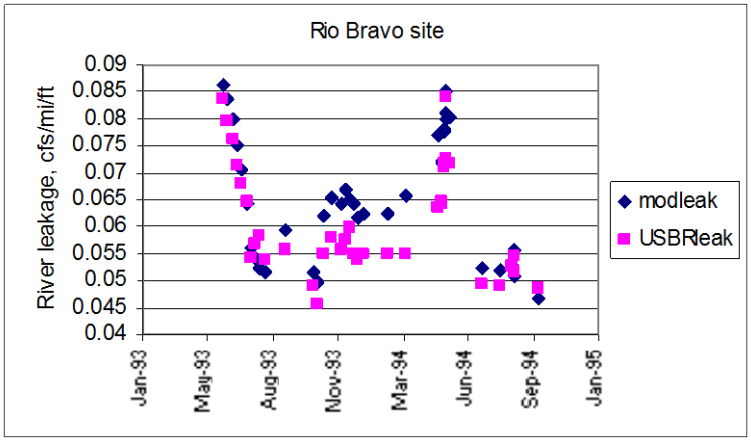

Figure 22. Comparison of USBR leakage rates with FORTRAN computed leakage rates at Rio Bravo site.

Table 37 provides statistics relative to the match and the horizontal hydraulic conductivity used at each of the site.

Table 37. Statistical summary of USBR and FORTRAN hydraulic conductivity at each site

Site	Number of days	FORTRAN average leakage (cfs/mi/ft)	USBR average leakage (cfs/mi/ft)	Average flow difference (cfs/mi/ft)	Horizontal hydraulic conductivity (ft/day)
Sandia	36	0.27156	0.26814	-0.00341	250
Paseo del Norte	36	0.07197	0.07185	-0.00012	125
Interstate 40	23	0.04348	0.04282	-0.00066	78
Tingley	30	0.02051	0.02098	0.00048	60
Rio Bravo	41	0.06544	0.06144	-0.00401	100

The RiverWare model uses leakage for entire reaches so the horizontal hydraulic conductivity values for the sites were averaged. There were no USBR sites in the Below Cochiti to San Felipe reach to calibrate against so the value used at the Sandia site of 250 ft/day was used. In the San Felipe to Central reach the Sandia, Paseo del Norte, and Interstate 40 sites were used for an average of 150 ft/day. The Tingley and Rio Bravo sites were used in the Central to Bernardo reach with an average hydraulic conductivity of 80 ft/day. Jack Veenhuis reported a gross leakage from the river of about 285 to 295 cfs per day in a reach from about 3 miles below the Highway 44 bridge and the Rio Bravo bridge. Flows were measured in the winters of 1994-95 through 1997-98. During 4 measurement efforts river flow was measured at several places along the reach and all inflows to the reach were measured. An assumption was made that all flows in the drains that returned to the river originated as leakage from the river. Using the gradients and the horizontal hydraulic conductivities reported above the average river leakage computed by the FORTRAN program for this reach was about 110 cfs per day. The discrepancy between flow reported by Veenhuis and that computed by the FORTRAN program might be because not all flow returning to the river originated as river leakage. If there were another source of water for flows returning in the drains then the leakage values reported by Veenhuis would be decreased.

Average gross leakage from each reach, by month, is shown in **figure 23**.

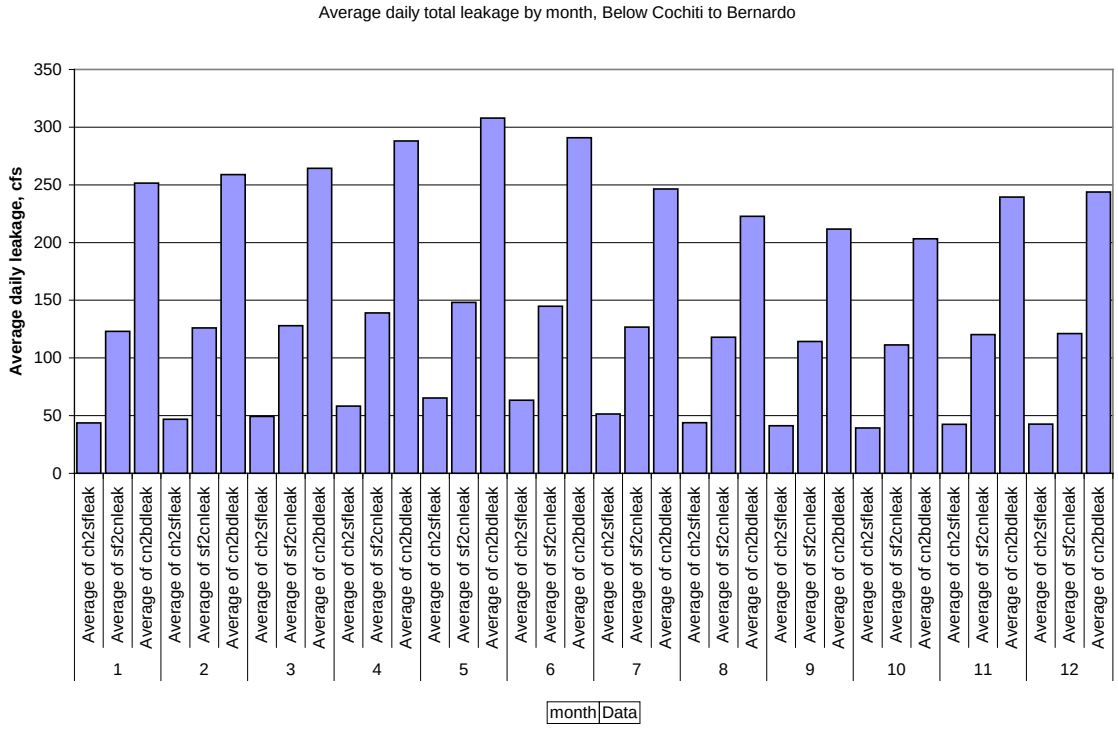

Figure 23. Average daily leakage, by month, Cochiti to Bernardo

Basically the same method of estimating leakage as that described from the reach from Cochiti to Bernardo was used for the reach from Bernardo to below the gage at San Acacia. Although this analysis went as far downstream as San Marcial, a completely different method was used for the reach from San Acacia to San Marcial. Differences for the analysis reach are (1) drain stage elevations are known at each of the gage sites (Bernardo Conveyance Channel, San Acacia Conveyance Channel, and San Marcial Conveyance Channel) and (2) drains or conveyance channels are only on the west side of river for most of the lower reach. The lower reach was divided into 68 cells using selected USBR aggradation-degradation cross sections as north and south cell boundaries. The cells were extended east and west a sufficient distance to include the river and drains or conveyance channels. The cells are about 1 river mi in length except at the San Acacia diversion structure and in the vicinity of the Tiffany Channel. The lengths of the river and drain or conveyance channels in each cell were determined from 7½-minute digital raster graphic maps. The maps were displayed in Arc/Info and overlain by an Arc/Info coverage of the cells. River and drain water surface elevations for each cell were computed using the method described for the upper reach.

Distances from the river channel to the drain or conveyance channel that are needed to compute the gradient from the river to the shallow ground-water system were computed using aggradation-degradation cross section data from February 1992. Zero distance was on the left side of each section and distance increased to the right. Each distance was accompanied by an elevation of the land or water surface. Data were entered into a spreadsheet and plotted. After the river and drain or conveyance channel locations were visually verified, the distance between the channels was determined. The river-to-drain distance for a cell is the average of the distance at the upstream and downstream ends of the cell. Ground-water-level data for 1985 to 1997 for shallow

wells near the river were retrieved from the USGS Ground-Water Site-Inventory (GWSI) data base. These data were used to compute gradients from the river to the shallow ground-water system to the east. For those days for which there were shallow ground-water-level gradients to the east, gradients to the east were compared with those to the west. Because the averages of the east and west gradients were nearly identical, the gradients to the east of the river were assumed to be equal to the computed gradients to the west.

Vertical flow from the river channel is computed using the area of the river channel in each cell and the vertical gradient. Vertical gradient data were taken from work done by Bartolino and Niswonger (1999). The average vertical gradient at sites upstream from the Highway 44 Bridge, above the Rio Rancho sewage plant outfall, near the Paseo del Norte Bridge, and near the Rio Bravo Bridge is 0.0058. Data were collected sporadically from 1996 through 1998. Vertical hydraulic conductivity was assumed to be 1/100 of horizontal hydraulic conductivity.

River depth is needed to determine the area through which water can flow from the river channel. Relations between river gage height and river depth were poorly defined in the upper reach. The lower reach, however, has no such relations, except at Bernardo. In the interest of computation consistency in the Fortran program, the relation at Bernardo was not used. Monthly average river depth was determined at the Bernardo Floodway, San Acacia Floodway, and San Marcial Floodway gages using USGS discharge measurements from 1970 to 1998. **Table 38** shows these average monthly depths.

Table 38. Average depth of Rio Grande at three floodway gages

	Average river depth, in feet		
Month	Bernardo	San Acacia	San Marcial
Jan	1.55	0.44	1.73
Feb	1.69	0.79	3.49
Mar	1.38	1.41	2.89
Apr	1.48	1.15	1.95
May	1.64	0.96	1.62
June	1.64	1.31	1.22
July	2.20	2.01	2.27
Aug	2.75	2.99	1.80
Sept	1.72	2.21	1.90
Oct	2.16	3.30	1.70
Nov	2.26	2.45	1.82
Dec	1.71	2.47	1.61

The area of the channel through which water can flow from the river to the shallow ground-water system is needed to compute vertical leakage from the river. The length of the river channel in each cell had been determined; the width of the channel is estimated using average monthly river widths taken from USGS discharge measurements from 1970 to 1998. **Table 39** shows the monthly average river widths at the three floodway gages in this reach.

Table 39. Average width of Rio Grande at three floodway gages

	Average river width, in feet		
Month	Bernardo	San Acacia	San Marcial
Jan	262	85	204
Feb	232	101	232
Mar	266	97	237
Apr	312	99	219
May	406	163	220
June	370	122	178
July	243	106	169
Aug	189	79	157
Sept	172	82	148
Oct	165	56	155
Nov	256	76	209
Dec	244	71	223

The Fortran program was modified to compute the water surface elevation in the drains and conveyance channel on the west side of the Rio Grande. This computation is done in addition to computing the water surface elevation of the river, as described previously. The estimated water surface elevation in the river and drain or conveyance channel in each cell was used to compute the gradient between the river and drain or conveyance channel.

A spreadsheet developed that duplicated the logic in the Fortran program ensured that the Fortran program was computing leakage using the correct stage in the river and the drain or conveyance channel at each cell, the correct gradient from the river to the drain, and the correct flow depth of the river. An input dataset used in the FORTRAN program was developed that should give the same answers as those in the spreadsheet. The FORTRAN program and the spreadsheet gave identical calculations of leakage.

Leakage from the river to the shallow ground-water system was estimated for 1985 through 1997. **Figure 24** shows the average daily estimated leakage by month for the Bernardo to San Acacia, San Acacia to San Marcial, and below San Marcial reaches.

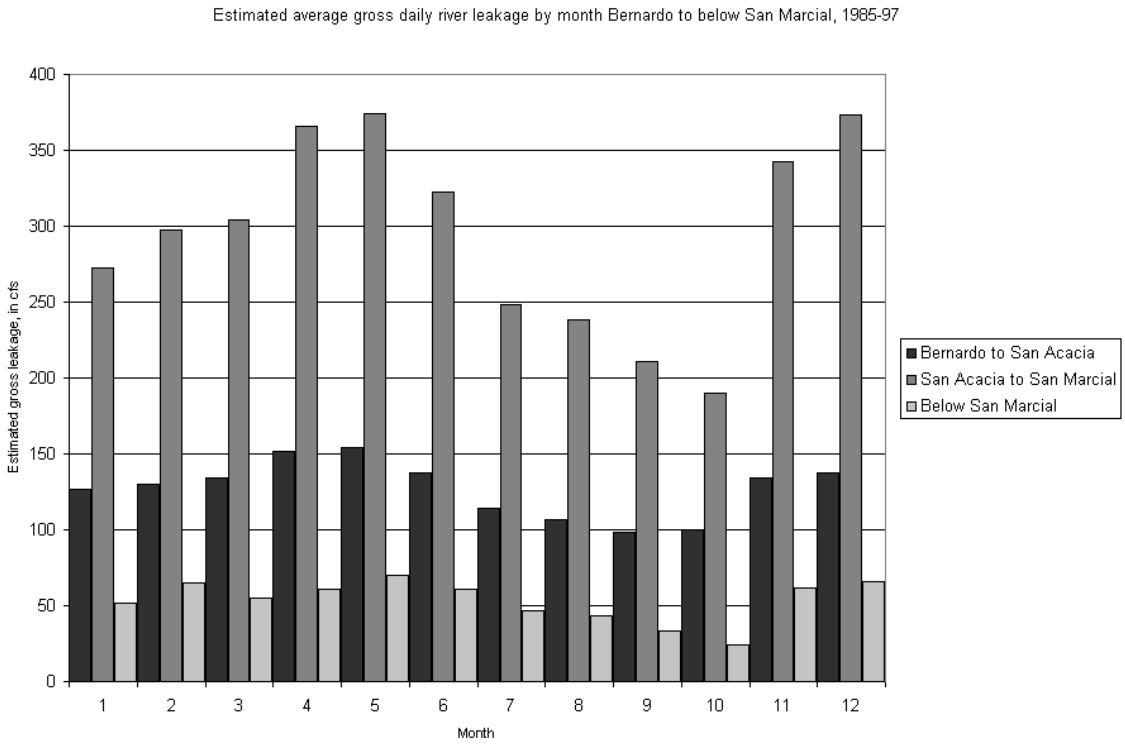

Figure 24. Average gross leakage calculated by FORTRAN program (in cfs) by month, Bernardo to below San Marcial, 1985-97.

The floodway reach from the Bernardo gage to the San Acacia gage loses water most days. As in the upper river reach/shallow ground-water system, not all water that leaks from the river stays in the shallow ground-water system. Some water is used by riparian vegetation, some flows to the deep ground-water system, and some enters the Unit 7 Drain. An estimate was needed of the amount of river water that leaks to the shallow ground-water system and actually enters the Unit 7 Drain channel. No seepage measurements in the Bernardo to San Acacia reach have been conducted that could be used to estimate that part of total river leakage entering the Unit 7 Drain channel by way of the shallow ground-water system; therefore, this volume of water was estimated using discharge data at the Bernardo and San Acacia floodway gages and calculated leakage to the Unit 7 Drain. Only data for the winter months of December through February were considered. Inflow from the Rio Puerco was subtracted from the gaged flow at San Acacia. Only those days when calculated leakage from the river was greater than loss shown by the gage data were used in the analysis. Only those days met the assumption that water lost from the river goes to riparian vegetation and the deeper ground-water system and enters the Unit 7 Drain channel. This analysis showed that 47 percent of the water that leaves the river channel enters the Unit 7 Drain channel. For this reach, the RiverWare model adjusts the leakage from the river to the Unit 7 Drain channel to be 47 percent of the calculated leakage. This percentage is very preliminary and needs to be refined for later versions of the model.

A calibrated ground/surface-water simulation model of the San Acacia to San Marcial reach requires the development of two look-up tables. The look-up tables are used to determine the losses or gains in the floodway and the low-flow conveyance channel based on the upstream flows at both upstream gages. Since the losses or gains in the reach are dependent on the amount of flow at the top of the reach (San Acacia), the look-up tables are incremented by flow.

The increments used in the look-up table for the floodway flow at the gage at San Acacia are 0, 250, 500, 1,000, 2,000, 4,000, 8,000, and 12,000. The increments for the low LFCC at the gage at San Acacia are 0, 250, 500, 1,000, and 2,000.

The NMISC has developed a surface water/groundwater model of the Rio Grande reach from San Acacia to Elephant Butte reservoir (Shafike 2005). The purpose of the model is to evaluate potential system-wide depletions that may result from changes in operation of the LFCC, riparian vegetation restoration projects, and riverbed aggradation. The model simulates the Rio Grande channel, the LFCC, and the main irrigation canals and drains as well as the alluvial and the Santa Fe group aquifers. The USGS program MODBRANCH (Swain et al, 1997) is used to represent the surface water/groundwater system. The surface water component is represented by solving the one-dimensional form of the continuity and momentum equations, known as Saint-Venant equation. The groundwater component is dynamically linked to the surface water component. The physical processes represented in the model are surface water routing, surface water/groundwater interaction, discharge from springs, riparian and crop depletions, groundwater withdrawals and groundwater levels. The model provides groundwater elevation, surface water flow and riparian and crop depletion.

For the purpose of computing the loss/gain in this reach of the river the model was run using stream package on a daily time step for each of the incremental flow mentioned above and the average monthly loss/gain of the river channel and the LFCC channel was computed. Daily riparian evapotranspiration measured at the Bosque del Apache ET-tower was used to represent the impact of riparian water use. Results indicated that on average this reach of the river loses about 300 cfs and LFCC channel gains about 200 cfs. However the river loss or the LFCC channel gain vary by month with the highest loss occur during the month of June. This resulted in the monthly gain or loss in the reach by the flow in both the floodway and the LFCC. The gain or loss was put into twelve monthly three-column table slots in the two data objects FloodwaySanAcaciaToSanMarcialLoss and LFCCSanAcaciaToSanMarcialLoss.

To set the loss or gain to the reach objects in the San Acacia to San Marcial reach two rules were needed to use the look-up tables. The rules looked at the previous days flows at the San Acacia gages on the Rio Grande Floodway and the low flow conveyance channel and used the three-dimension table look-up function to determine the loss or gain for each of the reaches and set the local inflow on the reach object to the loss or gain value. The two rules were placed in a rule group named “Middle Valley Loss”.

Computational verification and calibration was completed on the new San Acacia to San Marcial reach. To ensure that the Physical model would perform the simulation of the gains or losses in the reach properly, a test model was used that included only the San Acacia to San Marcial reach and the adjacent Socorro Main Canal irrigation area. The actual flows for both the LFCC and the Rio Grande Floodway were used for the initial verification. After the simulation of the calendar year 1968 was completed, the results were compared to the actual flows for the two gages at San Marcial. There appeared to be a constant difference between the actual and the simulated gains or losses over the range of flows in June and July. After some analysis, a constant was added to the gain and loss values in the look-up tables for these two months. A verification simulation was then run for three additional years (1969, 1973, and 1975). The results for the verification simulation indicated that the results of the simulation were very close to the actual flows at both San Acacia gages for all three years. Additional calibration work can be done to fine tune the look-up tables.

As part of the upgrade of the San Acacia to San Marcial reach and the use of the look-up tables, the RiverWare objects in this reach were either moved, replaced, or deleted. The first change to the model was the move of the SocorroWastewater data object. Further investigation of the location of the outflow of the Socorro Waste Water Treatment Plant indicated that the data object was located in the wrong place in the model and linked to the wrong reach object. The treatment plant effluent was actually put into one of the drains that flowed into the Low Flow Conveyance

Channel. Because of the issue with the location, the object was moved near and linked to the Return Flow slot of the SanAcaciaToElephantButteCropDeepPercLosses object.

In the San Acacia to San Marcial reach many objects were removed or replaced by the look-up table design. The objects removed from the model are:

1) SanAcaciaLFCCToSanMarcialLFCCGWGains reach object
2) LFCCBifurcation bifurcation object
3) SanAcaciaToSanMarcialSeepageCalibration reach object
4) SanAcaciaToSanMarcialSeepageLag reach object
5) BlwSocorroWastewaterReach reach object
6) SanAcaciaToSanMarcial reach object
7) SanAcaciaToSanMarcialLocalInflow reach object.

The SanAcaciaToSanMarcialLosses reach object was used in the new setup but the methods used in reach calculations were changed. The seepage calculations were removed and the routing method was set to time lag routing. A new reach object was added to the Low Flow Conveyance Channel part of the reach, LFCCSanAcacia ToSanMarcialLosses. The new object was set up the same as the SanAcaciaToSanMarcialLosses reach object. These two reach objects have there slot for local inflow set to the loss or gain from the look-up table by rules.

Method for Determining Travel Time Lag (River Routing)

River routing describes the techniques used to account for the attenuation and downstream travel time of streamflow (hydrograph). The variable time lag method, which was described in the Rio Chama section, is also used for the reach from Cochiti to Elephant Butte Reservoir. Because river-channel morphology in the Middle Valley can be highly variable and the stream-gaging sites at the upstream and downstream ends of the reach may be unrepresentative of the reach as a whole, the variable time lags were further refined. Travel time lags were shifted using a range of multiplier factors. The appropriate shift factor was chosen on the basis of the series of routed flows that minimized the standard error with the observed flow at the downstream gage. In addition, travel times were calculated for identifiable peaks that could be tracked from an upstream to a downstream gage. In the shorter reaches of the Middle Valley, the standard error was insensitive and adjusting the multiplier chosen was necessary so that the standard error was small, yet the observed travel time for peaks was not violated. The following summarizes travel time determinations for reaches in the Middle Valley.

Rio Grande from Cochiti to San Felipe

The stream gage Rio Grande below Cochiti Dam is 700 ft downstream from Cochiti Dam. For approximately 15 mi, from Cochiti Dam to San Felipe, the Rio Grande consists of a sand and gravel riverbed and highly erodible, sandy banks. A reduction of sediment load from the dam has resulted in degradation and armoring of the riverbed and made relatively erodible banks increasingly more vulnerable. The storage and release of floodwaters have diminished the magnitude of peak flows, increased the duration of lower flows, and narrowed the river channel. Throughout this reach the river channel averages approximately 320 ft wide and the river's longitudinal slope is approximately 7 ft/mi.

Cochiti Dam is the beginning of the Middle Rio Grande Conservancy District (MRGCD) Cochiti Division. Diversions of water into the Sili Canal and the Cochiti East Side Main Canal bypass the gage Rio Grande below Cochiti Dam. These diversions are measured and are used in agricultural-depletion computations for the Middle Valley. Galisteo Creek is a major east-side tributary to the Rio Grande in this reach. It contributes little water, but is included in this reach routing.

Table 40 summarizes stream-gage and calibration data used in determining the power coefficient (wave velocity exponent) that is applied to average velocity measurements to determine river travel time lags in this reach (**graphs 105 and 106)**.

Table 40. Summary of stream-gage and calibration data for the reach of the Rio Grande from Cochiti to San Felipe

	Below Cochiti Dam	San Felipe	Total Δ
Period of analysis	10/23/79 – 7/31/98	9/21/70 – 10/7/98	
River mile (above mouth)	1588	1573	15
Elevation (feet above sea level)	5226	5116	110
Drainage area (square miles)	14,900	16,100	1200
Number of measurements	258	202	
Wave velocity exponent (β)	0.384	0.616	
Coefficient of determination (R^2)	0.85	0.92	

Table 41 summarizes factors used to determine travel time lags in this reach (**graph 107).**

Table 41. Adopted travel time lags (TL) for the reach of the Rio Grande from Cochiti to San Felipe

			Time lag (hours) for indicated flow rate (cfs)						
Gage	TL vs. Q equation	R^2	50	200	500	750	1000	3000	6000
San Felipe	$TL = 59.518Q^{-0.3834}$	0.8105	13	8	5	5	4	3	2
Adopted travel times for reach using a multiplier of 2.0→			27	16	11	9	8	6	4

When the wave velocity was computed, the gage cross sections were assumed to represent the entire routing reach. The Rio Grande below Cochiti Dam cross section is fixed because it has rip-rapped banks and the area remains relatively the same for most measurements. The Rio Grande at San Felipe cross section has a sand and gravel riverbed. The wave velocity exponent for the Rio Grande at San Felipe cross section has the greater R^2 value (**table 41**) and was used to determine a wave velocity for the reach from Cochiti to San Felipe. To test whether this cross section gives velocities that represent the entire reach, multipliers were applied to the routed flow and checked against the observed flow. A multiplier of 2.0 (**table 42**) best matched the observed flow, indicating that velocities obtained from the wave velocity formula were too fast. Increasing the travel time by a factor of 2.0 gave the best match. Nine data points from San Felipe stream-gage data were not used to determine the wave velocity exponent and travel times.

Rio Grande from San Felipe to Albuquerque

The stream gage Rio Grande at San Felipe is located 0.8 mi upstream from San Felipe Pueblo. The Rio Grande consists of a sand and gravel riverbed from San Felipe to Bernalillo and of a predominantly sand riverbed from Bernalillo to Albuquerque. The river has low, sandy, erodible banks in this area, and the wide sandy river channel has many bars. Levees line both sides of the river to protect heavily developed valley areas. A strip of riparian cottonwood bosque lies between the levees and riverbanks. Throughout this reach, the river channel averages approximately 420 ft wide and the river's longitudinal slope is approximately 5 ft/mi. The Water Control Manual for Cochiti Dam (U.S. Army Corps of Engineers, 1996b) designates 7000 cfs as the channel capacity at Albuquerque.

The effect of cutting off the sediment supply at Cochiti Dam has manifested itself in the upper part of this reach. The river channel is presently degrading throughout the reach, and gravel is appearing in the riverbed material.

Major tributaries in this reach include the Arroyo de las Barrancas, Arroyo de las Calabacillas, and Las Huertas Creek. In addition, AMAFCA's North Floodway Channel discharges into the Rio Grande and the Jemez River enters the Rio Grande just below Angostura Diversion Dam. Formerly, the Jemez River contributed a heavy sediment load to the Rio Grande, but Jemez Dam now controls the Jemez River sediment load near its mouth. Tributary inflow from the North Floodway Channel, Jemez River, and diversions at Angostura are modeled. The remaining tributaries are modeled as unmeasured local inflows. Wastewater inflow from the Bernalillo and Rio Rancho wastewater treatment plants is also modeled.

Table 42 summarizes stream-gage and calibration data used in determining the power coefficient (wave velocity exponent) that is applied to average velocity measurements to determine river travel time lags in this reach (**graphs 106 and 108**).

Table 42. Summary of stream-gage and calibration data for the reach of the Rio Grande from San Felipe to Albuquerque

	Rio Grande at San Felipe	Rio Grande at Albuquerque	Total Δ
Period of analysis	9/21/70 – 10/7/98	9/28/70 – 3/10/00	
River mile (above mouth)	1573	1540	33
Elevation (feet above sea level)	5116	4946	170
Drainage area (square miles)	16,100	17,440	1340
Number of measurements	202	991	
Wave velocity exponent (β)	0.616	0.734	
Coefficient of determination (R^2)	0.92	0.98	

Table 43 summarizes factors used to determine travel time lags in this reach (**graph 109**).

Table 43. Adopted travel time lags (TL) for the reach of the Rio Grande from San Felipe to Albuquerque

			Time lag (hours) for indicated flow rate (cfs)						
Gage	TL vs. Q equation	R^2	50	200	500	750	1000	3000	6000
Albuquerque	$TL = 92.49Q^{-0.2664}$	0.847	33	23	18	16	15	11	9
Adopted travel times for reach using a multiplier of 1.2→			39	27	21	19	18	13	11

The San Felipe and Albuquerque cross sections were assumed to represent the entire routing reach. The wave velocity exponent for the Rio Grande at Albuquerque cross section has the greater R^2 value (**table 42**) and was used to determine a wave velocity for the reach from San Felipe to Albuquerque. To test whether this cross section gives velocities representative of the entire reach, multipliers were applied to the routed flow and checked against the observed flow. A multiplier of 1.2 (**table 43**) best matched the observed flow, indicating that velocities obtained from the wave velocity formula were too fast. Increasing the travel time by a factor of 1.2 gave the best match. Nine data points from the stream-gage data for Rio Grande at San Felipe were not used in development of the wave velocity exponent determination. A total of 179 data points from the stream-gage data for Rio Grande at Albuquerque were not used to develop the wave velocity exponent or travel times.

Rio Grande from Albuquerque to Rio Grande Floodway near Bernardo

The stream gage for the Rio Grande at Albuquerque is on the downstream side of the Central Avenue Bridge. For approximately 53 mi from Albuquerque to the Rio Grande Floodway near Bernardo, the Rio Grande has a sand riverbed. The presence of numerous alternating bars and middle islands is a strong characteristic of this reach. In the lower part of the reach, the flood plain widens and salt cedar stands become denser. Throughout this reach the river channel averages between 420 and 510 ft wide when flowing bankfull.

AMAFCA's South Floodway Channel discharges into Tijeras Arroyo, which discharges into the Rio Grande in this reach. In the Albuquerque area over-bank flows are limited. Over-bank flooding starts below the Isleta diversion. In this reach riverbanks are well vegetated and more stable.

Discharge from the Albuquerque, Los Lunas, and Belen wastewater treatment plants; Tijeras Arroyo; and the diversions at Isleta Dam are modeled.

Table 44 summarizes stream-gage and calibration data used in determining the power coefficient (wave velocity exponent) that is applied to average velocity measurements to determine river travel time lags in this reach (**graphs 108 and 110)**.

Table 44. Summary of stream-gage and calibration data for the reach of the Rio Grande from Albuquerque to Rio Grande Floodway near Bernardo

	Rio Grande at Albuquerque	Rio Grande Floodway near Bernardo	Total Δ
Period of analysis	9/28/70 – 3/10/00	6/10/70 – 2/29/00	
River mile (above mouth)	1540	1487	53
Elevation (feet above sea level)	4946	4723	223
Drainage area (square miles)	17,440	19,230	1790
Number of measurements	991	649	
Wave velocity exponent (β)	0.734	0.751	
Coefficient of determination (R^2)	0.98	0.96	

Table 45 summarizes factors used to determine travel time lags in this reach (**graph 111**).

Table 45. Adopted travel time lags (TL) for the reach of the Rio Grande from Albuquerque to Rio Grande Floodway near Bernardo

Gage	TL vs. Q equation	R^2	Time lag (hours) for indicated flow rate (cfs)						
			50	200	500	750	1000	3000	6000
Albuquerque	$TL = 149.34Q^{-0.2664}$	0.847	53	36	29	26	24	18	15
Adopted travel times for reach using a multiplier of 1.5→			79	54	43	38	36	27	22

Fifteen data points for the gage Rio Grande Floodway near Bernardo were removed and not used to determine wave velocity exponent and travel times.

Rio Grande Floodway near Bernardo to Rio Grande Floodway at San Acacia

The gage Rio Grande Floodway near Bernardo is on the downstream side of the U.S. Highway 60 Bridge, 2 mi east of Bernardo, and 5 mi above the mouth of the Rio Puerco. The Rio Grande begins a transition below the confluence of the Rio Puerco between aggrading and degrading conditions. The system is generally degrading but periodically is subject to heavy sediment loads

from the Rio Puerco and the Rio Salado. Both tributaries are ephemeral and contribute heavy, sediment-laden flows during the summer. Between Bernardo and the Rio Puerco are dense salt cedar stands. The river channel averages approximately 560 ft wide when bankfull.

The RiverWare model for this reach includes flow routing, local inflow, tributary inflow, diversions, return flow from drains, evaporation, and ground-water gain or loss. The model includes reach objects for routing flow and computing local inflow. Tributary inflow from the Rio Puerco and diversions at the San Acacia Diversion Dam to the Socorro Main Canal and the Rio Grande Conveyance Channel are modeled. Also modeled in this reach is return flow from the lower San Francisco Riverside Drain and the Unit 7 Drain. Four streamflow gages near Bernardo measure the combined flow of the river and drains. Downstream near San Acacia, three streamflow gages measure the combined flow of the river and drains.

Table 46 summarizes stream-gage and calibration data used in determining the power coefficient (wave velocity exponent) that is applied to average velocity measurements to determine river travel time lags in this reach (**graphs 110 and 112**).

Table 46. Summary of stream-gage and calibration data for the reach of the Rio Grande from Rio Grande Floodway near Bernardo to Rio Grande Floodway at San Acacia

	Rio Grande Floodway near Bernardo	Rio Grande Floodway at San Acacia	Total Δ
Period of analysis	6/10/70 – 2/29/00	9/29/70 – 11/20/98	
River mile (above mouth)	1487	1473	14
Elevation (feet above sea level)	4723	4655	68
Drainage area (square miles)	19,230	26,770	7540
Number of measurements	646	881	
Wave velocity exponent (β)	0.751	0.755	
Coefficient of determination (R^2)	0.96	0.98	

Table 47 summarizes factors used to determine travel time lags in this reach (**graph 113**).

Table 47. Adopted travel time lags (TL) for the reach of the Rio Grande from Rio Grande Floodway near Bernardo to Rio Grande Floodway at San Acacia

Gage	TL vs. Q equation	R^2	Time lag (hours) for indicated flow rate (cfs)						
			50	200	500	750	1000	3000	6000
San Acacia	$TL = 26.776Q^{-0.2455}$	0.844	10	7	6	5	5	4	3
Adopted travel times for reach using a multiplier of 2.0→			21	15	12	11	10	8	6

Seven data points for the gage Rio Grande Floodway at San Acacia were removed and not used in determining wave velocity exponent and time lags.

Accounting of Measured Diversions, Return Flows, and Inflows

The Middle Valley model reaches isolate many losses or gains on the river. The model represents diversions from the MRGCD starting below Cochiti Lake. Historical diversion information from 1985 to 2001 was obtained from the MRGCD. Some of the water diverted for agricultural uses is known to eventually return to the river; until recently, however, return flow had never been measured. Return flow is now being measured, which will greatly increase the ability to predict the amount of water in the river. Because of a lack of historical return-flow data, the model was

built and calibrated to estimate total return flows on the basis of other known or empirically derived values.

All known measured diversions and returns to the Rio Grande are accounted for as described below. These data represent the effects of human activities in the basin, such as diversions and return flows for agricultural, municipal, and industrial uses.

Middle Rio Grande Conservancy District Diversion Data

Diversion data for the four MRGCD diversions are available and used in the agricultural-depletion and return-flow calculations for the Middle Rio Grande Valley. The USGS collects and publishes data on diversions at Cochiti Dam into the Cochiti Eastside Main Canal and Sili Canal and on flow of the Socorro Main Canal at San Acacia.

The records of daily diversion by the MRGCD at the Angostura Diversion Dam for the Atrisco feeder, Albuquerque Main Canal, and Algodones Riverside Drain, when available, and the Isleta Diversion Dam for the Belen High Line Canal and Peralta Main Canal were reviewed by plotting monthly hydrographs of average monthly discharge for each year to determine changes or trends in monthly diversions for each year of available data. Monthly hydrographs of daily data were plotted to compare each year's operation, view any abrupt or unusual changes in daily discharge, and evaluate the data relative to canal capacities. The review did not include evaluating the reliability of the stage-discharge relation or the record of stage. The USGS records of diversion at Cochiti Dam and San Acacia were not reviewed.

Data on the capacity of selected irrigation canals were taken from table F-8 of the Plan for Development (Bureau of Reclamation, 1947) and were listed as follows:

- Albuquerque Main Canal (intake capacity below heading): 570 cfs;
- Peralta Main Canal (intake capacity): 350 cfs; and
- Belen High Line Canal (intake capacity): 410 cfs.

Records were not reviewed of the relatively small discharge of the Cacique Acequia, Chical Acequia, and Chical Lateral, which all divert water from the Isleta Diversion Dam. The periods of record of data used in the review were 1978-95 for the Angostura diversions and 1974-95 for the Isleta diversions.

Monthly hydrographs of discharge for each year show greater amounts of water diverted during dry years, smaller amounts during wet years, and no major, long-term anomalies. Plots of daily data are difficult to interpret because of changing irrigation demands or operating practices.

Flow measured in the Socorro Main Canal may include flow from the Unit 7 Drain; flow diverted from the San Acacia Diversion Dam, or a combination from both sources. Flow in Unit 7 Drain was not measured on a daily basis prior to 2001. In the model flow in Unit 7 Drain is assumed to be equal to the sum of flow in the conveyance channel near Bernardo and the Bernardo Interior Drain. When flow in the Socorro Main Canal is less than flow in the Unit 7 Drain, the excess flow in the Unit 7 Drain is assumed to return through a gate to the Rio Grande above the San Acacia diversion. When flow in the Socorro Main Canal is more than flow in the Unit 7 Drain, additional flow to the Socorro Main Canal is assumed to divert from the Rio Grande through the San Acacia Diversion.

Estimate of Middle Rio Grande Conservancy District Agricultural Depletions

One part of estimating return-flow values is predicting how much water irrigated crops might use on a daily basis. Currently, no technology in the MRGCD fields accurately measures how much water each farmer is applying. One way to estimate crop usage, often called consumptive use, is to empirically derive the evapotranspiration (ET) rate for crops grown in the valley and multiply

the ET rate by the irrigated crop acreage. Although ET rates are still being investigated, some rates are available and are used to estimate crop water use. A USBR web site (ET toolbox) has been established that reports precipitation, temperature, solar radiation, and wind speed at pertinent weather stations along the Rio Grande. This information allows the USBR to compute ET rates using the modified Penman method. This information is then compiled and used in conjunction with geographic information system (GIS) land coverages of crop acreage in the Middle Valley to compute consumptive use. In the URGWOM model ET Toolbox crop evapotranspiration rates were multiplied by MRGCD and USBR estimates of annual, irrigated crop acreages to get annual estimates of crop consumptive use. Each Middle Valley reach in the URGWOM model accounts for historical irrigation diversions. The diversion request at each diversion dam is subtracted from river flow. Estimates of crop consumptive use, canal seepage, and deep percolation of applied irrigation water are subtracted, resulting in a daily estimate of agriculture depletions. Crop types predominantly grown and represented in the model are:

Alfalfa	Pasture grasses	Grapes
Sorghum	Wheat	Barley
Corn/silage	Chile peppers	Cotton
Nursery	Orchards	Silage
Oats	Misc. fruits	Melons
Misc. vegetables	Apples	

Measured Tributary Inflows and Return Flows

Measured inflows to the reach of the Rio Grande between Cochiti and Elephant Butte Reservoir that are modeled are compiled in **table 48**.

Table 48. Measured inflows that are modeled

Tributary inflow	Irrigation- and wastewater-return flow
Galisteo Creek	Bernalillo wastewater treatment plant
Jemez River	Rio Rancho wastewater treatment plant
AMAFCA North Floodway Channel	Albuquerque wastewater treatment plant
Tijeras Arroyo	Los Lunas wastewater treatment plant
South Diversion Channel	Belen wastewater treatment plant
Rio Puerco	Socorro wastewater treatment plant

Jemez River from the Gage near Jemez to Jemez Canyon Reservoir

The discharge from the Jemez River is accounted for as a measured inflow to the Rio Grande. This reach is 23.5 miles long. Inflow to this reach is from the Jemez Mountains and from snowpack runoff March through early June. The Rio Salado is the major tributary to the Jemez and enters the Jemez River near San Ysidro. About 2,700 acres are irrigable with water diverted from the Jemez River; however, no major diversion structures are in this reach. Inflow to this reach is recorded by the gage Jemez River near Jemez. Outflow from the reach and inflow to the Jemez Reservoir are estimated by the USBR on a daily basis. From 1953 to 1958 there was a gage above Jemez Canyon Dam. Outflow from Jemez Canyon Dam is recorded by the gage Jemez River below Jemez Canyon Dam and is the flow that the model uses as inflow to the Rio Grande at the confluence. No lag time or losses are considered between Jemez Canyon Dam and the confluence.

Table 49 summarizes stream-gage and calibration data used in determining the power coefficient (wave velocity exponent) that is applied to average velocity measurements to determine river travel time lags in this reach (**graph 114**).

Table 49. Summary of stream-gage and calibration data for the reach of the Jemez River near Jemez

	Jemez River near Jemez
Period of analysis	10/5/70 – 10/25/99
River mile (above mouth)	29.5
Elevation (feet above sea level)	5622
Drainage area (square miles)	470
Number of measurements	251
Wave velocity component (β)	0.5847
Coefficient of determination (R^2)	0.8719

Table 50 summarizes factors used to determine travel time lags in this reach (**graph 115**).

Table 50. Adopted travel time lags (TL) for the reach of the Jemez River near Jemez

			Time lag (hours) for indicated flow rate (cfs)					
Gage	TL vs. Q equation	R^2	25	50	100	200	400	1000+
Near Jemez	$TL=30.901Q^{-0.4167}$	0.766	11	7	5	4	3	1
	Adopted travel times for reach→		11	7	5	4	3	1

Channel losses were estimated using daily flows at the gage near Jemez and daily inflows to the Jemez Canyon Dam computed by the USBR. For some months, the coefficient of determination was very low. As a check, the 1953-58 data for the gages near Jemez and above Jemez Canyon Dam were used to determine channel losses. The remaining dataset, after filtering and removal of the data when flows had to be estimated at one or both gages, was sparse and probably not representative of the reach. In addition, the 1953-58 period was dry and not representative of the model period of 1985-96. Regressions using data for the gage above Jemez Canyon Dam and estimated daily inflows are presented in **table 51 and graphs 116-127**.

Table 51. Correlations between routed flow and estimated inflow and adopted monthly loss coefficients for the reach of the Jemez River from near Jemez to above Jemez Canyon Reservoir, 1985-96

Month	n (days)	y-slope	y-intercept	y-R^2	0-slope	R^2	Model coefficient	Adopted model coefficient	Adopted model constant
Jan	62	0.8708	-5.7	0.538	0.7014	0.515	-0.06	-0.06	-10.6
Feb	95	0.9427	-10.6	0.89	0.7476	0.837	-0.06	-0.06	-10.6
Mar	70	0.8798	-11.7	0.908	0.7727	0.888	-0.12	-0.12	-11.7
Apr	52	0.9226	-8.9	0.994	0.9013	0.993	-0.1	-0.1	0
May	88	0.9502	-21.9	0.958	0.8692	0.949	-0.13	-0.13	0
June	89	0.9098	-10.3	0.886	0.7897	0.886	-0.21	-0.21	0
July	53	0.6936	-3.2	0.702	0.6128	0.688	-0.16	-0.16	-6.4
Aug	39	0.8419	-6.4	0.826	0.6617	0.777	-0.16	-0.16	-6.4
Sept	34	0.5736	-1.9	0.702	0.5215	0.693	-0.16	-0.16	-6.4
Oct	62	0.5055	2.7	0.32	0.625	0.299	-0.14	-0.14	0
Nov	35	1.0198	-11	0.947	0.8611	0.906	-0.14	-0.14	0
Dec	29	0.2666	2	0.079	0.3774	0.064	-0.06	-0.06	-10.6

Regression equations with a 0-intercept were used for April through June and for October and November. For the other months the 0-intercept regression equation did not fit the data and equations with a non-0-intercept were used.

Estimates of Canal Seepage

Seepage from irrigation canals and laterals was modeled as infiltration to the ground-water system. Water infiltrating the ground-water system was assumed to percolate to the deep aquifer or to the water table. Canal seepage that percolated to the deep aquifer was assumed to be lost to the surface-water system, and canal seepage that percolated to the water table was assumed to return to the Rio Grande through the Middle Valley drain system. Canal seepage was apportioned to the deep aquifer and the water table on the basis of a USBR study.

The USBR studied the Middle Rio Grande Valley and analyzed seepage from canals and laterals (Bureau of Reclamation, 1997). This study identified seepage losses to the deep aquifer and the water table for 1935, 1955, 1975, and 1993 using soil surveys and other field data. The seepage rates and apportioning of water summarized in **table 52** for 1975 and 1993 were used in the RiverWare model. An average, canal, wetted perimeter of 15 ft was assumed. Some URGWOM study reaches included two USBR study units with different seepage rates. The increase in seepage rates between 1975 and 1993 for the San Felipe to Albuquerque reach is a result of the sediment-control effects of Cochiti Lake. In the RiverWare model, 1975 seepage rates were used for 1975-84 and 1993 seepage rates were used for 1985 to the present. Canal seepage was assumed to occur during the irrigation season (March 1 – October 31).

Table 52. Canal seepage rates for the Middle Rio Grande Valley

Reach	Canal length (miles)	Seepage rate (feet/day)	Daily seepage loss to deep aquifer (cfs)	Daily seepage loss to water table (cfs)
		1975		
Below Cochiti to San Felipe	99	0.4	0	36
San Felipe to Central Ave.	128 77	0.2 0.3	0 21	23 0
Central Ave. to Bernardo	98 386	0.3 0.2	27 0	0 71
Bernardo to San Acacia	175	0.2	0	32
San Acacia to Elephant Butte	103	0.2	0	19
		1993		
Below Cochiti to San Felipe	101	0.4	0	37
San Felipe to Central Ave.	134 78	0.4 0.3	0 21	49 0
Central Ave. to Bernardo	97 401	0.3 0.2	27 0	0 74
Bernardo to San Acacia	173	0.2	0	32
San Acacia to Elephant Butte	103	0.2	0	19

Historical Crop Acreage Data

Table 53 is a tabulation of annual irrigated-crop acreage for 1975-99 obtained from MRGCD and USBR annual crop acreage reports. The reporting of crop acreage categories by each entity was not consistent for 1975-99, so certain assumptions were made to make the categories consistent. Although these assumptions and some unreliable data resulted in some questionable values of individual crop acreage, the data in these tables represent the best effort at compiling the acreage values consistently.

For reaches above San Acacia, these data were then disaggregated into division data on the basis of percentage of irrigated acreage in each division to total, District-wide irrigated acreage. The data then were adjusted to estimate irrigated-crop acreage by URGWOM river reach. Irrigated acreage below San Acacia corresponds to the Socorro Division. The Socorro Division contains 18 percent of total MRGCD irrigated acreage. Annual crop acreage below San Acacia was estimated by multiplying total crop acreage by 0.18.

Table 53. Middle Rio Grande Conservancy District total irrigated-crop acreage, 1975-99

Year	Alfalfa	Pas-ture grass	Sor-ghum	Wheat	Corn	All pep-pers	Grapes	Melons	Fruit	Nur-sery	Other cere-al and oats
1975	36,726	9501	1331	773	1683	344	0	28	78	45	386
1976	32,004	8295	792	1074	2054	339	3	6	290	63	6329
1977	35,428	9854	967	1096	2697	765	10	145	307	176	660
1978	34,602	9739	487	813	1763	384	7	31	265	16	881
1979	31,486	9595	311	517	1968	403	19	16	287	7	310
1980	29,473	10,928	244	538	1752	394	35	71	165	41	399
1981	29,609	9103	176	490	2541	285	11	51	229	68	652
1982	31,779	9917	694	271	2184	430	75	48	286	111	730
1983	33,770	10,221	64	494	2248	480	90	60	305	123	91
1984	33,445	11,371	95	475	2222	455	115	50	290	132	125
1985	32,225	12,448	115	525	2241	505	140	55	290	150	171
1986	28,625	13,273	360	721	2755	560	180	105	290	175	285
1987	28,455	12,445	375	740	2645	555	180	81	275	185	310
1988	28,725	12,565	380	945	2843	575	140	90	275	185	355
1989	31,526	14,274	28	369	2673	687	73	104	547	516	1007
1990	28,697	13,979	168	564	576	719	56	29	407	625	0
1991	28,725	12,565	380	945	2843	575	140	90	275	185	355
1992	28,835	13,125	400	915	2867	595	140	105	175	190	330
1993	20,921	15,677	48	2024	2000	1376	9	57	342	2343	2433
1994	30,837	15,848	0	0	0	896	7	0	294	22	0
1995	23,336	17,517	0	0	0	811	64	0	202	0	0
1996	25,712	17,813	184	652	3860	631	19	0	197	0	859
1997	25,739	16,204	562	910	4057	606	40	30	207	243	954
1998	26,974	15,611	214	557	3774	523	11	19	192	296	1001
1999	26,699	15,604	172	475	3849	506	28	48	180	318	1002

Table 53. Middle Rio Grande Conservancy District total irrigated-crop acreage, 1975-99—Concluded

Year	Misc. fruit	Misc. vege-tables	Garden	Not har-ves-ted	Barley	Hay	Si-lage	Cotton	Sum of irriga-ted acres	Fallow land	Sum of irriga-ted + fallow
1975	4	398	712	1173	668	988	3461	0	58,299	9076	67,375
1976	0	246	239	4	864	2889	3802	0	59,293	8195	67,488
1977	0	843	420	128	817	2161	3757	0	60,231	6919	67,150
1978	4	311	507	421	740	3610	4284	0	58,865	9945	68,810
1979	7	312	287	663	312	2366	4263	0	53,129	13,991	67,120
1980	0	554	583	715	632	2781	4566	0	53,871	14,256	68,127
1981	0	430	125	842	543	3952	5284	0	54,391	13,541	67,932
1982	6	565	495	117	9	3227	3484	0	54,428	14,902	69,330
1983	18	668	625	250	349	3625	2848	0	56,329	13,812	70,141
1984	18	646	635	265	375	3740	2873	0	57,327	12,945	70,272
1985	21	730	759	275	380	4608	2945	0	58,583	11,648	70,231
1986	21	943	885	285	395	5042	3331	0	58,231	11,821	70,052
1987	21	869	795	290	390	4696	2995	0	56,302	13,680	69,982
1988	21	944	825	283	395	4512	3433	0	57,491	12,343	69,834
1989	0	939	825	400	0	2651	0	12	56,631	12,549	69,180
1990	0	611	599	400	56	4640	2306	38	54,470	14,481	68,951
1991	21	944	825	283	395	4512	3433	0	57,491	12,343	69,834
1992	21	931	975	295	395	4343	3067	0	57,704	12,241	69,945
1993	15	1244	552	2329	7	1952	1296	0	54,625	14,511	69,136
1994	0	0	168	300	0	2664	3621	0	54,657	15,000	69,657
1995	0	0	159	0	0	3601	3998	0	49,718	5087	54,805
1996	1	17	835	0	0	2131	4104	0	57,015	10,240	67,255
1997	44	192	185	0	0	2244	0	0	52,217	9443	61,660
1998	29	149	133	0	0	1441	15	0	50,937	10,073	61,010
1999	39	276	126	0	0	1357	0	0	50,680	10,366	61,046

Table 54 lists the irrigable acreage and percentage of total acreage in each MRGCD division to the District total based on 1995 MRGCD land-use coverage (GIS) that included irrigated crops, pasture, idle, and fallow. The annual crop census data were then adjusted, as described below, to develop crop acreages that could be used in URGWOM river reaches.

Table 54. Middle Rio Grande Conservancy District (MRGCD) irrigable acreage, by division, and as percentage of total irrigated acreage

MRGCD division	Irrigable acreage	Percentage of total
Cochiti	4593	6
Albuquerque	23,456	29
Belen	37,303	47
Socorro	14,524	18
Total	79,876	100

The URGWOM river reach from Cochiti to San Felipe extends to the gage Rio Grande at San Felipe; the MRGCD's Cochiti Division extends an additional 6 mi downstream to the Angostura

Diversion Dam. Based on 1995 MRGCD GIS land-use coverage, an estimated 25 percent of irrigable lands in the Cochiti Division are in the reach between San Felipe and Angostura. This percentage was applied to annual irrigated acreage in the Cochiti Division, and the crop acreage for the Cochiti Division was reduced by 25 percent to calculate crop data for the URGWOM reach from Cochiti to San Felipe.

Table 55 is a tabulation of annual irrigated-crop acreage used in the Cochiti to San Felipe reach.

Table 55. Annual irrigated-crop acreage, Cochiti to San Felipe, 1975-99

Year	Alfalfa	Pas-ture grass	Sor-ghum	Wheat	Corn	All pep-pers	Grapes	Melons	Fruit	Nur-sery	Other cereal and oats
1975	1653	428	60	35	76	15	0	1	4	2	17
1976	1440	373	36	48	92	15	0	0	13	3	285
1977	1594	443	44	49	121	34	0	7	14	8	30
1978	1557	438	22	37	79	17	0	1	12	1	40
1979	1417	432	14	23	89	18	1	1	13	0	14
1980	1326	492	11	24	79	18	2	3	7	2	18
1981	1332	410	8	22	114	13	0	2	10	3	29
1982	1430	446	31	12	98	19	3	2	13	5	33
1983	1520	460	3	22	101	22	4	3	14	6	4
1984	1505	512	4	21	100	20	5	2	13	6	6
1985	1450	560	5	24	101	23	6	2	13	7	8
1986	1288	597	16	32	124	25	8	5	13	8	13
1987	1280	560	17	33	119	25	8	4	12	8	14
1988	1293	565	17	43	128	26	6	4	12	8	16
1989	1419	642	1	17	120	31	3	5	25	23	45
1990	1291	629	8	25	26	32	3	1	18	28	0
1991	1293	565	17	43	128	26	6	4	12	8	16
1992	1298	591	18	41	129	27	6	5	8	9	15
1993	941	705	2	91	90	62	0	3	15	105	109
1994	1388	713	0	0	0	40	0	0	13	1	0
1995	1051	788	0	0	0	36	3	0	9	0	0
1996	1157	802	8	29	174	28	1	0	9	0	39
1997	1158	729	25	41	183	27	2	1	9	11	43
1998	1214	703	10	25	170	24	0	1	9	13	45
1999	1201	702	8	21	173	23	1	2	8	14	45

Table 55. Annual irrigated-crop acreage, Cochiti to San Felipe, 1975-99—Concluded

Year	Misc. fruit	Misc. vege-tables	Garden	Not harvested	Barley	Hay	Si-lage	Cotton	Sum of irriga-ted acres	Fallow land	Sum of irriga-ted + fallow
1975	0	18	32	53	30	44	156	0	2623	408	3032
1976	0	11	11	0	39	130	171	0	2668	369	3037
1977	0	38	19	6	37	97	169	0	2710	311	3022
1978	0	14	23	19	33	162	193	0	2649	448	3096
1979	0	14	13	30	14	106	192	0	2391	630	3020
1980	0	25	26	32	28	125	205	0	2424	642	3066
1981	0	19	6	38	24	178	238	0	2448	609	3057
1982	0	25	22	5	0	145	157	0	2449	671	3120
1983	1	30	28	11	16	163	128	0	2535	622	3156
1984	1	29	29	12	17	168	129	0	2580	583	3162
1985	1	33	34	12	17	207	133	0	2636	524	3160
1986	1	42	40	13	18	227	150	0	2620	532	3152
1987	1	39	36	13	18	211	135	0	2534	616	3149
1988	1	42	37	13	18	203	154	0	2587	555	3143
1989	0	42	37	18	0	119	0	1	2548	565	3113
1990	0	27	27	18	3	209	104	2	2451	652	3103
1991	1	42	37	13	18	203	154	0	2587	555	3143
1992	1	42	44	13	18	195	138	0	2597	551	3148
1993	1	56	25	105	0	88	58	0	2458	653	3111
1994	0	0	8	14	0	120	163	0	2460	675	3135
1995	0	0	7	0	0	162	180	0	2237	229	2466
1996	0	1	38	0	0	96	185	0	2566	461	3026
1997	2	9	8	0	0	101	0	0	2350	425	2775
1998	1	7	6	0	0	65	1	0	2292	453	2745
1999	2	12	6	0	0	61	0	0	2281	466	2747

The MRGCD Albuquerque Division extends from Angostura to Isleta; the URGWOM San Felipe to Albuquerque reach extends to the gage Rio Grande at Albuquerque, 14 mi above Isleta Dam. Based on MRGCD GIS land-use coverage, about 46 percent of irrigated lands in the Albuquerque District are located between the Albuquerque gage and Isleta Dam. Therefore, the irrigated-crop acreage for the San Felipe to Albuquerque reach was estimated by adding 25 percent of Cochiti Division crop acreage to Albuquerque Division acreage after reducing the initial Albuquerque Division acreage by 46 percent. **Table 56** is a tabulation of annual irrigated-crop acreage for the reach from San Felipe to Albuquerque.

Table 56. Annual irrigated-crop acreage, San Felipe to Albuquerque, 1975-99

Year	Alfalfa	Pas-ture grass	Sor-ghum	Wheat	Corn	All pep-pers	Grapes	Melons	Fruit	Nur-sery	Other cereal and oats
1975	6302	1630	228	133	289	59	0	5	13	8	66
1976	5492	1423	136	184	352	58	1	1	50	11	1086
1977	6079	1691	166	188	463	131	2	25	53	30	113
1978	5938	1671	84	140	303	66	1	5	45	3	151
1979	5403	1647	53	89	338	69	3	3	49	1	53
1980	5058	1875	42	92	301	68	6	12	28	7	68
1981	5081	1562	30	84	436	49	2	9	39	12	112
1982	5453	1702	119	47	375	74	13	8	49	19	125
1983	5795	1754	11	85	386	82	15	10	52	21	16
1984	5739	1951	16	82	381	78	20	9	50	23	21
1985	5530	2136	20	90	385	87	24	9	50	26	29
1986	4912	2278	62	124	473	96	31	18	50	30	49
1987	4883	2136	64	127	454	95	31	14	47	32	53
1988	4929	2156	65	162	488	99	24	15	47	32	61
1989	5410	2449	5	63	459	118	13	18	94	89	173
1990	4924	2399	29	97	99	123	10	5	70	107	0
1991	4929	2156	65	162	488	99	24	15	47	32	61
1992	4948	2252	69	157	492	102	24	18	30	33	57
1993	3590	2690	8	347	343	236	2	10	59	402	418
1994	5292	2720	0	0	0	154	1	0	50	4	0
1995	4010	3006	0	0	0	139	11	0	35	0	0
1996	4412	3057	32	112	662	108	3	0	34	0	147
1997	4417	2781	96	156	696	104	7	5	36	42	164
1998	4629	2679	37	96	648	90	2	3	33	51	172
1999	4582	2678	30	82	660	87	5	8	31	55	172

Table 56. Annual irrigated-crop acreage, San Felipe to Albuquerque, 1975-99—Concluded

Year	Misc. fruit	Misc. vege-tables	Garden	Not har-vested	Barley	Hay	Si-lage	Cotton	Sum of irriga-ted acres	Fallow land	Sum of irriga-ted + fallow
1975	1	68	122	201	115	170	594	0	10,004	1557	11,562
1976	0	42	41	1	148	496	652	0	10,175	1406	11,581
1977	0	145	72	22	140	371	645	0	10,336	1187	11,523
1978	1	53	87	72	127	619	735	0	10,101	1707	11,808
1979	1	54	49	114	54	406	732	0	9117	2401	11,518
1980	0	95	100	123	108	477	784	0	9244	2446	11,691
1981	0	74	21	144	93	678	907	0	9333	2324	11,657
1982	1	97	85	20	2	554	598	0	9340	2557	11,897
1983	3	115	107	43	60	622	489	0	9666	2370	12,036
1984	3	111	109	45	64	642	493	0	9837	2221	12,059
1985	4	125	130	47	65	791	505	0	10,053	1999	12,052
1986	4	162	152	49	68	865	572	0	9992	2028	12,021
1987	4	149	136	50	67	806	514	0	9661	2347	12,009
1988	4	162	142	49	68	774	589	0	9865	2118	11,984
1989	0	161	142	69	0	455	0	2	9718	2153	11,871
1990	0	105	103	69	10	796	396	7	9347	2485	11,832
1991	4	162	142	49	68	774	589	0	9865	2118	11,984
1992	4	160	167	51	68	745	526	0	9902	2101	12,003
1993	3	213	95	400	1	335	222	0	9374	2490	11,864
1994	0	0	29	51	0	457	621	0	9379	2574	11,953
1995	0	0	27	0	0	618	686	0	8532	873	9405
1996	0	3	143	0	0	366	704	0	9784	1757	11,541
1997	8	33	32	0	0	385	0	0	8960	1620	10,581
1998	5	26	23	0	0	247	2	0	8741	1728	10,469
1999	7	47	22	0	0	233	0	0	8697	1779	10,476

The MRGCD Belen Division extends from Isleta Dam to just above San Acacia Dam. The URGWOM reach from Albuquerque to Bernardo extends to the gage Rio Grande Floodway at Bernardo, about 14 mi above the San Acacia dam. Based on 1995 MRGCD GIS land-use coverage, all irrigated acres in the Belen Division were assumed to be located above the Bernardo gage. Therefore, the irrigated-crop acreage for the Albuquerque to Bernardo reach was estimated by adding 46 percent of Albuquerque Division irrigated-crop acreage to Belen Division irrigated-crop acreage. **Table 57** is a tabulation of annual irrigated-crop acreage for the reach from Albuquerque to Bernardo.

Table 57. Annual irrigated-crop acreage, Albuquerque to Rio Grande Floodway near Bernardo, 1975-99

Year	Alfalfa	Pas-ture grass	Sor-ghum	Wheat	Corn	All pep-pers	Grapes	Melons	Fruit	Nur-sery	Other cereal and oats
1975	22,160	5733	803	466	1016	208	0	17	47	27	233
1976	19,311	5005	478	648	1239	205	2	4	175	38	3819
1977	21,377	5946	583	661	1627	462	6	87	185	106	398
1978	20,879	5877	294	491	1064	232	4	19	160	10	532
1979	18,999	5790	188	312	1187	243	11	10	173	4	187
1980	17,784	6594	147	325	1057	238	21	43	100	25	241
1981	17,866	5493	106	296	1533	172	7	31	138	41	393
1982	19,175	5984	419	164	1318	259	45	29	173	67	440
1983	20,377	6167	39	298	1356	290	54	36	184	74	55
1984	20,181	6861	57	287	1341	275	69	30	175	80	75
1985	19,445	7511	69	317	1352	305	84	33	175	91	103
1986	17,272	8009	217	435	1662	338	109	63	175	106	172
1987	17,170	7509	226	447	1596	335	109	49	166	112	187
1988	17,333	7582	229	570	1715	347	84	54	166	112	214
1989	19,023	8613	17	223	1613	415	44	63	330	311	608
1990	17,316	8435	101	340	348	434	34	17	246	377	0
1991	17,333	7582	229	570	1715	347	84	54	166	112	214
1992	17,399	7920	241	552	1730	359	84	63	106	115	199
1993	12,624	9460	29	1221	1207	830	5	34	206	1414	1468
1994	18,607	9563	0	0	0	541	4	0	177	13	0
1995	14,099	10,570	0	0	0	489	39	0	122	0	0
1996	15,515	10,748	111	393	2329	381	11	0	119	0	518
1997	15,531	9778	339	549	2448	366	24	18	125	147	576
1998	16,276	9420	129	336	2277	315	7	11	116	179	604
1999	16,110	9416	104	287	2322	305	17	29	109	192	604

Table 57. Annual irrigated-crop acreage, Albuquerque to Rio Grande Floodway near Bernardo, 1975-99—Concluded

Year	Misc. fruit	Misc. vege-tables	Gar-den	Not har-vested	Barley	Hay	Si-lage	Cotton	Sum of irriga-ted acres	Fallow land	Sum of irriga-ted + fallow
1975	2	240	430	708	403	596	2088	0	35,178	5476	40,654
1976	0	148	144	2	521	1743	2294	0	35,777	4945	40,722
1977	0	509	253	77	493	1304	2267	0	36,343	4175	40,518
1978	2	188	306	254	447	2178	2585	0	35,519	6001	41,520
1979	4	188	173	400	188	1428	2572	0	32,058	8442	40,500
1980	0	334	352	431	381	1678	2755	0	32,506	8602	41,108
1981	0	259	75	508	328	2385	3188	0	32,820	8171	40,990
1982	4	341	299	71	5	1947	2102	0	32,842	8992	41,834
1983	11	403	377	151	211	2187	1718	0	33,989	8334	42,323
1984	11	390	383	160	226	2257	1734	0	34,591	7811	42,402
1985	13	440	458	166	229	2780	1777	0	35,349	7028	42,377
1986	13	569	534	172	238	3042	2010	0	35,137	7133	42,269
1987	13	524	480	175	235	2834	1807	0	33,973	8255	42,227
1988	13	570	498	171	238	2723	2071	0	34,690	7448	42,138
1989	0	567	498	241	0	1600	0	7	34,171	7572	41,743
1990	0	369	361	241	34	2800	1391	23	32,867	8738	41,605
1991	13	570	498	171	238	2723	2071	0	34,690	7448	42,138
1992	13	562	588	178	238	2621	1851	0	34,819	7386	42,205
1993	9	751	333	1405	4	1178	782	0	32,961	8756	41,717
1994	0	0	101	181	0	1607	2185	0	32,980	9051	42,031
1995	0	0	96	0	0	2173	2412	0	30,000	3069	33,069
1996	1	10	504	0	0	1286	2476	0	34,403	6179	40,582
1997	27	116	112	0	0	1354	0	0	31,508	5698	37,206
1998	17	90	80	0	0	869	9	0	30,735	6078	36,813
1999	24	166	76	0	0	819	0	0	30,580	6255	36,835

La Joya Community Ditch serves irrigated lands in the Bernardo to San Acacia reach. Because this ditch is not part of the MRGCD, MRGCD does not report acreage for these irrigated lands. Based on 2000 New Mexico Interstate Stream Commission GIS irrigated-acreage data, irrigable acreage in this reach was estimated to be 250 acres. This 250 acres is not currently modeled, but could be added as a model object should historical data for annual crop acreage become available. **Table 58** is a tabulation of annual irrigated-crop acreage for the reach from Rio Grande Floodway near San Acacia to Elephant Butte Reservoir.

Table 58. Annual irrigated-crop acreage, Rio Grande Floodway at San Acacia to Elephant Butte Reservoir

Year	Alfalfa	Pas-ture grass	Sor-ghum	Wheat	Corn	All pep-pers	Grapes	Melons	Apple fruit	Nur-sery	Other cereal and oats
1975	6611	1710	240	139	303	62	0	5	14	8	69
1976	5761	1493	143	193	370	61	1	1	52	11	1139
1977	6377	1774	174	197	485	138	2	26	55	32	119
1978	6228	1753	88	146	317	69	1	6	48	3	159
1979	5667	1727	56	93	354	73	3	3	52	1	56
1980	5305	1967	44	97	315	71	6	13	30	7	72
1981	5330	1639	32	88	457	51	2	9	41	12	117
1982	5720	1785	125	49	393	77	14	9	51	20	131
1983	6079	1840	12	89	405	86	16	11	55	22	16
1984	6020	2047	17	86	400	82	21	9	52	24	23
1985	5801	2241	21	95	403	91	25	10	52	27	31
1986	5153	2389	65	130	496	101	32	19	52	32	51
1987	5122	2240	68	133	476	100	32	15	50	33	56
1988	5171	2262	68	170	512	104	25	16	50	33	64
1989	5675	2569	5	66	481	124	13	19	98	93	181
1990	5165	2516	30	102	104	129	10	5	73	113	0
1991	5171	2262	68	170	512	104	25	16	50	33	64
1992	5190	2363	72	165	516	107	25	19	32	34	59
1993	3766	2822	9	364	360	248	2	10	62	422	438
1994	5551	2853	0	0	0	161	1	0	53	4	0
1995	4206	3153	0	0	0	146	12	0	36	0	0
1996	4628	3206	33	117	695	114	3	0	35	0	155
1997	4633	2917	101	164	730	109	7	5	37	44	172
1998	4855	2810	38	100	679	94	2	3	35	53	180
1999	4806	2809	31	86	693	91	5	9	32	57	180

Table 58. Annual irrigated-crop acreage, Rio Grande Floodway at San Acacia to Elephant Butte Reservoir—Concluded

Year	Misc. fruit	Misc. vege-tables	Gar-den	Not har-vested	Barley	Hay	Si-lage	Cotton	Cropped delta	Sum of irriga-ted acres	Fallow land	Sum of irriga-ted + fallow
1975	1	72	128	211	120	178	623	0	0	10,494	1634	12,128
1976	0	44	43	1	156	520	684	0	-20	10,652	1475	12,128
1977	0	152	76	23	147	389	676	0	0	10,842	1245	12,087
1978	1	56	91	76	133	650	771	0	0	10,596	1790	12,386
1979	1	56	52	119	56	426	767	0	-63	9500	2518	12,019
1980	0	100	105	129	114	501	822	0	-39	9658	2566	12,224
1981	0	77	23	152	98	711	951	0	-87	9703	2437	12,140
1982	1	102	89	21	2	581	627	0	-12	9785	2682	12,467
1983	3	120	113	45	63	653	513	0	-15	10,124	2486	12,610
1984	3	116	114	48	68	673	517	0	-17	10,302	2330	12,632
1985	4	131	137	50	68	829	530	0	-27	10,518	2097	12,615
1986	4	170	159	51	71	908	600	0	-27	10,455	2128	12,582
1987	4	156	143	52	70	845	539	0	-32	10,103	2462	12,565
1988	4	170	149	51	71	812	618	0	-27	10,321	2222	12,543
1989	0	169	149	72	0	477	0	2	-54	10,140	2259	12,398
1990	0	110	108	72	10	835	415	7	-60	9744	2607	12,351
1991	4	170	149	51	71	812	618	0	-27	10,321	2222	12,543
1992	4	168	176	53	71	782	552	0	-32	10,355	2203	12,559
1993	3	224	99	419	1	351	233	0	0	9833	2612	12,444
1994	0	0	30	54	0	480	652	0	-162	9676	2700	12,376
1995	0	0	29	0	0	648	720	0	0	8949	916	9865
1996	0	3	150	0	0	384	739	0	-47	10,216	1843	12,059
1997	8	35	33	0	0	404	0	0	-106	9293	1700	10,993
1998	5	27	24	0	0	259	3	0	0	9169	1813	10,982
1999	7	50	0	0	0	244	0	0	0	9100		

Estimates of Crop Consumptive Use

Crop consumptive use is equal to the estimated annual crop census acreages multiplied by the evapotranspiration rates developed for the ET Toolbox (King and Bawazir, 1998). In the model, crop consumptive use is subtracted from irrigation diversions, thus reducing the amount of irrigation water available to return to the river.

Estimates of Riparian Consumptive Use

Riparian consumptive use is equal to the consumptive use reported for bosque by the ET Toolbox. In the model, riparian consumptive use is subtracted from the river leakage, if river leakage is positive and greater than riparian consumptive use. If river leakage is positive but less than riparian consumptive use, the amount of the consumptive use equal to the river leakage is subtracted. If river leakage is negative, meaning that there is a groundwater gradient toward the river and the river reach is a gaining reach rather than a losing reach, then the riparian consumptive use is not subtracted from river leakage.

Estimate of Deep Percolation for Irrigation Diversion

Deep percolation is the amount of infiltrated water per irrigation event that is not used by crops, moves through the soil profile to the water table, and does not return to the river by way of drains. Deep percolation from rainfall on crops is assumed to be negligible. The USBR (1997, supporting document 7) analyzed soil texture and permeability in the Middle Rio Grande Valley. Deep percolation rates for soil series and crop types range from 0.10 to 1.22 ft/yr in that document. A deep percolation rate of 1.0 acre-ft/acre/yr was applied to crop acreages. Deep percolation is modeled as a loss to the amount diverted.

Computation of Unmeasured Return Flows

Water diverted into MRGCD canals is depleted by crop consumptive use, canal seepage, and deep percolation. The remainder of diverted water returns to the river through MRGCD drains and wasteways. The model allows a proportion of river leakage to be intercepted by riverside drains. Below San Acacia, modelers assumed that the low-flow conveyance channel intercepted a proportion of river leakage. The model calculates the remainder of diverted water that may return to the river or flow downstream in the parallel channel that represents combined flow in the drains and canals. The proportion of river leakage intercepted by riverside drains is set during the calibration process. A mass-balance process constrained by the known flow at streamflow gages at the upstream and downstream ends of the channel representing combined flow in the drains and canals computes the excess flow and returns it to the main channel as return flow.

Computation of Unmeasured Tributary Inflow

Unmeasured Tributary Inflow in the middle valley represents the unmeasured streamflow gain within a reach resulting from a precipitation event. A rainfall-runoff model, such as the U.S. Geological Survey's Modular Modeling System or the U.S. Army Corps of Engineers' Hydrologic Engineering Center Hydrological Modeling System, is planned to calculate inflow resulting from a precipitation event and would be entered into the URGWOM model as a local inflow.

Rio Grande Floodway at San Acacia to Rio Grande Floodway at San Marcial

This reach begins at the San Acacia Diversion Dam. Flow arriving at the dam is divided into three components: (1) the Rio Grande Floodway, the actual river channel, (2) the Rio Grande Conveyance Channel, also referred to as the low-flow conveyance channel (LFCC), a manmade channel constructed in the late 1950's to efficiently carry Rio Grande flows to Elephant Butte Reservoir, and (3) the Socorro Main Canal, the source of irrigation water for farms to the south. The other inflow into the reach is the Unit 7 Drain, which flows into the Socorro Main Canal just below the dam. The gage on the Rio Grande Floodway is approximately 0.2 mi below the dam, the gage on the LFCC is 1.2 mi south of the dam, and the gage on the Socorro Main Canal is 0.5 mi below the dam **(fig. 12)**.

During the 1960's and 1970's most non-flood flow in the Rio Grande was diverted into the LFCC. The LFCC has a capacity of approximately 2000 cfs. During the 1980's and 1990's, however, water was diverted infrequently, then eventually not at all.

The floodway has seen significant aggradation. Toward the lower section of the reach, the river is above the level of the surrounding valley. Leakage is significant from the river channel into the LFCC. The channel profile varies greatly through the reach: some sections are broad and shallow, whereas others are narrow and deep.

Currently, water from the LFCC can be returned to the floodway in only one location by gravity. Prior to aggradation of the floodway channel, discharge from the LFCC was diverted to the floodway at other locations as operation and maintenance dictated.

The LFCC also serves as both a drain collecting irrigation-return flows at certain locations and as a source of irrigation supply. Check structures provide adequate head to deliver water into adjoining laterals.

Table 59 summarizes stream-gage and calibration data used in determining the power coefficient (wave velocity exponent) that is applied to average velocity measurements to determine river travel time lags in this reach (**graphs 112 and 128**).

Table 59. Summary of stream-gage and calibration data for the reach of the Rio Grande from Rio Grande Floodway at San Acacia to Rio Grande Floodway at San Marcial

	Rio Grande Floodway at San Acacia	Rio Grande Floodway at San Marcial	Total Δ
Period of analysis	1970-84	1970-84	
River mile (above mouth)	1473	1425	48
Elevation (feet above sea level)	4654	4455	199
Drainage area (square miles)	26,770	27,700	930
Number of measurements	483	340	
Wave velocity exponent (β)	0.7469	0.7058	
Coefficient of determination (R^2)	0.98	0.97	

Table 60 summarizes factors used to determine travel time lags in this reach (**graphs 129 and 130**).

Table 60. Adopted travel time lags (TL) for the reach of the Rio Grande from Rio Grande Floodway at San Acacia to Rio Grande Floodway at San Marcial

			Time lag (hours) for indicated flow rate (cfs)						
Gage	TL vs. Q equation	R^2	50	200	500	750	1000	3000	6000
San Acacia	$TL = 136.15Q^{-0.255}$	0.87	49	35	27	25	23	17	15
San Marcial	$TL = 161.78Q^{-0.2942}$	0.85	49	32	25	22	20	15	12
	Adopted travel times for reach→		49	34	26	23	22	16	13

The two gages used for this reach are Rio Grande Floodway at San Acacia and Rio Grande Floodway at San Marcial. The Rio Grande has been gaged at San Acacia since 1936, but the site has been moved several times since its installation. The site was moved to its present location in 1965. From 1958 to 1964, flow into the conveyance channel was included in total flow; since 1964, data for the conveyance channel and the floodway have been reported separately. The Rio Grande has been gaged at San Marcial since 1895. Flows in the floodway were separated from those in the conveyance channel in 1964.

The velocities obtained from the wave velocity formula appeared to be too high based on observed conditions. Because this is a highly variable reach, the cross sections at the gaging stations may not be representative of cross sections found along the length of the reach. After the model was run using several different lag times both greater and less than that obtained from the formula, it was determined that increasing the lag time by 60 percent increased the R^2 value obtained for the regression equation of computed versus observed flow. The lag times also were very close to those widely used as estimates of travel time lags from San Acacia to San Marcial.

Rio Grande Floodway and Low-Flow Conveyance Channel at San Marcial to Elephant Butte Reservoir

Flow into Elephant Butte Reservoir from San Marcial is through both the Rio Grande Floodway and the LFCC. Flow from the two waterways used to merge above the reservoir. Flooding and sediment deposition have now caused the flows to enter separately.

There are gaging stations on the river and LFCC at San Marcial. Inflow into the reservoir is calculated using a reservoir budget computation, which takes into account outflows and evaporation losses. The top of the conservation pool is at an elevation of 4407 ft. At this elevation the beginning of the reservoir is just below the San Marcial gage. Elephant Butte Dam is approximately 42 mi downstream from the gage. The reservoir stage has been as low as 4220 ft in 1953 and as high as 4409 ft in 1942. This wide range of pool elevations also means a wide range of reservoir lengths that would affect routing. The model currently does not have a method to vary the lag time of a reach based on a changing reach length caused by a rising or falling reservoir stage downstream. The distance between the San Marcial gage and the head of the reservoir was varied to determine the best relation (highest R^2) between observed flow and routed flow.

No diversions or drains (except for the LFCC) are in this reach. There is a large expanse of riparian vegetation, mainly west of the river, from below San Marcial to the head of the reservoir.

Table 61 summarizes stream-gage and calibration data used in determining the power coefficient (wave velocity exponent) that is applied to average velocity measurements to determine river travel time lags in this reach (**graph 128).**

Table 61. Summary of stream-gage and calibration data for the reach of the Rio Grande from Rio Grande Floodway at San Marcial to Rio Grande at Elephant Butte Reservoir

	Rio Grande Floodway at San Marcial	Rio Grande at Elephant Butte Reservoir	Total Δ
Period of analysis	1970-84	1970-84	
River mile (above mouth)	1425	1383	42
Elevation (feet above sea level)	4455	[1]4209	246
Drainage area (square miles)	27,700	29,400	2600
Number of measurements	340	n/a	
Wave velocity exponent (β)	0.7058	n/a	
Coefficient of determination (R^2)	0.97	n/a	

[1]Power-house tail-water elevation.

Table 62 summarizes factors used to determine travel time lags in this reach (**graph 131**).

Table 62. Adopted travel time lags (TL) for the reach of the Rio Grande from Rio Grande Floodway at San Marcial to Elephant Butte Reservoir

			Time lag (hours) for indicated flow rate (cfs)						
Gage	TL vs. Q equation	R^2	50	200	500	750	1000	3000	6000
San Marcial	$TL = 84.521Q^{-0.2942}$	0.85	27	18	14	12	11	8	7
	Adopted travel times for reach→		27	18	14	12	11	8	7

Flow into Elephant Butte Reservoir is through both the Rio Grande and the LFCC. Because only one inflow to the reservoir is calculated, all flow was assumed to be routed in the same manner.

Elephant Butte is a large reservoir, so calculating the proper lag times was difficult. Values were obtained using regression analysis that yielded the highest R^2 values. Actual inflow values were sometimes very suspect, which made calibration difficult. This is a highly variable reach as evident from the low R^2 values obtained for the loss analysis.

The San Acacia to San Marcial Floodway reach was calibrated using data from January 1, 1987, to October 5, 1996. The reach from San Marcial to Elephant Butte was not calibrated because there is no downstream gage with which to compare the San Acacia routed flows. Computed flows into Elephant Butte Reservoir are the sum of the floodway, LFCC, and return flows from the Socorro Main Canal. Between San Acacia and San Marcial there are no diversions or drain-return flows. The LFCC has very little flow at San Acacia but has 200-400 cfs of flow at San Marcial. This gain in flow is a result of leakage from the Rio Grande and from irrigation-return flow through the shallow ground-water system. There are no diversions from and no drain-return flows to the river and the LFCC gains water primarily from river leakage in this reach. The modeled floodway and LFCC were calibrated by adjusting the amount of leakage from the river and the amount of water intercepted by the LFCC. Average monthly routed floodway flows were compared to average monthly San Marcial Floodway flow at the San Marcial gage. From January 1, 1989, to March 31, 1989, water was removed from both the floodway and LFCC flows. The USBR was conducting a study of the LFCC, and removed river water above the San Acacia Floodway gage and dumped it into the LFCC above the San Acacia LFCC gage. Also, the USBR removed water from the LFCC above the San Marcial LFCC gage and dumped it back into the river above the San Marcial Floodway gage. The best match of average monthly floodway gage data and routed data, using visual inspection, was with leakage in the winter, January through March and November and December, reduced to 85 percent of computed leakage and summer leakage reduced to 95 percent of computed leakage. With river leakage adjusted as described above, the amount of leakage intercepted by the LFCC was 80 percent for winter and 100 percent for summer. Average summer monthly modeled flow in the LFCC was generally lower than gaged flow at the San Marcial gage. Because the amount of flow in the LFCC at the San Marcial gage in summer was greater than 100 percent of the modeled river leakage, either river leakage is too low or applied irrigation water is returning to the LFCC through the shallow ground-water system during the irrigation season. River leakage is probably not low because the average monthly river flows are best matched using 95 percent of calculated leakage.

RESERVOIRS IN THE MIDDLE VALLEY

DESCRIPTION OF PHYSICAL PROPERTIES

Three reservoirs were constructed on the Rio Grande in the Middle Valley and its tributaries. Only two, Jemez Canyon Reservoir and Cochiti Lake, are modeled. Jemez Canyon and Cochiti Dams are operated for flood- and sediment-control purposes only. **Table 63** summarizes general information about these facilities.

Table 63. General information about Middle Rio Grande Valley reservoirs

	Cochiti	Jemez Canyon
Type:	Earth fill	Earth fill
Year completed:	1973	1953
Structural height (feet):	251	149
Top width (feet):	30	23
Width at base (feet):	1760	835
Crest length (feet):	28,815	861
Crest elevation (feet above sea level):	5479	5271.6
Outlet works discharge capacity (cfs):	14,790	9700

Cochiti Lake

Cochiti Lake is owned and is operated by the Corps in coordination with other Corps projects in the basin. Cochiti Lake has maintained a permanent recreation pool of approximately 50,000 acre-ft since the dam was completed. The permanent pool, which includes an intermittent pond in the arm of the Santa Fe River, provides sediment-control benefits, trapping about 1000 acre-ft of sediment per year. The permanent pool was established by and is maintained by San Juan-Chama Project water. The remaining capacity of the reservoir, totaling about 545,000 acre-ft, is reserved for flood and sediment control.

Cochiti Dam is operated to bypass all inflow to the lake to the extent that downstream channel conditions are capable of safely bypassing the flow. Flood-control operations are initiated when inflow to the lake is in excess of the downstream channel capacity. Stored floodwaters are released when downstream channel conditions permit, all in accordance with the provisions of Public Law 86-645 and the Rio Grande Compact. **Table 64** contains elevation information about Cochiti Lake.

Table 64. Elevation-related information about Cochiti Lake

	Elevation (feet)	Area (acres)	Total capacity (acre-feet)
Top of dam:	5479.00	--	--
Maximum pool:	5474.10	--	--
Total storage at spillway crest:	5460.50	--	--
Permanent pool (varies):	5335.92	1,037	44,712
Conduit invert:	5255.00	0	0

Jemez Reservoir

Jemez Canyon Dam is owned and operated by the Corps for flood- and sediment-control purposes. Establishment and maintenance of a permanent pool significantly enhanced the sediment-control function of Jemez Canyon Reservoir. A sediment retention pool was about 2000 acre-ft in 1979, which has grown to its present size of about 17,000 acre-ft. Jemez Canyon Dam is operated in conjunction with Cochiti Dam to limit downstream flow to existing channel capacity. **Table 65** contains elevation information about Jemez Canyon Dam.

Table 65. Elevation-related information about Jemez Canyon Dam

	Elevation (feet)	Area (acres)	Total capacity (acre-feet)
Top of embankment:	5271.6	--	--
Maximum pool:	5271.2	--	--
Total storage at spillway crest:	5232.0	2,943	94,450
Sediment retention pool:	5196.7	1,364	24,566
Zero storage:	5154.0	--	--

MATHEMATICAL DESCRIPTION OF MIDDLE VALLEY RESERVOIR CALCULATIONS

Cochiti Lake and Jemez Canyon Reservoirs follow the general mass-balance equation for reservoirs:

$$S_t - S_{t-1} - I - P_t + E_t + O = 0$$

where:

S_t = total storage today, in acre-ft;
S_{t-1} = total storage yesterday, in acre-ft;
I = inflow into the reservoir, in acre-ft/day;
P_t = physical model precipitation, in acre-ft/day;
E_t = physical model evaporation, in acre-ft/day; and
O = outflow from the reservoir, in acre-ft/day.

Physical model precipitation is determined by using the equation:

$$P_t = R_t (A_{res})/12$$

where:

R_t = rainfall, in inches/day; and

A_{res} = average reservoir area, in acres.

Physical model evaporation is determined by using one of two equations, depending on the time of year. The summer equation is:

$$E_t = Ep(coeff)(A_{res})/12$$

where:

Ep = pan evaporation, in inches/day; and

$coeff$ = pan evaporation coefficient (0.7 for reservoirs in the Rio Grande Basin).

The winter equation is:

$$E_t = [(T_{max} + T_{min})/2] * (k/days) * (1\text{-}cov) * A_{res}$$

where:

T_{max} = maximum daily temperature, in °F;

T_{min} = minimum daily temperature, in °F;

k = factor for month, in inches per °F;

days = days in the month; and

cov = reservoir ice cover, in percent.

MODEL SIMULATION OF MIDDLE VALLEY RESERVOIR SYSTEM

Jemez Reservoir and Cochiti Lake are simulated as storage reservoirs in the model. Each reservoir solves a mass-balance equation as well as many user-defined solutions. The start of construction of the reservoir object is setting up the object and selecting user-defined methods or solutions. Data are then put into the object's slots (variable or primary data storage container on any object), which are defined by user-defined methods. With all reservoir objects, the default slots are inflow, storage, pool elevation, release, and an elevation-volume table.

Methods for accounting of real-time sediment deposition in Jemez Canyon Reservoir and Cochiti Lake have been developed using empirical data and assumptions unique to each reservoir. These methods provide an estimate of sediment accumulation in storage, resulting in a more accurate accounting of water in storage in the reservoirs.

LOWER VALLEY

PHYSICAL DESCRIPTION OF MODEL REACHES

The Lower Valley is defined in this part of the model as the main stem Rio Grande from Elephant Butte Dam to the stream gage Rio Grande at El Paso, Texas (**fig. 25**). As in the Middle Valley, this 130-mi section is a succession of valleys separated by canyons and narrows. Of these valleys, the Rincon and Mesilla Valleys compose the New Mexico part of the Rio Grande Project. Elevations in the lower valley range from 4200 ft at Elephant Butte to about 3720 ft at El Paso.

The Lower Valley was analyzed in reaches that were delineated at points along the river where discharge measurements were available. The first reach starts at Elephant Butte Dam and extends to Caballo Reservoir, where computed inflow to the reservoir is used for routing streamflow and determining losses. The second reach starts at the gage below Caballo Dam and extends to the gage below the Leasburg Diversion Dam. The third reach begins at the gage below Leasburg Diversion Dam and extends to the gage below Mesilla Diversion Dam. The fourth reach extends from the gage below Mesilla Diversion Dam to the stream gage at Courchesne Bridge (Rio Grande at El Paso, Texas).

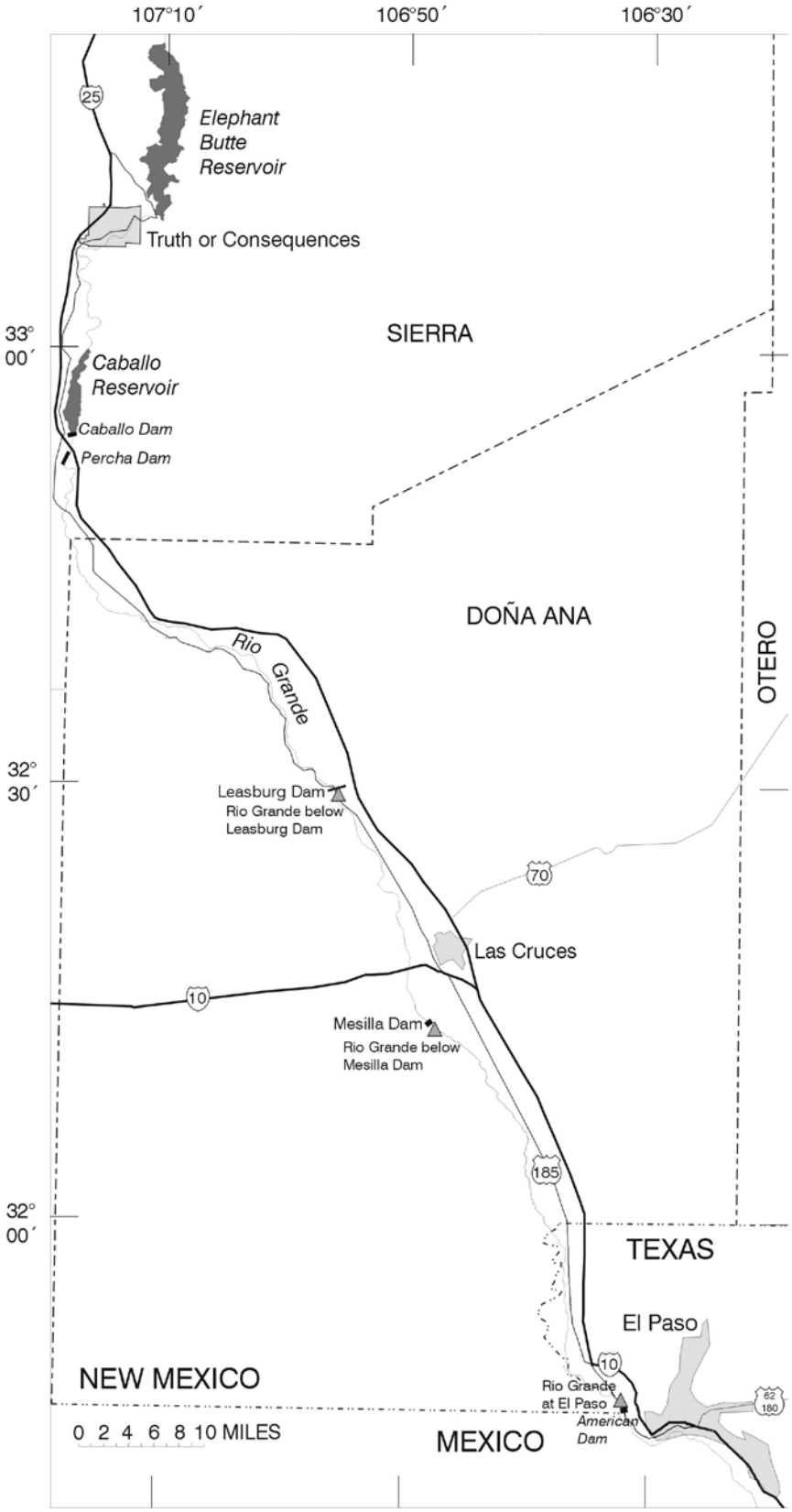

Figure 25. Rio Grande from Elephant Butte Reservoir to El Paso, Texas.

DESCRIPTION OF MODEL METHODS

The focus of the modeling effort for the Lower Valley reaches of the Rio Grande is on flood-control operations and transport of floodwater. Although ample data are available on surface-water diversion from the river for agricultural purposes and return flow thereto, these data are not used in the model. Diversion and return flow and unmeasured tributary inflows are not represented in the model except as an unidentified component of a loss coefficient applied to the reach or of local inflow.

Reach Travel Time and Loss Analysis

The following steps are necessary for implementing the variable time lag routing method and for developing loss coefficients and local inflows in a reach:

1. Select an overall dataset. Datasets used to determine travel times and loss rates are based on discharge data for gages at the upstream or downstream ends of each URGWOM reach that are available or that have been put in electronic format. The period of record used in the analysis of each reach is included in the description of each reach.

2. Calibrate the variable time lag routing method for each reach using methods described previously.

3. To calibrate the travel time lags, multiply the travel time lags determined in step 2 by appropriate multipliers—for example, 0.5, 0.8, 1.0, 1.2, 1.5 and 2.5—to provide a series of routed flows.

4. Compare the series of routed flows to the observed flow at the downstream gage. Use regression analysis and the standard error of the predicted routed flow at the downstream gage for each observed flow at the downstream gage. Using the series of routed flows that minimize the standard error, choose the appropriate multiplier for the travel time.

5. Create a routed hydrograph by routing the upstream-observed hydrograph using the appropriate multiplier for travel time.

6. Create a filtered dataset to determine only loss relations. Keep data for the days when routed flow is greater than downstream-observed flow in groups of 3 or more consecutive days.

7. Plot the (filtered) downstream-observed hydrograph versus the (filtered) routed hydrograph and perform a regression analysis on the data.

8. Create a monthly regression coefficient for each calendar month by using daily data in the regression analyses of the filtered dataset. The slope of the linear regression line of best fit represents the loss coefficient. Regression lines of best fit are computed with y-intercepts and with the line forced through the zero y-intercept. If the y-intercept and zero y-intercept regression lines were not judged to be significantly different, the y = 0 intercept regression line was used. The R^2 value that gives the proportion of the total variability of the y-values that is accounted for by the independent variable x (Ott, 1988, p. 323) was used to judge whether the y-intercept and the zero y-intercept lines were significantly different.

9. Create a “routed with losses” hydrograph using the monthly regression coefficient -1 and the appropriate y-intercept for the overall routed hydrograph.

10. Create a local inflow hydrograph that represents gains within the reach by subtracting the routed with losses hydrograph from the downstream-observed flow hydrograph, both for the overall dataset.

11. (Optional) Smooth the local inflow hydrograph to minimize large negative daily local inflows using a moving average technique.

Rio Grande from below Elephant Butte Dam to Caballo Reservoir

This reach of the Rio Grande is about 18 mi long. Inflow to the reach is water released from Elephant Butte Reservoir at the dam and is recorded by the gage Rio Grande below Elephant Butte Dam. Outflow is calculated from USBR storage, outflow, and evaporation data for Caballo Reservoir. This reach of the river flows through the towns of Truth or Consequences and Williamsburg. Two major ephemeral tributaries, Cuchillo Negro Creek and Palomas Creek, drain from mountains to the west of the river and enter this reach.

Table 66 summarizes stream-gage and calibration data used in determining the power coefficient (wave velocity exponent) that is applied to average velocity measurements to determine river travel time lags in this reach (**graph 132).**

Table 66. Summary of stream-gage and calibration data for the reach of the Rio Grande from Elephant Butte Dam to Caballo Reservoir

	Rio Grande below Elephant Butte Dam
Period of analysis	9/14/70 – 3/1/99
River mile	1382.2
Elevation (feet above sea level)	4241.09
Drainage area (square miles)	29,450
Number of measurements	676
Wave velocity exponent (β)	0.7352
Coefficient of determination (R^2)	0.96

Flow of the Rio Grande from below Elephant Butte Dam to Caballo Reservoir was assumed to be equal to inflow for Caballo Reservoir. Because Caballo Reservoir has no gaged or measured inflow, inflow was calculated using the equation:

inflow = change in reservoir storage + outflow + reservoir evaporation.

Change in reservoir storage was calculated as the previous day's storage minus the current day's storage. Outflow from Caballo Reservoir was calculated from the stream gage Rio Grande below Caballo Dam. The discharge of Bonito Ditch, which diverts water above the gage Rio Grande below Caballo Dam, was not included in this analysis. Reservoir evaporation was calculated from pan evaporation records using the standard 0.7 pan coefficient, the surface area of the reservoir, and the appropriate unit conversion factors. USBR storage, outflow, and evaporation data for Caballo Reservoir were concurrently available for January 1, 1989, through December 31, 1995. The calculated inflow values for Caballo Reservoir were used to calibrate and verify the time lags for this reach. **Table 67** summarizes factors used to determine travel time lags in this reach (**graph 133).**

Table 67. Adopted travel time lags (TL) for the reach of the Rio Grande from below Elephant Butte Dam to Caballo Reservoir

Gage	TL vs. Q equation	R^2	Time lag (hours) for indicated flow rate (cfs)						
			50	200	500	750	1000	3000	6000
Elephant Butte	$TL = 43.908Q^{-0.2634}$	0.783	16	11	9	8	7	5	4
	Adopted travel times for reach using a multiplier of 2.5→		39	27	21	19	18	13	11

Once the travel time lags were determined and verified for this reach, the monthly loss expected in this reach was analyzed using the data filtering procedure described previously with a slight modification for October through December. This filtering procedure resulted in no data points for November and 3 data points for December; although 24 data points were used for October, the data were restricted to a small range of values and produced a poor correlation coefficient. October through December flow in this reach was considerably less than flow during the rest of the year. Measurement and analytical errors appeared to affect low-flow data more than the rest of the data. For example, seepage or other inflow to the reach during low-flow conditions may cause outflow from the reach to be greater than inflow to the reach. Thus, the reach has no loss, and the filtering process will eliminate these data. To expand the number of data points available for the analysis, a filtered dataset of flows less than 1000 cfs for September through February was created and a relation was determined. This relation is referred to as the "low-flow relation." The loss coefficients determined for the low-flow relation were adopted for October through December.

Table 68 summarizes the adopted monthly loss coefficients and y-intercepts for this reach (**graphs 134-143).**

Table 68. Correlations between routed flow and observed flow and adopted monthly loss coefficients and y-intercepts for the reach of the Rio Grande from below Elephant Butte Dam to Caballo Reservoir, 1989-95

Month	n (days)	Slope	y-intercept	R^2	Slope (y=0)	R^2	Adopted loss coefficient	Adopted y-intercept
Jan	15	0.925	-19	0.972	0.901	0.971	-0.10	0
Feb	25	0.956	-30	0.977	0.932	0.977	-0.07	0
Mar	41	1.021	-146	0.962	0.950	0.957	-0.05	0
Apr	63	1.004	-164	0.897	0.924	0.891	-0.08	0
May	95	0.924	-27	0.973	0.915	0.973	-0.08	0
June	78	0.893	84	0.979	0.920	0.978	-0.08	0
July	62	0.998	-127	0.991	0.951	0.989	-0.05	0
Aug	30	1.040	-226	0.942	0.914	0.926	-0.09	0
Sept	42	0.899	8	0.940	0.904	0.940	-0.10	0
Oct[1]		0.861	-5	0.869	0.854	0.869	-0.15	0
Nov[1]		0.861	-5	0.869	0.854	0.869	-0.15	0
Dec[1]		0.861	-5	0.869	0.854	0.869	-0.15	0
Sept-Feb low flow	55	0.861	-5	0.869	0.854	0.869	-0.15	0

[1]Based on Sept – Feb low-flow data.

Rio Grande from below Caballo Dam to below Leasburg Dam

This reach of the Rio Grande is about 45 mi long. Percha and Leasburg Dams divert water from and a number of drains and wasteways return water to the Rio Grande. None of these are included in modeling except as a component of a loss coefficient applied to the reach or of local inflow.

Table 69 summarizes stream-gage and calibration data used to calculate the power coefficient (wave velocity exponent) applied to average velocity measurements for determination of river travel time lags in this reach (**graph 144**).

Table 69. Summary of stream-gage and calibration data for the reach Rio Grande below Caballo Dam to below Leasburg Dam

	Rio Grande below Caballo Dam
Period of analysis	2/17/90 – 10/12/98
River mile	1355.6
Elevation (feet above sea level)	4140.9
Drainage area (square miles)	30,700
Number of measurements	422
Wave velocity exponent (β)	0.368
Coefficient of determination (R^2)	0.848

Table 70 summarizes factors used to determine travel time lags in this reach **(graph 145).**

Table 70. Adopted travel time lags (TL) for the reach of the Rio Grande from below Caballo Dam to below Leasburg Dam

			Time lag (hours) for indicated flow rate (cfs)						
Gage	TL vs. Q equation	R^2	50	200	500	750	1000	3000	6000
Below Caballo Dam	$TL = 1507.1Q^{-0.632}$	0.94	127	53	30	23	19	10	6
	Adopted travel times for reach using a multiplier of 1.5→		191	79	44	35	29	14	9

Table 71 summarizes correlations and the adopted loss coefficients and y-intercepts for this reach **(graphs 146-156).**

Table 71. Correlations between routed flow and observed flow and adopted monthly loss coefficients and y-intercepts for the reach of the Rio Grande from below Caballo Dam to below Leasburg Dam, 1986-99

Month	n (days)	Slope	y-intercept	R^2	Slope (y=0)	R^2	Adopted loss coefficient	Adopted y-intercept
Jan	44	0.982	-122	0.981	0.910	0.972	-0.09	0
Feb	226	0.834	-131	0.909	0.734	0.892	-0.27	0
Mar	434	0.816	-138	0.899	0.749	0.893	-0.25	0
Apr	420	0.870	-277	0.921	0.705	0.886	-0.30	0
May	430	0.885	-314	0.937	0.723	0.902	-0.28	0
June	408	0.838	-260	0.895	0.733	0.880	-0.27	0
July	428	0.866	-225	0.928	0.780	0.918	-0.22	0
Aug	389	0.717	44	0.826	0.739	0.825	-0.26	0
Sept	385	0.724	-38	0.833	0.696	0.832	-0.30	0
Oct	154	1.050	-441	0.881	0.695	0.772	0.05	-441
Nov - Dec	51	0.965	-8	0.993	0.961	0.993	-0.04	0

Data used to develop monthly loss rates for the Caballo to Leasburg reach are generally in the low to moderate flow range rather than the flood-flow range. Also, the data used are affected by surface-water diversions for irrigation, particularly during the months of the irrigation season. Therefore, the loss coefficients and y-intercepts in **table 71** do not apply to a flood-flow situation. A monthly “flood-flow” value is chosen so that flows (in cfs) at or above this rate are assigned a uniform loss rate of 5 percent. Loss rates for flows below the flood-flow value are based on monthly correlation. The flood-flow value for September through February is 1500 cfs and for March through August is 2500 cfs. **Table 72** summarizes the monthly loss coefficients and y-intercepts used in the model for selected flow ranges.

Table 72. Adopted monthly loss coefficients and y-intercepts for the reach of the Rio Grande from below Caballo Dam to below Leasburg Dam for selected flow ranges

	0-1500 cfs		1500-2500 cfs		2500-1,000,000 cfs	
Month	Adopted loss coefficient	Adopted y-intercept	Adopted loss coefficient	Adopted y-intercept	Adopted loss coefficient	Adopted y-intercept
Jan	-0.09	0	-0.05	0	-0.05	0
Feb	-0.27	0	-0.05	0	-0.05	0
Mar	-0.25	0	-0.25	0	-0.05	0
Apr	-0.30	0	-0.30	0	-0.05	0
May	-0.28	0	-0.28	0	-0.05	0
June	-0.27	0	-0.27	0	-0.05	0
July	-0.22	0	-0.22	0	-0.05	0
Aug	-0.26	0	-0.26	0	-0.05	0
Sept	-0.30	0	-0.05	0	-0.05	0
Oct	0.05	-441	-0.05	0	-0.05	0
Nov	-0.04	0	-0.05	0	-0.05	0
Dec	-0.09	0	-0.05	0	-0.05	0

Rio Grande from below Leasburg Dam to below Mesilla Dam

This reach of the Rio Grande is about 23 mi long. The East Side and West Side Canals divert water from the river at Mesilla, and numerous wasteways and drains return water to the river. None of them are included in the modeling of this reach except as a component of a loss coefficient applied to the reach or of the local inflow.

Table 73 summarizes stream-gage and calibration data used to calculate the power coefficient (wave velocity exponent) applied to average velocity measurements for determination of river travel time lags in this reach (**graph 157**).

Table 73. Summary of stream-gage and calibration data for the reach of the Rio Grande from below Leasburg Dam to below Mesilla Dam

	Rio Grande below Mesilla Dam
Period of analysis	9/24/92 – 6/25/99
River mile	1287.5
Elevation (feet above sea level)	3865
Drainage area (square miles)	
Number of measurements	101
Wave velocity exponent (β)	0.724
Coefficient of determination (R^2)	0.9521

Table 74 summarizes factors used to determine travel time lags in this reach **(graph 158).**

Table 74. Adopted travel time lags (TL) for the reach of the Rio Grande from below Leasburg Dam to below Mesilla Dam

			Time lag (hours) for indicated flow rate (cfs)						
Gage	TL vs. Q equation	R^2	50	200	500	750	1000	3000	6000
Below Mesilla Dam	$TL = 55.22Q^{-0.2513}$	0.65	21	15	12	11	10	7	6
	Adopted travel times for reach using a multiplier of 1.5→		31	22	17	16	15	11	9

Table 75 summarizes the adopted loss coefficients and y-intercepts for this reach **(graphs 159-170).**

Table 75. Correlations between routed flow and observed flow and adopted monthly loss coefficients and y-intercepts for the reach of the Rio Grande from below Leasburg Dam to below Mesilla Dam, 1985-98

Month	n (days)	Slope	y-intercept	R^2	Slope (y=0)	R^2	Adopted loss coefficient	Adopted y-intercept
Jan	205	0.935	-36	0.978	0.903	0.97	-0.10	0
Feb	333	0.770	-106	0.870	0.661	0.84	-0.23	-106
Mar	423	0.905	-458	0.861	0.616	0.76	-0.09	-458
Apr	420	0.985	-491	0.875	0.584	0.71	-0.02	-491
May	432	1.060	-636	0.925	0.629	0.74	0.06	-636
June	410	0.969	-618	0.856	0.635	0.74	-0.03	-618
July	415	1.000	-655	0.919	0.689	0.81	0	-655
Aug	406	0.562	-52	0.511	0.526	0.51	-0.47	0
Sept	417	0.598	-175	0.673	0.423	0.61	-0.40	-175
Oct	300	0.840	-193	0.771	0.650	0.71	-0.16	-193
Nov	140	0.662	16	0.859	0.686	0.85	-0.31	0
Dec	154	0.975	-12	0.999	0.968	0.99	-0.03	0

Data used to develop monthly loss rates for the Leasburg to Mesilla reach are generally in the low to moderate flow range rather than the flood-flow range. Also, the data used are affected by surface-water diversions and returns for irrigation, particularly during the months of the irrigation season. Therefore, the loss coefficients and y-intercepts in **table 75** do not apply to the flood-flow situation. A monthly “flood-flow” value is chosen so that flows (in cfs) at or above this rate are assigned a uniform loss rate of 5 percent. Loss rates for flows below the flood-flow value are based on monthly correlation. The flood-flow value for September through February is 1000 cfs and for March through August is 2000 cfs. **Table 76** summarizes the monthly loss coefficients and y-intercepts used in the model for selected flow ranges.

Table 76. Adopted monthly loss coefficients and y-intercepts for the reach of the Rio Grande from below Leasburg Dam to below Mesilla Dam for selected flow ranges

	0-1000 cfs		1000-2000 cfs		2000-1,000,000 cfs	
Month	Adopted loss coefficient	Adopted y-intercept	Adopted loss coefficient	Adopted y-intercept	Adopted loss coefficient	Adopted y-intercept
Jan	-0.10	0	-0.05	0	-0.05	0
Feb	-0.23	-106	-0.05	0	-0.05	0
Mar	-0.09	-458	-0.09	-458	-0.05	0
Apr	-0.02	-491	-0.02	-491	-0.05	0
May	0.06	-636	0.06	-636	-0.05	0
June	-0.03	-618	-0.03	-618	-0.05	0
July	0.00	-655	0.00	-655	-0.05	0
Aug	-0.47	0	-0.47	0	-0.05	0
Sept	-0.40	-175	-0.05	0	-0.05	0
Oct	-0.16	-193	-0.05	0	-0.05	0
Nov	-0.31	0	-0.05	0	-0.05	0
Dec	-0.03	0	-0.05	0	-0.05	0

Rio Grande from below Mesilla Dam to El Paso, Texas

This reach of the Rio Grande is about 38 mi long. Although the Rio Grande has no diversions in this reach, numerous wasteways and drains return water to the river. These wasteways and drains are not included in the model, except as a component of local inflow.

Table 77 summarizes stream-gage and calibration data used to calculate the power coefficient (wave velocity exponent) applied to average velocity measurements for determination of river travel time lags in this reach (**graph 171**).

Table 77. Summary of stream-gage and calibration data for the reach of the Rio Grande from below Mesilla Dam to El Paso, Texas

	Rio Grande at El Paso
Period of analysis	12/6/84 – 7/21/99
River mile	1249
Elevation (feet above sea level)	3722
Drainage area (square miles)	32,207
Number of measurements	245
Wave velocity exponent (β)	0.659
Coefficient of determination (R^2)	0.959

Table 78 summarizes factors used to determine travel time lags in this reach **(graph 172).**

Table 78. Adopted travel time lags (TL) for the reach of the Rio Grande from below Mesilla Dam to El Paso, Texas

Gage	TL vs. Q equation	R^2	Time lag (hours) for indicated flow rate (cfs)						
			50	200	500	750	1000	3000	6000
El Paso	$TL = 172.55Q^{-0.339}$	0.854	46	29	21	18	17	11	9
	Adopted travel times for reach using a multiplier of 1.0→		46	29	21	18	17	11	9

The returns of water to the river result in a gaining reach most of the time. Monthly loss rates established and used for this reach are based on fewer observations than in the two upstream reaches. For September through December the number of observations was too few to do the analysis; therefore, data were combined for the periods November through January and for February through October. Results for these two analytical periods were used to fill in the missing data for November and December and for September and October, respectively.

Table 79 summarizes the adopted loss coefficients for this reach **(graphs 173-182).**

Table 79. Correlations between routed flow and observed flow and adopted monthly loss coefficients and y-intercepts for the reach of the Rio Grande from below Mesilla Dam to El Paso, Texas, 1985-98

Month	n (days)	Slope	y-intercept	R^2	Slope (y=0)	R^2	Adopted loss coefficient	Adopted y-intercept
Jan	15	0.985	-50	0.994	0.958	0.993	-0.04	0
Feb	30	0.869	-15	0.978	0.856	0.977	-0.14	0
Mar	73	0.905	-35	0.957	0.882	0.956	-0.12	0
Apr	12	0.888	82	0.927	0.946	0.923	-0.05	0
May	24	0.980	-80	0.978	0.930	0.975	-0.07	0
June	34	0.872	0	0.873	0.872	0.873	-0.13	0
July	74	0.824	87	0.888	0.856	0.886	-0.14	0
Aug	10	0.671	181	0.875	0.778	0.849	-0.22	0
Sept[1]		0.854	29	0.946	0.868	0.946	-0.13	0
Oct[1]		0.854	29	0.946	0.868	0.946	-0.13	0
Nov[2]		0.974	-48	0.985	0.948	0.984	-0.05	0
Dec[2]		0.974	-48	0.985	0.948	0.984	-0.05	0
Feb-Oct	257	0.854	29	0.946	0.868	0.946	-0.13	0
Nov-Jan	20	0.974	-48	0.985	0.948	0.984	-0.05	0

[1]Based on Feb – Oct data.
[2]Based on Nov – Jan data.

Data used to develop monthly loss rates for the Mesilla to El Paso reach are generally in the low to moderate flow range rather than the flood-flow range. Also, the data used are affected by surface-water returns from irrigation. Therefore, the loss coefficients and y-intercepts in **table 79** do not apply to the flood-flow situation. A monthly "flood-flow" value is chosen so that flows (in cfs) at or above this rate are assigned a uniform loss rate of 5 percent. Loss rates for flows below the flood-flow value are based on monthly correlation. The flood-flow value for September through February is 1000 cfs and for March through August is 2000 cfs. **Table 80** summarizes the monthly loss coefficients and y-intercepts used in the model for selected flow ranges.

Table 80. Adopted monthly loss coefficients and y-intercepts for the reach of the Rio Grande from below Mesilla Dam to El Paso for selected flow ranges

	0-1000 cfs		1000-2000 cfs		2000-1,000,000 cfs	
Month	Adopted loss coefficient	Adopted y-intercept	Adopted loss coefficient	Adopted y-intercept	Adopted loss coefficient	Adopted y-intercept
Jan	-0.04	0	-0.05	0	-0.05	0
Feb	-0.14	0	-0.05	0	-0.05	0
Mar	-0.12	0	-0.12	0	-0.05	0
Apr	-0.05	0	-0.05	0	-0.05	0
May	-0.07	0	-0.07	0	-0.05	0
June	-0.13	0	-0.13	0	-0.05	0
July	-0.14	0	-0.14	0	-0.05	0
Aug	-0.22	0	-0.22	0	-0.05	0
Sept	-0.13	0	-0.05	0	-0.05	0
Oct	-0.13	0	-0.05	0	-0.05	0
Nov	-0.05	0	-0.05	0	-0.05	0
Dec	-0.05	0	-0.05	0	-0.05	0

RESERVOIRS IN THE LOWER VALLEY

Description of Physical Properties

Two reservoirs were constructed on the Rio Grande in the Lower Valley as part of the Rio Grande Project: Elephant Butte Reservoir and Caballo Reservoir. Elephant Butte Reservoir is authorized to operate for conservation storage and generation of hydroelectric power. Caballo Reservoir is operated for conservation storage and flood control. **Table 81** summarizes general information about these two facilities.

Table 81. General information about Lower Rio Grande Valley dams

	Elephant Butte	Caballo
Type:	Concrete gravity	Earth fill
Year completed:	1916	1938
Structural height (feet):	301	96
Top width (feet):	18	35
Crest length (feet):	1674	4558
Crest elevation (feet above sea level):	4407	4190
Outlet works discharge capacity (cfs):	10,800	5000

Elephant Butte Reservoir

Elephant Butte Reservoir is owned and operated by the USBR and is the principal water storage facility for 178,000 irrigated acres of the Rio Grande Project in south-central New Mexico and west Texas. The reservoir is operated to maintain a 25,000-acre-ft pool vacant for flood-control purposes in the winter months and 50,000 acre-ft for flood control in the summer months. A 50,000-acre-foot minimum recreation pool is authorized and is maintained with San Juan-Chama Project water, when available. **Table 82** lists elevation, surface area, and capacity information about Elephant Butte Dam and Reservoir.

Table 82. Elevation-related information about Elephant Butte Dam and Reservoir

	Elevation (feet)	Area (acres)	Total capacity (acre-feet)
Top of dam:	4414	39,853	2,332,748
Maximum pool:	4410	38,019	2,177,003
Total storage at spillway crest:	4407	36,643	2,065,010
Inactive:	4231.5	--	--

Caballo Reservoir

Caballo Dam and Reservoir is operated for conservation storage purposes by the USBR for flood-control purposes by the U.S. Section of the International Boundary and Water Commission (IBWC). Completed in 1938, Caballo Dam provides flood protection for the El Paso/Juarez area by the reservation of 100,000 acre-ft of total capacity for a dedicated flood-control pool, which is under the jurisdiction of IBWC. The reservoir also serves to re-regulate releases made from Elephant Butte Reservoir for the generation of hydroelectric power. **Table 83** contains elevation, surface area, and capacity information about Caballo Dam and Reservoir.

Table 83. Elevation-related information about Caballo Dam and Reservoir

	Elevation (feet)	Area (acres)	Total capacity (acre-feet)
Top of dam:	4190	--	-
Total storage at spillway crest:	4182	--	331,510
Top of conservation storage pool:	4172.44	--	231,467
Top of dead storage:	4104	--	0

Mathematical Description of Lower Valley Reservoir Calculations

Elephant Butte and Caballo Reservoirs follow the general mass-balance equation for reservoirs:

$$S_t - S_{t-1} - I - P_t + E_t + O = 0$$

where:

S_t = total storage today, in acre-ft;
S_{t-1} = total storage yesterday, in acre-ft;
I = inflow into the reservoir, in acre-ft/day;
P_t = physical model precipitation, in acre-ft/day;
E_t = physical model evaporation, in acre-ft/day; and
O = outflow from the reservoir, in acre-ft/day.

Physical model precipitation is determined by using the equation:

$$P_t = R_t(A_{res})/12$$

where:

R_t = rainfall, in inches/day; and

A_{res} = average reservoir area, in acres.

Physical model evaporation is determined by using the equation:

$$E_t = Ep(coeff)(A_{res})/12$$

where:

E_p = pan evaporation, in inches/day; and

coeff = pan evaporation coefficient (0.7 for reservoirs in the Rio Grande Basin).

Model Simulation of Lower Valley Reservoir System

Elephant Butte is simulated as a level power reservoir, and Caballo is simulated as a storage reservoir in the model. Each reservoir solves a mass-balance equation as well as many user-defined solutions. The start of construction of the reservoir object is setting up the object and selecting user-defined methods or solutions. Data are then put into the object's slots (variable or primary data storage container on any object), which are defined by user-defined methods. With all reservoir objects, the default slots are inflow, storage, pool elevation, release, and an elevation-volume table.

REFERENCES CITED

Barlow, P.M., and Moench, A.F., Analytical solutions and computer programs for hydraulic interaction of stream-aquifer systems: U.S. Geological Survey Open-File Report 98-415A, 85 p., 1998.

Bartolino, J.R., and Niswonger, R.G., Numerical simulation of vertical ground-water flux of the Rio Grande from ground-water temperature profiles, central New Mexico: U.S. Geological Survey Water-Resources Investigations Report 99-4212, 34 p., 1999.

Blanchard, P.J., Ground-water-level fluctuations in the Cochiti Dam-Peña Blanca area, Sandoval County, New Mexico: U.S. Geological Survey Water-Resources Investigations Report 92-4193, 72 p., 1993.

Brater, E.F., and King, H.W., Handbook of hydraulics (6th ed.): New York, McGraw-Hill, 1976.

Bureau of Reclamation, Plan for development, Middle Rio Grande Project: app. v. 2 of 2, table F-8, August 1947.

_____San Juan-Chama Project—Incremental loss studies between Cochiti Dam and Elephant Butte Reservoir: Upper Rio Grande Basin Projects Office, 43 p., 1985.

_____ Middle Rio Grande Project-New Mexico, aggredation-degredation range lines, Cochiti Dam to Range Line 1794, 1992.

_____Middle Rio Grande water assessment—supporting documents 6, 7, 10, 12, and 15: Upper Rio Grande Area Office, Albuquerque, N. Mex., 1997.

Bureau of Reclamation and U.S. Army Corps of Engineers, Programmatic biological assessment, Water operations and river maintenance on the Middle Rio Grande, New Mexico, Rio Grande silvery minnow, southwestern willow flycatcher, and bald eagle: 190 p., May 1998.

Chow, V.T., Open channel hydraulics: New York, McGraw-Hill, 1959.

Fenton, K.H., 1992 Rio Grande high/low flow wetted area and river channel study: Bureau of Reclamation Technical Memorandum no. 8260-96-03, 7 p., 1996.

Hansen, Steve, no date, Middle Rio Grande Assessment Riparian Corridor alluvium steady-state, groundwater investigation concerning Rio Grande channel loss contributions to recharge conducted by Bureau of Reclamation Albuquerque Projects Office, final draft.

Hawley, J.W., and Haase, C.S., Hydrogeologic framework of the northern Albuquerque Basin: Socorro, New Mexico Bureau of Mines and Mineral Resources Open-File Report 387, p. II-4, 1992.

Kernodle, J.M., McAda, D.F., and Thorn, C.R., Simulation of ground-water flow in the Albuquerque Basin, central New Mexico, 1901-1994, with projections to 2020: U.S. Geological Survey Water-Resources Investigations Report 94-4251, 114 p., 1995.

King, J.P., and Bawazir, Salim, Evapotranspiration crop coefficients as a function of heat units for some agricultural crops in New Mexico: Las Cruces, New Mexico Water Resources Research Institute, 19 p., May 1998.

Leopold, L.B., and Maddock, T., The hydraulic geometry of stream channels and some physiographic implications: U.S. Geological Survey Professional Paper 252, 1953.

Leopold, L.B., Wolman, M.G., and Miller, J.P., Fluvial processes in geomorphology: San Francisco, W.H. Freeman, 1964.

Ortiz, David, Lange, Kathy, and Beal, Linda, Water resources data, New Mexico, water year 1997: U.S. Geological Survey Water-Data Report NM-1997-1, 574 p., 1998.

Ott, Lyman, An introduction to statistical methods and data analysis: Boston, PWS-Kent, 1988.

Seddon, J.A., River hydraulics: Transactions, American Society of Civil Engineers, v. 43, no. 9, p. 179-229, 1900.

Shafike, Nabil (2005) (undergoing review)

Sorey, M.L., and Matlock, W.G., Evaporation from an ephemeral streambed: Journal of the Hydraulics Division, American Society of Civil Engineers, v. 95, no. HY2, Proc. Paper 636, p. 423-438, January 1969.

Tiedeman, C.R., Kernodle, J.M., and McAda, D.P., Application of nonlinear-regression methods to a ground-water-flow model of the Albuquerque Basin, New Mexico: U.S. Geological Survey Water-Resources Investigations Report 98-4172, 90 p., 1998.

U.S. Army Corps of Engineers, Elevation-area-capacity table, Cochiti Lake, Rio Grande Basin, Sandoval County, New Mexico: Albuquerque District, 1990.

_____Rio Chama, Abiquiu Dam to Española: Reconnaissance Report, 1995.

_____Elevation-area-capacity table, Cochiti Lake, Rio Grande Basin, Sandoval County, New Mexico: Albuquerque District, 1996a.

_____Water control manual, Cochiti Dam and Lake, Sandoval County, New Mexico: Albuquerque District, May 1996b.

U.S. Geological Survey, Surface water records in New Mexico: 1964.